EXCISION, TRANSFER, AND INTEGRATION OF THE *BACTEROIDES* INTEGRATIVE AND CONJUGATIVE ELEMENT CTnDOT

BY

CRYSTAL MARIE HOPP

DISSERTATION

Submitted in partial fulfillment of the requirements
for the degree of Doctor of Philosophy in Microbiology
in the Graduate College of the
University of Illinois at Urbana-Champaign, 2016

Urbana, Illinois

Doctoral Committee:

Professor Jeffrey F. Gardner, Chair
Professor Gary J. Olsen
Professor Peter A. B. Orlean
Associate Professor Rachel J. Whitaker

ABSTRACT

Increased resistances to antibiotics is a pressing problem in the world today. When new antibiotics are introduced, resistance to that antibiotic within the microbial community soon follows. One of the many contributing factors to increased resistances to antibiotics is the spread of mobile genetic elements that encode antibiotic resistance genes. These elements are able to transfer themselves to new host cells by conjugation, which may result in the widespread dissemination of an element throughout a given microbial population.

The *Bacteroides sp.* are known for harboring wide array of integrative and conjugative elements. One of the most well studied examples is the 65kb CTnDOT, which encodes both erythromycin and tetracycline resistances. *Bacteroides* are prevalent within the human gastrointestinal tract, which means that CTnDOT is capable of transferring to other resident microbes within this environment.

The transfer of CTnDOT is repressed under normal conditions, but when tetracycline is present the propagation of the element is stimulated through a complex regulatory cascade. The excision operon is a key component of this regulation, and is involved at many different levels of the regulatory cascade. As the name implies, the expression of the excision operon promotes the excision of CTnDOT from the host chromosome. Once the element is excised it needs somewhere to go, which the excision operon also facilitates by increasing the transcription of both the mobilization (*mob*) and transfer (*tra*) operons. These operons encode the proteins needed to assemble the mating apparatus, and the proteins responsible for shuttling the excised element to the mating apparatus for transfer.

The work presented within this dissertation focuses on the different aspects of the excision operon. First the mechanistic properties of the excision proteins at the *mob* and *tra* region were investigated. It was shown that the Xis2d protein binds the DNA between the *mob* and *tra* promoters, and that the Exc protein can be recruited in the presence of Xis2d to help initiate the transcription of the *mob* operon.

The contribution of each of the excision genes to the *in vivo* excision reaction was also analyzed. It was shown that each of the genes within the excision operon play a significant role in the excision reaction. The presence of *xis2c, xis2d,* and *exc* was essential for detecting excised product, which confirms that *exc* is required for *in vivo* excision. Also, a deletion of *orf3* significantly reduced the production of excised products, which is the first time this gene has shown a discernable effect in a CTnDOT assay. This wasn't the only discovery of gene functionality that was uncovered, the previously uncharacterized *orf2a* and *orf2b* genes were found to contribute to the excision reaction.

The excision, transfer, and mobilization of CTnDOT ultimately lead to propagation of this element into new recipients. Once within the recipient cell, the element integrates into an *attB* site located within the recipient chromosome. This dissertation also provides an *in vivo* analysis of CTnDOT integration, where 18 alternative *attB* sites were identified. In summation, the work presented within this dissertation has clarified the main aspects of CTnDOT propagation, by revealing important contributions of the excision operon to the regulation of the element.

TABLE OF CONTENTS

CHAPTER 1: INTRODUCTION

1.1 Beneficial Aspects of *Bacteroides*

Humans are composed of cells, but not all of those cells originate from the host. In terms of prevalence, there are 10 times more bacterial cells than human cells within our bodies [60]. Within our gastrointestinal tract alone there are 10^{13} to 10^{14} bacterial cells [25]. Key players in this microbial community are members of the *Bacteroides* genus, which makes up about 25% of the adult human intestinal tract [78].

In many ways *Bacteroides* sp. form a mutualistic relationship with their human hosts. They help us break down indigestible carbohydrates into usable energy sources, which allows us to gain energy from the food we eat more efficiently [2, 17, 73, 77, 78]. For example, germ free rats require 30% more calories than non-germ free rats to maintain a normal body mass [26]. While all bacteria are capable of metabolizing a subset of carbohydrates, *Bacteroides* are equipped with more genes for this purpose than any other characterized bacterium [2, 73]. *Bacteroides thetaiotaomicron* contains 163 genes that are homologous to the starch utilization genes *susC* and *susD*, whose products bind starch so that glycosylhydrolases can degrade the substrate [17, 77, 78]. *Bacteroides thetaiotaomicron* contains 172 glycosylhydrolases from 23 distinct classes of enzymes [17, 77, 78]. Around 11% of the glycosylhydrolases are located on the surface of *Bacteroides* cells, so the released products can be used by *Bacteroides*, the host, or neighboring bacteria [17, 26, 78]. To keep *Bacteroides* in close proximity, host epithelial cells respond to *Bacteroides* in the environment by releasing fucosylated glycans, which

Bacteroides can use as an energy source [26]. The host cells can then pilfer an array of energy sources that *Bacteroides* produce before they are taken up by the bacterial cell.

In addition to breaking down macromolecules into usable energy sources, *Bacteroides* can synthesize vitamins [53]. The vitamin K that is produced by *Bacteroides* can be absorbed through the bowel and contribute to host nutrition [53].

Not only do *Bacteroides* help their human host obtain more sources of energy, their prevalence also seems to correlate with healthier observed weights. Obese individuals contain fewer *Bacteroides* and more Firmicutes than healthy weight individuals [41, 42]. When obese individuals are put on diet therapy, their levels of *Bacteroides* rise, while their levels of Firmicutes decrease [42].

As young children we are taught that our immune system helps us fight off disease and infection. Therefore, it is probably surprising to the general public that our body's system of defense against microorganisms heavily relies on microorganisms for proper maintenance. *Bacteroides* helps out the host immune system in several ways. *Bacteroides* play an important role in the development of gut associated lymphoid tissue (GALT). A combination of *Bacteroides fragilis* and *Bacillus subtilis* promoted GALT development in rabbits [55]. *Bacteroides fragilis* also plays a pivotal role in optimizing the balance between T helper cell types (T_H1 and T_H2), in addition to regulating T cell differentiation [24]. Paneth cells are immune cells in the gastrointestinal epithelia that secrete antimicrobial compounds [73]. *Bacteroides thetaiotaomicron* has been shown influence Paneth cell protein expression by stimulating the production of a protein that kills harmful pathogenic bacteria [73].

Bacteroides have the ability to induce T regulatory cells, which are required for reducing the symptoms of chronic inflammation [23]. Even non-intestinal inflammation, like asthma and allergies, can be influenced by gastrointestinal species. *Bacteroides fragilis* produces polysaccharide A (PSA), which is a capsular polysaccharide that has been shown to help balance and regulate cytokine levels [46]. When the cytokine levels in our bodies are balanced it helps relieve the negative symptoms associated with asthma and allergies.

Many bacteria would be able to thrive within the nutrient rich gastrointestinal tract of humans. However, not all bacteria would be hospitable partners to their human hosts. Fortunately *Bacteroides* prevent colonization of harmful bacteria by out-competing them in the gastrointestinal real estate market. The gut environment is hostile and constantly changing. The surface epithelium cells are constantly shedding within the small intestine and colon [78]. Our immune cells are also continuously monitoring the area. *Bacteroides* can evade the host immune response largely due to their polysaccharide capsule. The composition of the polysaccharides in the capsule is regulated by invertible promoters upstream of polysaccharide synthesis genes [37]. There could be as many as 256 unique capsular polysaccharide combinations [37].

When everything is in balance, this ability to adapt to the ever changing host environment is beneficial to maintaining the mutualistic relationship between *Bacteroides* and humans, however the ability to adapt can become detrimental when the balance is upset.

1.2 *Bacteroides* Gone Bad

The ability of *Bacteroides* to evade the host immune system is no longer beneficial when the balance is tipped towards virulence. The capsule that is capable of displaying a wide array of surface polysaccharides to evade the host immune system is also capable of shielding *Bacteroides* from complement killing and phagocytic uptake [73]. *Bacteroides fragilis* has the potential to prevent peritoneal macrophage activity, which is the first line of defense when the intestines are ruptured [73].

If *Bacteroides* do establish themselves outside of their normal niche within the gastrointestinal tract it can be hard to regain the upper hand due to the high instances of antibiotic resistance found within *Bacteroides* sp. These resistances are often acquired from a wide array of mobile genetic elements that *Bacteroides* tend to harbor. These elements can carry genes that encode antibiotic resistances, heavy metal resistances, carbon source utilization genes, symbiosis genes, pathogenesis genes, restriction and modification genes, bacteriocin synthesis genes, and biofilm formation genes [33].

1.3 Mobile Genetic Elements

Mobile genetic elements comprise a vast and diverse category of transferable DNA segments. Insertion sequences (IS) are small mobile pieces of DNA that encode a transposase gene and are flanked by inverted repeat sequences [28]. Transposons (Tn) are insertion sequences that carry additional genes other than the transposase gene [28]. Often transposons carry antibiotic resistance genes, or genes that can benefit the fitness of a bacterium in some way [54]. Transposons can be simple, like Tn3, or composite, like Tn10. Simple transposons contain a single set of inverted repeats that flank the encoded genes. For example, Tn3 contains the required transposase gene (*tnpA*), a repressor gene

(*tnpR*), and a β-lactamase antibiotic resistance gene (*bla*) flanked by a single set of inverted repeats [31]. Composite transposons contain two complete insertion sequences, each one containing a transposase gene flanked pair of inverted repeats [68]. These insertion sequences flank the additionally encoded genes in between them and the whole apparatus moves as a single element. For example, Tn10 contains a tetracycline resistance gene (*tetR*), flanked by IS10-left and IS10-right [21, 29]. Both insertion sequences and transposons tend to insert randomly within a genome.

The random nature of these types of elements can result in a variety of possible outcomes. The integration of these elements can lead to insertion mutations in the middle of genes, causing aberrant gene products, or cell death in the case of essential genes. Polarity can result from the insertion of transposons and insertion sequences into operons. When this happens the transcription of downstream genes can be negatively impacted, while the transcription of the upstream genes remains unaffected. Some insertion sequences and transposons actually provide promoters that regulate the host DNA once the elements integrate. A recent study in *Drosophila melanogaster* showed that transposable elements contributed 1300 promoters to the developmental transcriptome of the organism [4]. Insertion sequences and transposons can also cause genetic rearrangement to occur throughout the chromosome of the host organism via homologous recombination and alternative transposition [27]. The repression, activation, and rearrangement of genes throughout a chromosome aided by mobile genetic elements are thought to help drive evolution [5, 9, 10, 12].

Plasmids are self-replicating circular segments of extrachromosomal DNA that can encode a multitude of different genes [22, 28]. Usually the genes encode products

that are beneficial to the host bacterium, including: antibiotic resistance, virulence factors, detoxifying agents, secondary metabolic pathways, bacteriocins, and nitrogen fixation machinery [11, 20, 54]. Some plasmids are self-transmissible, meaning they encode the machinery needed to mobilize and transfer themselves into a new host. Other plasmids are incapable of self-transfer, so they must hijack the transfer machinery from a self-transmissible element to enter into a new host cell [28]. For example, *Salmonella typhimurium* strains contain a virulence plasmid that is self-transmissible in the strains LT2, 14028, and SR-11 [57]. However, the virulence plasmid in strain SL1344 is not self-transmissible [57].

Bacteriophages, or phages, use capsids to shuttle foreign genetic material to new hosts [22, 65]. Phages come in a variety of sizes and can be composed of either DNA or RNA, and can be single, or double stranded [22]. Once the foreign DNA is injected into the host cell, a few different outcomes are possible depending on the type of phage. A phage may begin to replicate and package new phage particles, and then lyse open the host cell to release the newly formed viruses [6]. This is known as a lytic cycle, and there is no real advantage for the host cell in this circumstance. However, some phages utilize the lysogenic life cycle. This is where phages enter the host cell and integrate into the host chromosome, becoming prophages [6]. Prophages repress the viral genes that are active during the lytic cycle, but there are often additional genes provided by the prophage that are beneficial to the host cell [6, 66]. Some phages encode gene products that alter the surface of the bacterium to make it resistant to additional phage uptake [6]. This prevents the possibility of a lytic phage entering the host and lysing the prophage's new host. Prophages also supply a wealth of different types of toxins and effector

molecules that the bacteria can use against eukaryotic host cells. The shiga toxin, cholera toxin, diphtheria toxin, and botulism toxin are all examples of exotoxins encoded by prophages [6, 66]. Often prophages encode proteins the bacteria can use to facilitate adhesion and resistance to the immune system, like the *bor* and *lom* genes of phage lambda [3, 66, 67]. The lysogenic cycle is stable until certain conditions, which vary according to phage, are encountered. Then the prophage can shut off the lysogenic cycle and enter into the lytic cycle for dissemination of the element.

Conjugative transposons have always had a bit of an identity crisis, since they share similarities with each of the previously mentioned mobile genetic elements. When first discovered they were thought to be regular transposons. Like transposons they contained several foreign genes flanked by inverted repeats and they were found integrated within the host genome [58]. This is why Tn916, one of the most well studied conjugative transposons, was not originally designated CTn916. Unlike regular transposons, conjugative transposons integrate into the bacterial chromosome in a site selective manner and they encode the genes necessary for constructing a cell-to-cell mating apparatus. Some lysogenic phages, like phage lambda, integrate site selectively [48]. However, conjugative transposons do not form any viral particles and they use the aforementioned mating bridge for transmission to new host cells. Once excised from the chromosome, conjugative transposons form a circular intermediate similar to a plasmid. However, conjugative transposons are unable to self-replicate when in the excised form. Instead they rely on getting passively replicated with the genome when integrated into the chromosome. After countless studies have been performed on various members of this family it has become clear that conjugative transposons are a unique group of elements.

Therefore, to distance them from the preconceptions associated with the word transposon they have been given a new name. They are now termed integrative and conjugative elements (ICEs).

Many of the mobile genetic elements found within *Bacteroides* belong to the CTnDOT family of ICEs. This is a diverse group of integrative and conjugative elements that appear to be regulated by tetracycline. This thesis focuses on the "king" of this family, CTnDOT, and the multi-faceted aspects of its intricate lifecycle (Figure 1.1). CTnDOT is not only one of the longest and most well studied ICEs within the *Bacteroides* sp., it is also one of the most well studied ICEs of all time.

CTnDOT has prompted sustained and continuous research projects for a plethora of different reasons. This element has numerous regulatory intricacies that have yet to be fully understood and it uses these intricacies to spread from host to new recipients. This has ultimately increased the drug resistance of microorganisms within the gastrointestinal tracts, since this element carries both tetracycline and erythromycin resistances.

1.4 CTnDOT Regulatory Cascade

The propagation of CTnDOT relies on this ICE's ability to excise itself from the chromosome of a host cell, transfer itself to a recipient cell, and integrate into the chromosome of the recipient cell (Figure 1.2). These major steps in the lifecycle of CTnDOT are highly regulated by a complex cascade of events (Figure 1.3). At the epicenter of this regulatory cascade is tetracycline, since all CTnDOT functions are governed by the presence, or absence of this antibiotic. When tetracycline is absent from the host environment, CTnDOT remains inactively maintained within the chromosome of

the host cell, being passively replicated through the cellular replication mechanisms of the host.

When tetracycline is present, it initially binds to ribosomes, causing them to stall on the mRNA [70]. When this stalling occurs on the leader peptide upstream of the *tetQ-rteA-rteB* operon, it destabilizes a hairpin loop in the mRNA that occludes the ribosomal binding site of *tetQ* [69]. Once the ribosomal binding site is free from the hairpin loop structure, incoming ribosomes can come in and start translation of the *tetQ* message. The TetQ protein provides ribosomal protection against tetracycline by causing a conformational change in the ribosome that prevents tetracycline from binding [43, 49]. The presence of this gene at the start of the regulatory cascade ensures that the process is self-limiting, because once TetQ is produced, it protects the ribosomes and prevents them from stalling. If stalling doesn't occur at the leader peptide of the *tetQ-rteA-rteB* operon, the regulatory cascade shuts down. This prevents the pointless overproduction of downstream factors.

The other two proteins in the *tetQ-rteA-rteB* operon show significant homology to known two component regulatory systems, with RteA resembling a histidine kinase sensor protein and RteB resembling a response regulator protein [61]. Based on the amino acid sequence it appears that RteA spans the plasma membrane and has an N-terminal receptor domain located in the extracellular space and a C-terminal cytoplasmic domain where the signal is delivered [61]. It is unknown what RteA is sensing in the environment. The response regulator, RteB, contains conserved aspartic acid residues in the N-terminus of the protein that can be phosphorylated by the C-terminal domain of

RteA [61]. RteB also has potential ATP binding sites and a helix-turn-helix domain at the C-terminus of the protein [61].

The phosphorylated response regulator, RteB, is then able to positively regulate the transcription of the downstream gene *rteC* [47, 62]. RteB is likely able to activate *rteC* transcription by binding directly to the DNA upstream of the *rteC* promoter using the helix-turn-helix DNA binding motif found in the C-terminus of the RteB protein. However, RteB has never been purified to confirm this *in vitro*.

RteC is a transcriptional activator of the *xis2c-xis2d-orf3-exc* operon [47, 50]. RteC binds upstream of the *xis2c-xis2d-orf3-exc* promoter using a C-terminal winged helix domain [50]. The closest homologs of RteC are not even in the bacterial domain of life. The structure of RteC most closely resembles the human transcription factors E2F-4 and DP2 [50]. If RteC is placed under an inducible promoter, the *tetQ-rteA-rteB* operon is no longer required for the induction of excision and transfer of CTnDOT [47].

Once the transcription of the *xis2c-xis2d-orf3-exc* operon is induced, a further layer of complexity regarding the regulation of CTnDOT unfolds. This single operon facilitates the excision, mobilization, and transfer components of CTnDOT propagation. The *xis2c-xis2d-orf3-exc* operon has been colloquially titled the excision operon, since this operon was first characterized when it was discovered to be required for the excision of CTnDOT [15]. Each of the four proteins encoded by the genes of this operon appear to individually contribute to the overall processes of excision, mobilization, and transfer in a different manner.

With regards to excision, the Xis2c and Xis2d proteins can be classified as recombination directionality factors (RDFs). RDFs bind DNA to influence whether the integrase protein binds in a way to promote the excision reaction, or the integration reaction [40]. The Xis2c and Xis2d proteins are small, basic proteins whose predicted secondary structure contains strong helix-turn-helix motifs. When Xis2c, Xis2d, and the integrase IntDOT are bound to the ends of the integrated CTnDOT element, known as *attL* and *attR*, the excision reaction is prompted [35]. The third gene in the excision operon, *orf3*, has two conserved domains of unknown function. These domains, DUF4099 and DUF3945, are archived in the NCBI conserved domains database, and were identified when human metagenome sequences were clustered. CTnDOT derivatives with in-frame deletions of *orf3* previously showed no discernable differences in excision and transfer levels, compared to the wild type excision operon. Therefore, this gene has remained largely unstudied. The final gene in the excision operon, *exc*, encodes a type III topoisomerase. This type of topoisomerase is functionally similar to type I topoisomerases in relaxing supercoils, but they have the added ability to facilitate disentangling recently replicated chromosomes [13]. While Exc is a functional topoisomerase that has been shown to relax supercoiled DNA *in vitro*, the topoisomerase activity is not required for excision to occur [64]. The contribution of Exc to the excision reaction has been much studied, but the mechanism of the protein remains elusive.

When CTnDOT excises from the host cell, the two integrated ends of the element, *attL* and *attR*, are cut and brought together to form a covalently closed circular intermediate [15, 19]. The newly formed junction that closes this circular intermediate is termed *attDOT*, and it can be detected through PCR and DNA blotting methods.

In vivo, Exc is required for producing detectable levels of an excised product by Southern blot analysis [15]. However, *in vitro* Exc has shown varying levels of involvement in the excision reaction. An intermolecular excision assay was constructed where the integrated ends of CTnDOT (*attL* and *attR*) are on separate plasmids and excision is detected by the formation of a co-integrate plasmid. In this intermolecular assay Exc did not show any effect on the levels of excision detected [63]. Since the excision of CTnDOT from the chromosome does not occur between two separate DNA elements, an intramolecular *in vitro* excision assay was then constructed. In this assay the integrated ends of CTnDOT, known as *attL* and *attR*, were provided on the same plasmid with *lacZα* between them. Excision results in the loss of *lacZα*, which was detectible by transforming the DNA into cells and screening for the frequency of white colonies on MacConkey agar. In this assay Exc was not required for CTnDOT excision, but it did show a stimulatory effect [34].

As previously mentioned, the excision proteins are not, as their name suggests, only involved in the excision of CTnDOT. More recent studies have indicated that members of the excision operon are responsible for the transcriptional activation of the divergently transcribed mobilization and transfer operons. These two operons are separated by 691 bps. There is a long 264 bp leader region between the start of *mobA* and the promoter of the *mob* operon, and there is a 318 bp leader region between the start of *traA* and the promoter of the *tra* operon. This means that the promoters of these operons are only 66 bps apart (Figure 1.4).

The proteins encoded by the mobilization operon are involved in nicking the *oriT* of the excised CTnDOT, and transporting a single strand of the element to the mating

apparatus [51, 72]. The mobilization operon consists of three proteins, *mobA-mobB-mobC*. MobA has similarities to nicking accessory proteins of the ribbon-helix-helix family, and it helps the relaxase protein (MobB) access the nick site within the origin of transfer (*oriT*) [51]. MobB is responsible for nicking the *oriT* and covalently binding to the strand of DNA that is going to be transferred [32, 51]. MobC shares homology to the VirD4 family of coupling proteins, which serve to escort the MobB-bound strand of DNA to the mating apparatus [32, 51]. The transcription of the mobilization operon appears to be suppressed under normal conditions, however the source of that suppression is currently unknown [72]. The excision proteins Xis2d and Exc appear to be required to overcome the transcriptional repression of the mobilization operon (Figure 1.5) [72].

It is worth mentioning that the mobilization operon of CTnDOT may have twice the workload of a typical mobile genetic element. Recent studies have shown that CTnDOT possesses two *oriT* sites that are both capable of initiating transfer of the excised form of CTnDOT [72]. All other characterized elements have a single origin of transfer.

The transfer operon is composed of 17 genes (traA-traQ) that encode the mating apparatus of CTnDOT. The exact role of the individual transfer genes is unknown, but studies were performed to test the necessity of the different transfer genes in the closely related element CTnERL. When the *traG*, *traI*, *traJ*, and *traM* genes were disrupted by insertion, the transfer of CTnERL was abolished [8]. Insertions into *traH* and *traN* resulted in a significant reduction in transfer frequency, but some transfer was detectible [8]. Limited protein localization studies were performed with TraG and TraN. These studies showed that TraG localized to the inner and outer cell membranes, while TraN

remained localized to the outer membrane [8]. This suggests that at least TraG and TraN are structural components of the mating apparatus. Surprisingly when the last three of the transfer genes (*traO*, *traP*, *traQ*) were disrupted, an increase in transfer frequency was seen, suggesting that some of the genes in the transfer operon may provide a self-regulatory role [8].

While the individual roles of the transfer genes are unknown, a few have some structural homology to the conjugation proteins of other systems. TraG has homology to several known conjugation proteins. It is most similar to the BctA protein, which is a *Bacteroides* protein found on the self-transmissible plasmid pBF4 and on the ICE BTF-37 [7, 30]. It also has similarity to VirB4, which is a multimeric inner membrane ATPase that helps coordinate and provide energy for the transfer of DNA strand to the VirB6 and VirB8 proteins of the mating apparatus in the Ti plasmid system [1, 7, 52]. It also shows some similarity to the TraC protein from the F plasmid, which is involved in assembling the F pillin into a mature F pillus structure [7, 59].

The transcription of the transfer operon is repressed under normal conditions by a constitutively transcribed small RNA known as RteR [71, 74]. To overcome this negative regulation, Xis2d and Xis2c must activate the transcription of the transfer operon (Figure 1.5).

1.5 CTnDOT Integration

When the excised CTnDOT is successfully transferred into a recipient cell through the mating apparatus, it needs to integrate into the chromosome of the host cell to be maintained. This is also true for the copy of CTnDOT that remains within the donor

cell. The donor cell would lose the antibiotic resistances that CTnDOT provides unless excised CTnDOT re-integrates into the chromosome.

As previously described, there are multiple tiers of regulation involved in controlling the excision of CTnDOT, however the integration of the element is more straightforward. The integration reaction requires the joined ends of CTnDOT (*attDOT*), the chromosomal insertion site (*attB*), the integrase (IntDOT), and a host factor (BHFa) [14, 16, 56]. Since the integrase, IntDOT, is needed for nicking, strand transfer, and ligation of the DNA in both the excision and integration reactions, it is a constitutively expressed protein. IntDOT is a member of the tyrosine recombinase family of integrases [44].

For integration to occur four InDOT monomers must bind to the *attDOT* and *attB* substrates [76]. These IntDOTs are able to make the proper contacts with the DNA when the *Bacteroides* host factor, BHFa, bends the DNA to move the IntDOT binding sites closer together [56]. For integration to occur, IntDOT must facilitate the reaction by nicking either the top or bottom strands of DNA, and coordinating the strand exchange and ligation between the CTnDOT element and the recipient chromosome [38, 45]. This sequence of events results in a Holliday junction intermediate [36, 76]. Once this intermediate is formed, the opposite strands of DNA are nicked, exchanged, and ligated to form the *attL* and *attR* sequences that result from the successful integration of CTnDOT [38, 45]. This process is summarized in Figure 1.6. The excision reaction also undergoes this type of mechanism. In the excision reaction the starting reactants are *attL* and *attR*, and the excision proteins are bound to these DNA sequences to promote the excision reaction that results in the *attDOT* and *attB* products.

To expand on the first step of integration, the C-terminal domains of IntDOT bind to sequences known as core type sites (D, D', B, B'), and the N-terminal domains of IntDOT bind to sequences known as arm type sites (R1, R1', R2, R2', L1, L2) [18, 39, 75]. The core type sites are flanking 7 bp of DNA that is known as the overlap region (Figure 1.7) [14, 18, 39, 75]. For most tyrosine recombinases, the 7bp in the overlap region need to be identical to each other for the reaction to proceed [76]. IntDOT is unique in that it requires the first two base pairs in the overlap region to identical, but the remaining 5 bp do not have to match for the reaction to proceed [76]. This increases the promiscuity of CTnDOT, which may help explain its omnipresent abundance in nature. Many genetic elements have a preferred *attB* site that they integrate into, but this does not appear to be the case with CTnDOT. Previous studies have sequenced 8 CTnDOT recombination events, with only two of the sequences possibly being the same [14]

1.6 Questions Addressed in This Dissertation

As described previously, the excision proteins of CTnDOT are pivotal for regulation of the element, as they are involved in multiple tiers of the regulatory cascade. Chapter 2 of my dissertation is dedicated to determining how the excision proteins are regulating the transcription of these divergently transcribed operons. There is a special focus placed on Xis2d, as it is involved in promoting the excision reaction of CTnDOT and in transcriptionally activating both the mobilization and transfer operons. To address this question, the Xis2d and Exc proteins were purified and subjected to *in vitro* analysis. The overall findings suggest that Xis2d binds in between the two promoters and bends the DNA. It is possible that Xis2d is the first to bind the region, as it is involved in the regulation of both operons. Then one of the other two excision proteins may come in and

switch transcription in a particular direction. It was shown that Exc appears to form higher order complexes when incubated with Xis2d and DNA from the promoter region.

In Chapter 3, I address the *in vivo* frequency of CTnDOT excision and integration. As stated earlier, there are conflicting results with regards to excision, depending on which assay is used. Previous *in vivo* studies used qualitative methods for analysis, so a quantitative *in vivo* assay was developed. This assay utilizes primers to measure the overall formation of *attDOT* and *attB*, while measuring the disappearance of *attR/attL* sequences using qPCR. This assay was not only able to test the excision levels for the wild type CTnDOT element, but it was also used to test numerous in-frame deletions of the excision proteins.

In addition to the qPCR assay, the excision and integration frequency of CTnDOT was analyzed using high throughput sequencing. The relative number of reads containing the *attDOT*, *attB*, and *attL/attR* sequences were analyzed to determine the excision frequency of the element. The added benefit of using HiSeq analysis was being able to pull out reads where CTnDOT had integrated into a new location on the chromosome. This allowed us identify 18 alternative *attB* sites within the *Bacteroides* chromosome. In addition to learning more about the excision and integration of CTnDOT, the HiSeq$_{2500}$ data was assembled to provide the first complete sequence of CTnDOT.

Chapter 4 focuses on the development of an *in vivo* mutagenesis screen I developed for isolating excision protein mutants. It is currently unknown how the structures of the different excision proteins contribute to their functionality. Regions of mutant proteins that are incapable of *in vivo* excision can be characterized, which could

result in the identification of the functional regions of the individual proteins. Finally, in Chapter 5 I will summarize the overall findings of my work, and discuss future studies that would build upon the work I have accomplished.

1.7 References

1. Atmakuri, K., E. Cascales, and P.J. Christie, *Energetic components VirD4, VirB11 and VirB4 mediate early DNA transfer reactions required for bacterial type IV secretion.* Mol Microbiol, 2004. **54**(5): p. 1199-211.

2. Backhed, F., et al., *Host-bacterial mutualism in the human intestine.* Science, 2005. **307**(5717): p. 1915-20.

3. Barondess, J.J. and J. Beckwith, *bor gene of phage lambda, involved in serum resistance, encodes a widely conserved outer membrane lipoprotein.* J Bacteriol, 1995. **177**(5): p. 1247-53.

4. Batut, P., et al., *High-fidelity promoter profiling reveals widespread alternative promoter usage and transposon-driven developmental gene expression.* Genome Res, 2013. **23**(1): p. 169-80.

5. Bohne, A., et al., *Transposable elements as drivers of genomic and biological diversity in vertebrates.* Chromosome Res, 2008. **16**(1): p. 203-15.

6. Bondy-Denomy, J. and A.R. Davidson, *When a virus is not a parasite: the beneficial effects of prophages on bacterial fitness.* J Microbiol, 2014. **52**(3): p. 235-42.

7. Bonheyo, G., et al., *Transfer Region of a Bacteroides Conjugative Transposon, CTnDOT.* Plasmid, 2001. **45**(1): p. 41-51.

8. Bonheyo, G.T., et al., *Transfer region of a Bacteroides conjugative transposon contains regulatory as well as structural genes.* Plasmid, 2001. **46**(3): p. 202-9.

9. Brookfield, J.F.Y., *Mobile DNAs: The Poacher Turned Gamekeeper.* Current Biology, 2003. **13**(21): p. R846-R847.

10. Burrus, V. and M.K. Waldor, *Shaping bacterial genomes with integrative and conjugative elements.* Res Microbiol, 2004. **155**(5): p. 376-86.

11. Carattoli, A., *Plasmids and the spread of resistance.* Int J Med Microbiol, 2013. **303**(6-7): p. 298-304.

12. Chalopin, D., et al., *Comparative analysis of transposable elements highlights mobilome diversity and evolution in vertebrates.* Genome Biol Evol, 2015. **7**(2): p. 567-80.

13. Champoux, J.J., *DNA topoisomerases: structure, function, and mechanism.* Annu Rev Biochem, 2001. **70**: p. 369-413.

14. Cheng, Q., et al., *Integration and excision of a Bacteroides conjugative transposon, CTnDOT.* J Bacteriol, 2000. **182**(14): p. 4035-43.

15. Cheng, Q., et al., *Identification of genes required for excision of CTnDOT, a Bacteroides conjugative transposon.* Mol Microbiol, 2001. **41**(3): p. 625-32.

16. Cheng, Q., et al., *Development of an in vitro integration assay for the Bacteroides conjugative transposon CTnDOT.* J Bacteriol, 2002. **184**(17): p. 4829-37.

17. Comstock, L.E. and M.J. Coyne, *Bacteroides thetaiotaomicron: a dynamic, niche-adapted human symbiont.* Bioessays, 2003. **25**(10): p. 926-9.

18. Dichiara, J.M., A.N. Mattis, and J.F. Gardner, *IntDOT interactions with core- and arm-type sites of the conjugative transposon CTnDOT.* J Bacteriol, 2007. **189**(7): p. 2692-701.

19. DiChiara, J.M., A.A. Salyers, and J.F. Gardner, *In vitro analysis of sequence requirements for the excision reaction of the Bacteroides conjugative transposon, CTnDOT.* Mol Microbiol, 2005. **56**(4): p. 1035-48.

20. Ding, H. and M.F. Hynes, *Plasmid transfer systems in the rhizobia.* Can J Microbiol, 2009. **55**(8): p. 917-27.

21. Foster, T.J., et al., *Genetic organization of transposon Tn10.* Cell, 1981. **23**(1): p. 201-13.

22. Frost, L.S., et al., *Mobile genetic elements: the agents of open source evolution.* Nat Rev Microbiol, 2005. **3**(9): p. 722-32.

23. Fujimura, K.E. and S.V. Lynch, *Microbiota in allergy and asthma and the emerging relationship with the gut microbiome.* Cell Host Microbe, 2015. **17**(5): p. 592-602.

24. Furusawa, Y., Y. Obata, and K. Hase, *Commensal microbiota regulates T cell fate decision in the gut.* Semin Immunopathol, 2015. **37**(1): p. 17-25.

25. Gill, S.R., et al., *Metagenomic analysis of the human distal gut microbiome.* Science, 2006. **312**(5778): p. 1355-9.

26. Gilmore, M.S. and J.J. Ferretti, *Microbiology. The thin line between gut commensal and pathogen.* Science, 2003. **299**(5615): p. 1999-2002.

27. Gray, Y.H., *It takes two transposons to tango: transposable-element-mediated chromosomal rearrangements.* Trends Genet, 2000. **16**(10): p. 461-8.

28. Gyles, C. and P. Boerlin, *Horizontally transferred genetic elements and their role in pathogenesis of bacterial disease.* Vet Pathol, 2014. **51**(2): p. 328-40.

29. Halling, S.M., et al., *DNA sequence organization of IS10-right of Tn10 and comparison with IS10-left.* Proc Natl Acad Sci U S A, 1982. **79**(8): p. 2608-12.

30. Hecht, D.W., et al., *Characterization of BctA, a mating apparatus protein required for transfer of the Bacteroides fragilis conjugal element BTF-37.* Res Microbiol, 2007. **158**(7): p. 600-7.

31. Heffron, F., et al., *DNA sequence analysis of the transposon Tn3: three genes and three sites involved in transposition of Tn3.* Cell, 1979. **18**(4): p. 1153-63.

32. Ilangovan, A., S. Connery, and G. Waksman, *Structural biology of the Gram-negative bacterial conjugation systems.* Trends Microbiol, 2015. **23**(5): p. 301-10.

33. Johnson, C.M. and A.D. Grossman, *Integrative and Conjugative Elements (ICEs): What They Do and How They Work.* Annual Review of Genetics, 2015. **49**(1): p. 577-601.

34. Keeton, C.M. and J.F. Gardner, *Roles of Exc protein and DNA homology in the CTnDOT excision reaction.* J Bacteriol, 2012. **194**(13): p. 3368-76.

35. Keeton, C.M., et al., *Interactions of the excision proteins of CTnDOT in the attR intasome.* Plasmid, 2013. **70**(2): p. 190-200.

36. Kim, S. and J.F. Gardner, *Resolution of Holliday junction recombination intermediates by wild-type and mutant IntDOT proteins.* J Bacteriol, 2011. **193**(6): p. 1351-8.

37. Krinos, C.M., et al., *Extensive surface diversity of a commensal microorganism by multiple DNA inversions.* Nature, 2001. **414**(6863): p. 555-8.

38. Laprise, J., S. Yoneji, and J.F. Gardner, *Homology-dependent interactions determine the order of strand exchange by IntDOT recombinase.* Nucleic Acids Res, 2010. **38**(3): p. 958-69.

39. Laprise, J., S. Yoneji, and J.F. Gardner, *IntDOT interactions with core sites during integrative recombination.* J Bacteriol, 2013. **195**(9): p. 1883-91.

40. Lewis, J.A. and G.F. Hatfull, *Control of directionality in integrase-mediated recombination: examination of recombination directionality factors (RDFs) including Xis and Cox proteins.* Nucleic Acids Res, 2001. **29**(11): p. 2205-16.

41. Ley, R.E., et al., *Obesity alters gut microbial ecology.* Proc Natl Acad Sci U S A, 2005. **102**(31): p. 11070-5.

42. Ley, R.E., et al., *Microbial ecology: human gut microbes associated with obesity.* Nature, 2006. **444**(7122): p. 1022-3.

43. Li, W., et al., *Mechanism of tetracycline resistance by ribosomal protection protein Tet(O).* Nat Commun, 2013. **4**: p. 1477.

44. Malanowska, K., A.A. Salyers, and J.F. Gardner, *Characterization of a conjugative transposon integrase, IntDOT.* Mol Microbiol, 2006. **60**(5): p. 1228-40.

45. Malanowska, K., et al., *CTnDOT integrase performs ordered homology-dependent and homology-independent strand exchanges.* Nucleic Acids Res, 2007. **35**(17): p. 5861-73.

46. Mazmanian, S.K., et al., *An Immunomodulatory Molecule of Symbiotic Bacteria Directs Maturation of the Host Immune System.* Cell, 2005. **122**(1): p. 107-118.

47. Moon, K., et al., *Regulation of excision genes of the Bacteroides conjugative transposon CTnDOT.* J Bacteriol, 2005. **187**(16): p. 5732-41.

48. Nash, H.A., *Integration and excision of bacteriophage lambda: the mechanism of conservation site specific recombination.* Annu Rev Genet, 1981. **15**: p. 143-67.

49. Nikolich, M.P., N.B. Shoemaker, and A.A. Salyers, *A Bacteroides tetracycline resistance gene represents a new class of ribosome protection tetracycline resistance.* Antimicrob Agents Chemother, 1992. **36**(5): p. 1005-12.

50. Park, J. and A.A. Salyers, *Characterization of the Bacteroides CTnDOT regulatory protein RteC.* J Bacteriol, 2011. **193**(1): p. 91-7.

51. Peed, L., A.C. Parker, and C.J. Smith, *Genetic and functional analyses of the mob operon on conjugative transposon CTn341 from Bacteroides spp.* J Bacteriol, 2010. **192**(18): p. 4643-50.

52. Rabel, C., et al., *The VirB4 family of proposed traffic nucleoside triphosphatases: common motifs in plasmid RP4 TrbE are essential for conjugation and phage adsorption.* J Bacteriol, 2003. **185**(3): p. 1045-58.

53. Ramakrishna, B.S., *Role of the gut microbiota in human nutrition and metabolism.* J Gastroenterol Hepatol, 2013. **28 Suppl 4**: p. 9-17.

54. Rankin, D.J., E.P. Rocha, and S.P. Brown, *What traits are carried on mobile genetic elements, and why?* Heredity (Edinb), 2011. **106**(1): p. 1-10.

55. Rhee, K.J., et al., *Role of commensal bacteria in development of gut-associated lymphoid tissues and preimmune antibody repertoire.* J Immunol, 2004. **172**(2): p. 1118-24.

56. Ringwald, K. and J. Gardner, *The Bacteroides thetaiotaomicron protein Bacteroides host factor A participates in integration of the integrative conjugative element CTnDOT into the chromosome.* J Bacteriol, 2015. **197**(8): p. 1339-49.

57. Rotger, R. and J. Casadesus, *The virulence plasmids of Salmonella.* Int Microbiol, 1999. **2**(3): p. 177-84.

58. Salyers, A.A., et al., *Conjugative transposons: an unusual and diverse set of integrated gene transfer elements.* Microbiol Rev, 1995. **59**(4): p. 579-90.

59. Schandel, K.A., M.M. Muller, and R.E. Webster, *Localization of TraC, a protein involved in assembly of the F conjugative pilus.* J Bacteriol, 1992. **174**(11): p. 3800-6.

60. Schippa, S. and M.P. Conte, *Dysbiotic events in gut microbiota: impact on human health.* Nutrients, 2014. **6**(12): p. 5786-805.

61. Stevens, A.M., et al., *Genes involved in production of plasmidlike forms by a Bacteroides conjugal chromosomal element share amino acid homology with two-component regulatory systems.* J Bacteriol, 1992. **174**(9): p. 2935-42.

62. Stevens, A.M., et al., *Tetracycline regulation of genes on Bacteroides conjugative transposons.* J Bacteriol, 1993. **175**(19): p. 6134-41.

63. Sutanto, Y., et al., *Factors required in vitro for excision of the Bacteroides conjugative transposon, CTnDOT.* Plasmid, 2004. **52**(2): p. 119-30.

64. Sutanto, Y., et al., *Characterization of Exc, a novel protein required for the excision of Bacteroides conjugative transposon.* Mol Microbiol, 2002. **46**(5): p. 1239-46.

65. Thierauf, A., G. Perez, and A.S. Maloy, *Generalized transduction.* Methods Mol Biol, 2009. **501**: p. 267-86.

66. Tinsley, C.R., E. Bille, and X. Nassif, *Bacteriophages and pathogenicity: more than just providing a toxin?* Microbes Infect, 2006. **8**(5): p. 1365-71.

67. Vica Pacheco, S., O. Garcia Gonzalez, and G.L. Paniagua Contreras, *The lom gene of bacteriophage lambda is involved in Escherichia coli K12 adhesion to human buccal epithelial cells.* FEMS Microbiol Lett, 1997. **156**(1): p. 129-32.

68. Wagner, A., *Cooperation is fleeting in the world of transposable elements.* PLoS Comput Biol, 2006. **2**(12): p. e162.

69. Wang, Y., et al., *Translational control of tetracycline resistance and conjugation in the Bacteroides conjugative transposon CTnDOT.* J Bacteriol, 2005. **187**(8): p. 2673-80.

70. Wang, Y., N.B. Shoemaker, and A.A. Salyers, *Regulation of a Bacteroides operon that controls excision and transfer of the conjugative transposon CTnDOT.* J Bacteriol, 2004. **186**(9): p. 2548-57.

71. Waters, J.L. and A.A. Salyers, *The small RNA RteR inhibits transfer of the Bacteroides conjugative transposon CTnDOT.* J Bacteriol, 2012. **194**(19): p. 5228-36.

72. Waters, J.L., G.R. Wang, and A.A. Salyers, *Tetracycline-related transcriptional regulation of the CTnDOT mobilization region.* J Bacteriol, 2013. **195**(24): p. 5431-8.

73. Wexler, H.M., *Bacteroides: the good, the bad, and the nitty-gritty.* Clin Microbiol Rev, 2007. **20**(4): p. 593-621.

74. Whittle, G., N.B. Shoemaker, and A.A. Salyers, *Characterization of genes involved in modulation of conjugal transfer of the Bacteroides conjugative transposon CTnDOT.* J Bacteriol, 2002. **184**(14): p. 3839-47.

75. Wood, M.M., et al., *CTnDOT integrase interactions with attachment site DNA and control of directionality of the recombination reaction.* J Bacteriol, 2010. **192**(15): p. 3934-43.

76. Wood, M.M. and J.F. Gardner, *The Integration and Excision of CTnDOT.* Microbiol Spectr, 2015. **3**(2): p. Mdna3-0020-2014.

77. Xu, J., et al., *A genomic view of the human-Bacteroides thetaiotaomicron symbiosis.* Science, 2003. **299**(5615): p. 2074-6.

78. Xu, J. and J.I. Gordon, *Honor thy symbionts.* Proc Natl Acad Sci U S A, 2003. **100**(18): p. 10452-9.

1.8 Figures

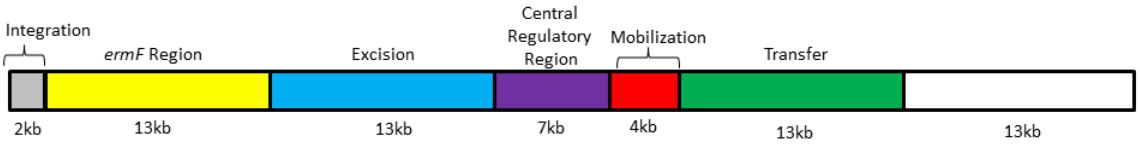

Figure 1.1: CTnDOT Overview. Schematic representation of the different functional regions of the 65 kbp CTnDOT element.

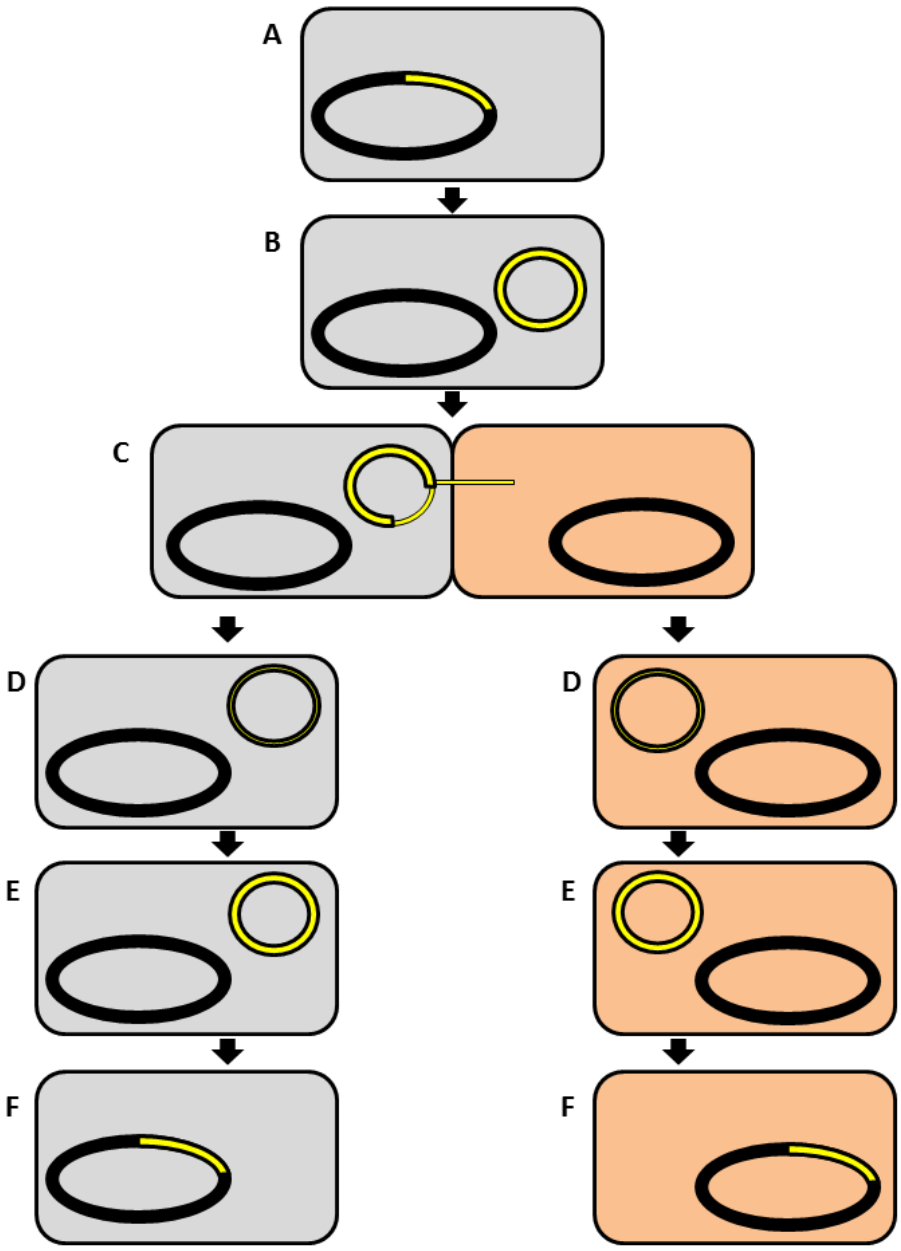

Figure 1.2: Propagation of CTnDOT. (A) CTnDOT can be stably maintained within the *Bacteroides* chromosome. (B) When stimulated CTnDOT can excise from the host chromosome and form a plasmid-like intermediate. (C) A single strand of the excised CTnDOT may then be transferred to a recipient cell. (D) Once transfer is complete, both the host and recipient cells contain a single stranded copy of CTnDOT. (E) CTnDOT undergoes replication to become double stranded. (F) CTnDOT may then integrate into the chromosome of the host and recipient cells. The host cell is shaded gray, while the recipient cell is shaded orange and CTnDOT is represented in yellow.

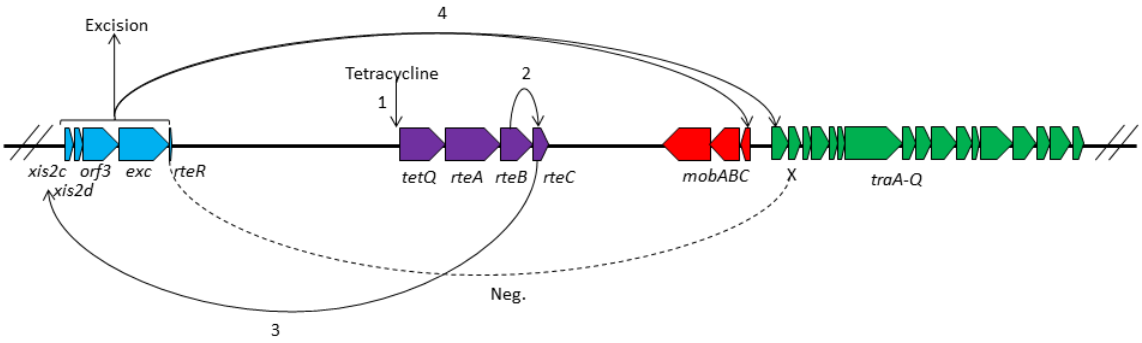

Figure 1.3: Regulation of CTnDOT. CTnDOT is positively regulated by tetracycline exposure. Presence of tetracycline upregulates the translation of the *tetQ-rteA-rteB* operon(1). RteB activates the transcription of *rteC* (2). RteC activates the transcription of the excision operon (3). The excision operon is responsible for activating the transcription of both the mobilization and transfer operons (4). When tetracycline is absent the small RNA *rteR* represses the transcription of the transfer operon (Neg.).

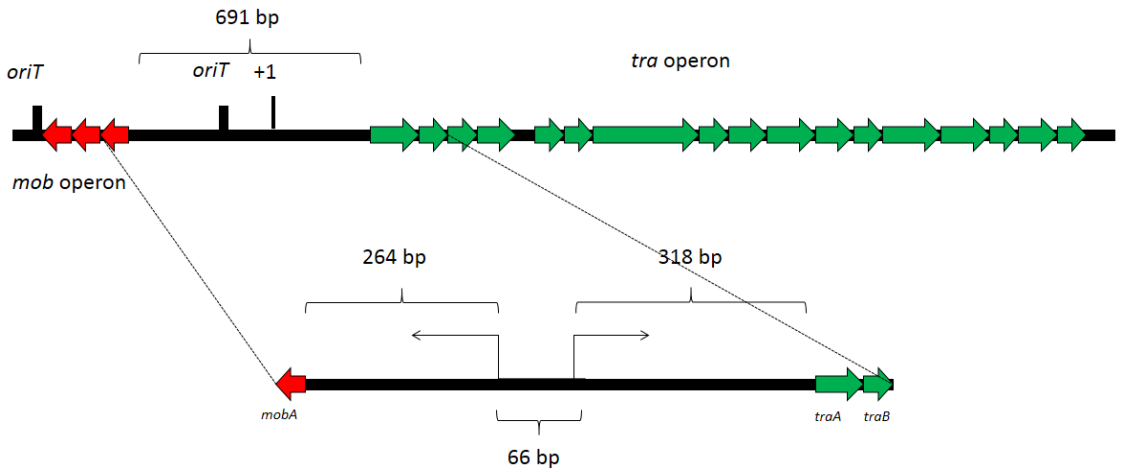

Figure 1.4: Layout of the mobilization and transfer operons. The mobilization operon (purple) is 264 bp away from the *mob* promoter and the transfer operon is 318 bp away from the *tra* promoter. The two promoters are themselves 66 bp away from each other, and they direct transcription in opposite directions (indicated by arrows).

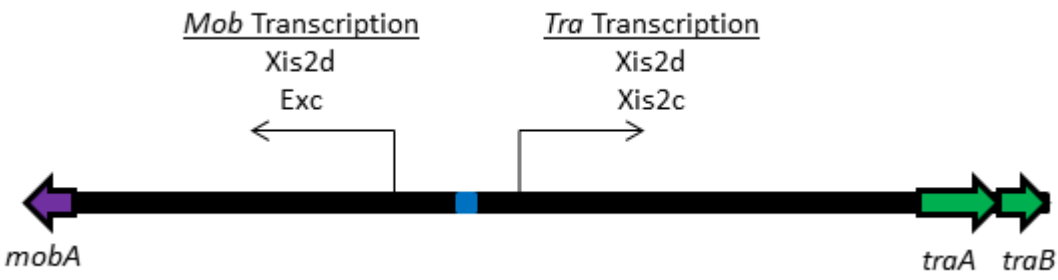

Figure 1.5: Excision Proteins Regulate Transcription of *mob* and *tra* Operons. The proteins encoded by the excision operon form alternative complexes to activate the transcription of other operons. The Xis2d and Exc proteins both contribute to the activation of the *mob* operon, while Xis2d works with Xis2c work together to activate the transcription of the *tra* operon.

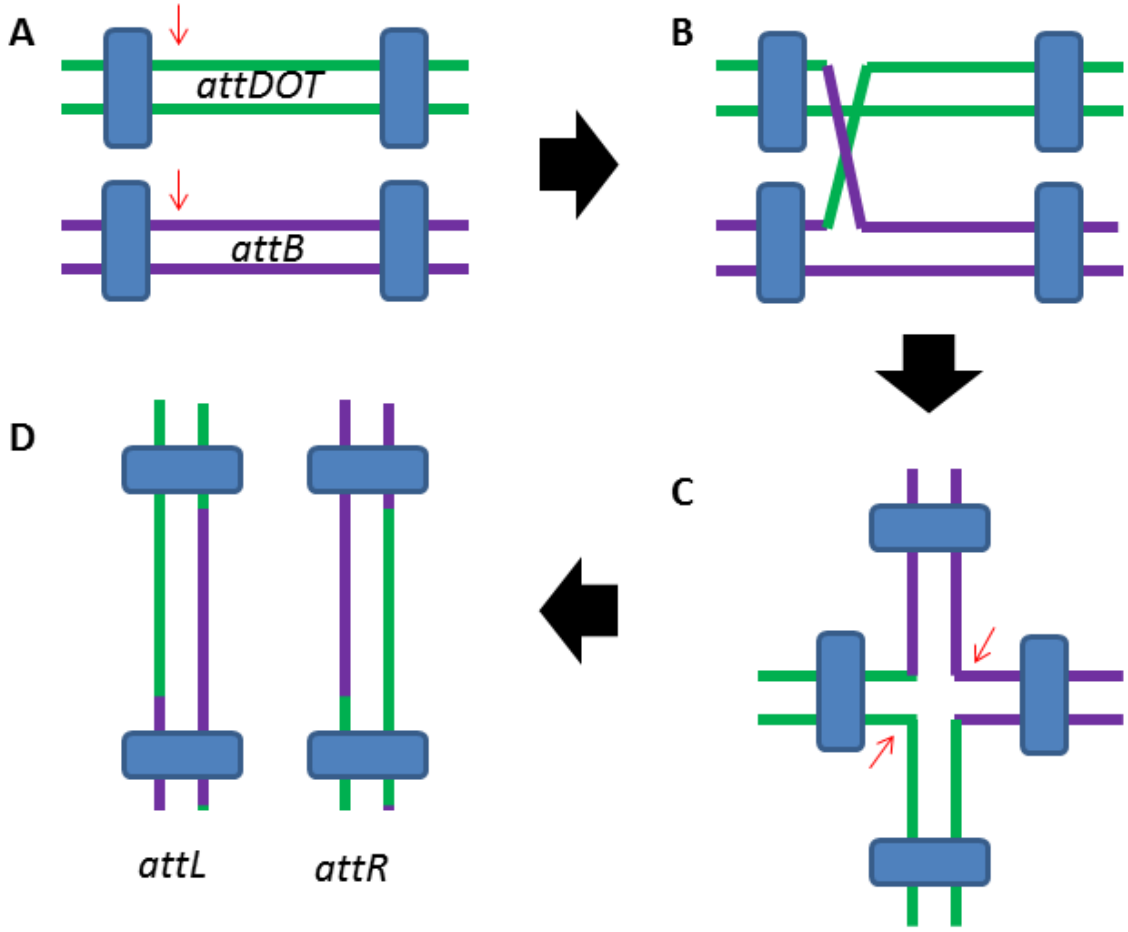

Figure 1.6: Overview of Integration. (A) Two monomers of IntDOT bind to each of the DNA substrates (*attDOT* and *attB*) and the top strands of each DNA substrate are nicked. (B) The nicked strands are swapped and ligated together. (C) This results in the formation of a Holliday junction intermediate. The bottom strands of the DNA substrates are then nicked by IntDOT. (D) The nicked strands are swapped and ligated together, resulting in the formation of the *attL* and *attR* products. IntDOT monomers are represented by blue rectangles. The DNA that originated from *attDOT* is green, while the DNA that originated from *attB* is purple. DNA nicking is represented by red arrows.

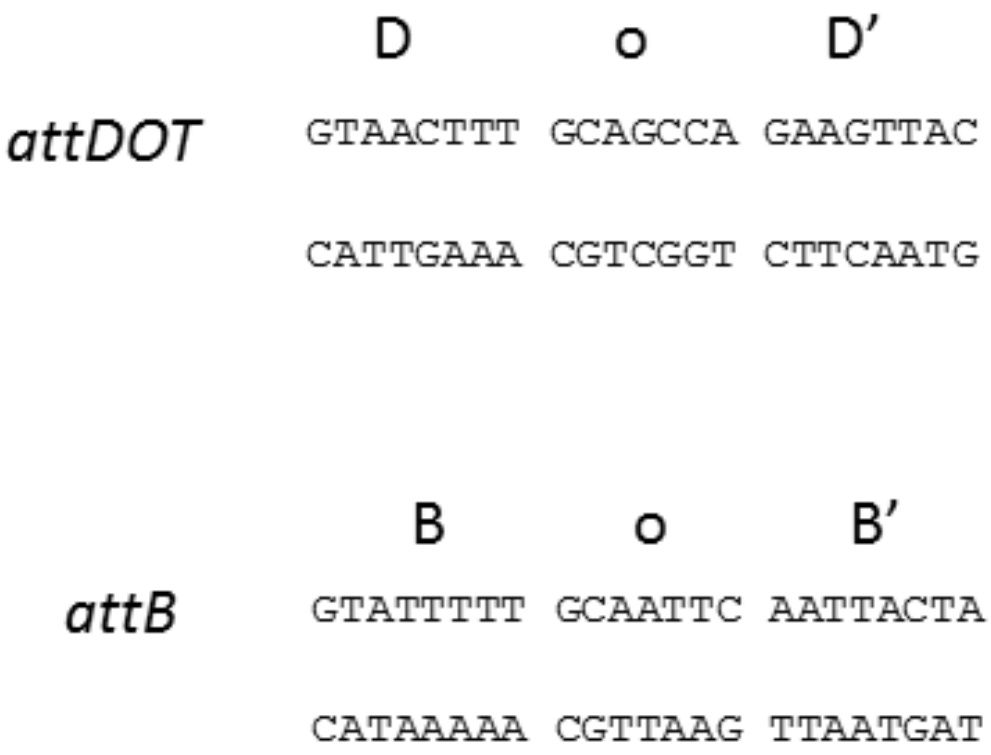

Figure 1.7: Overview of *attDOT* and *attB* sequences. The attachment sites for the chromosomal insertion site (*attB*) and the joined ends of CTnDOT (*attDOT*) are each comprised of two core binding sites (D, D', B, B') where the core binding domain of IntDOT binds. These core binding sites flank a seven nucleotide overlap region where the strand exchange occurs. In CTnDOT the first two nucleotides are conserved, but the last five nucleotides in the overlap region can be heterologous.

CHAPTER 2: THE XIS2D PROTEIN OF CTNDOT BINDS TO THE INTERGENIC REGION BETWEEN THE *MOB* AND *TRA* OPERONS

2.1 Abstract

CTnDOT is a 65 kbp integrative and conjugative element (ICE) that carries genes encoding both tetracycline and erythromycin resistances. The Excision operon of this element encodes Xis2c, Xis2d, and Exc proteins involved in the excision of CTnDOT from host chromosomes. These proteins are also required in the complex transcriptional regulation of the divergently transcribed transfer (*tra*) and mobilization (*mob*) operons of CTnDOT. Transcription of the *tra* operon is positively regulated by Xis2c and Xis2d, whereas, transcription of the *mob* operon is positively regulated by Xis2d and Exc. Xis2d is the only protein that is involved in the excision reaction, as well as the transcriptional regulation of both the *mob* and *tra* operons. This paper helps establish how Xis2d binds the DNA in the *mob* and *tra* region. Unlike other excisionase proteins, Xis2d binds a region of dyad symmetry. The binding site is located in the intergenic region between the *mob* and *tra* promoters, and once bound Xis2d induces a bend in the DNA. Xis2d binding to this region could be the preliminary step for the activation of both operons. Then the other proteins, like Exc, can interact with Xis2d and form higher order complexes.

2.2 Introduction

Bacteroides sp. are prevalent members of the human gut microbiome [5]. The predominance of these organisms in the gastrointestinal tract makes them an ideal reservoir for horizontal gene transfer, as many harbor integrative and conjugative elements (ICEs) that carry antibiotic resistance genes. *Bacteroides* sp. may initiate

genetic transfer of these elements to other members of the gut microbiome, or to bacteria that pass through the gastrointestinal tract [23]. This leads to the potential for significant dissemination of antibiotic resistances to a variety of bacteria. One well characterized ICE is the 65 kb CTnDOT, which carries both erythromycin and tetracycline resistance genes. CTnDOT and related elements are prevalent within the population.
In the 1990s, the *tetQ* gene carried by CTnDOT and related elements was detected in about 80% of *Bacteroides* isolates collected from both individuals with a *Bacteroides* infection and healthy volunteers [26].

Normally, CTnDOT is found integrated within the host chromosome and is passively replicated when cellular chromosomal replication occurs. Under favorable conditions CTnDOT excises from the chromosome and forms a non-replicating double-stranded circular intermediate. Once this circle is nicked at the *oriT* site, a single-stranded copy is transferred to the recipient cell via conjugation. Once inside the recipient cell, the single-stranded copy is re-circularized and replicated before integration into the recipient chromosome [24, 25, 34]. This transfer of CTnDOT DNA into a recipient cell is controlled by a highly complex regulatory cascade that is stimulated by tetracycline (Figure 2.1) [32].

Transfer is initiated by tetracycline-induced expression of three regulatory proteins: TetQ, RteA, and RteB [28, 30, 31]. TetQ is a tetracycline ribosomal protection protein, while RteA and RteB form a two component regulatory system. RteA functions as a sensor protein and RteB is a transcriptional activator of *rteC* expression [28]. RteC in turn activates the expression of the excision operon containing the *xis2c-xis2d-orf3-exc* genes [19, 20]. The first two genes in this operon, Xis2c and Xis2d, encode small, basic

proteins with helix-turn-helix motifs that bind DNA. They have been shown to function as excisionases by binding *attR* DNA to promote CTnDOT excision [11]. The function of *orf3* is unknown, as no phenotype is observed when *orf3* is deleted. Exc is a topoisomerase III, but the topoisomerase activity is not required for excision [29].

It is interesting to note that proteins expressed from the excision operon are not only involved in the excision reaction, they are also responsible for regulating transcription of the two divergently transcribed mobilization (*mob*) and transfer (*tra*) operons. Previous studies showed that Xis2c and Xis2d are involved in the transcriptional regulation of the *tra* operon, which consists of 17 genes (*traA-traQ*) encoding the mating apparatus of CTnDOT [9, 12, 35]. Deletion of either *orf3* or *exc* had no effect on the transcriptional regulation of the *tra* genes [12]. Recent studies showed that Xis2d and Exc are responsible for positively regulating the transcription of the *mob* operon [33]. The *mob* operon consists of three genes (*mobA-mobB-mobC*) that encode proteins in the relaxosome complex, which is responsible for transferring the CTnDOT DNA to the mating apparatus [21, 33]. Deletions of either *xis2c* or *orf3* have no effect on the transcriptional regulation of the *mob* genes [33].

The focus of this study is centered on Xis2d since it is involved in transcriptional activation of both the *mob* and *tra* operons. Prior to this study it was unclear where Xis2d interacts with DNA in the promoter region of these two operons to activate transcription. In this paper we show that Xis2d binds an area of dyad symmetry between the promoters of these two operons. Xis2d binding to this region is thought to be the initial step in the dual regulation of divergently transcribed operons, since Xis2d is required for the

positive regulation of both operons. Then additional proteins, like Exc, may be recruited to form higher order complexes.

2.3 Materials and Methods

Strains, Plasmids, and Growth Conditions

The bacterial strains and plasmids used in this study are listed in Table 2.1. *Escherichia coli* strains were grown aerobically in Luria-Bertani (LB) broth at 37°C, and supplemented with ampicillin (100 μg/ml) when appropriate.

Gel Filtration

The low molecular weight calibration kit (GE) was used as described by the manufacturer with a HiLoad 16/60 Superdex 75 pg column. The working concentration of Xis2d was 285 μM.

Electrophoretic Mobility Shift Assay (EMSA)

DNA substrates were amplified using primers listed in Table 2.2 and the resulting DNA products were purified by gel extraction as described by the manufacturer (Qiagen). Reactions were performed in 10 μL volumes containing 2 μL GSBA buffer [50 mM Tris-HCl (pH 8), 1 mM EDTA, 50 mM NaCl, 10% glycerol, and 0.01 mg/ml heparin] and the substrate DNA. Reactions were then incubated with indicated concentrations of protein for 20 min before samples are loaded onto a 6% DNA retardation gel (Invitrogen) running at 100 V/20 mA.

Gels were stained by shaking in 1X TBE-Sybergreen solution for 45 min and the DNA fragments were visualized using a transilluminator (Bio-Rad).

DNaseI Fluorescent Footprinting

A DNA substrate containing 235 bp of the transfer operon promoter region was amplified with a set of primers, with one primer containing a 5' 6-FAM label (Table 2.2). The reactions were conducted in 18 µl volumes consisting of 1 pmol DNA, 3 mM $CaCl_2$, 7 mM $MgCl_2$, 9.5% glycerol, 50 mM Tris-HCl pH 7.4, 250 µg/ml BSA, and 2 µL protein dilution buffer (50 mM Tris-HCl pH 7.4, 10% glycerol, 800 mM KCl, 2 mg/ml BSA). Reactions were incubated with indicated concentrations of protein for 30 min at room temperature. Then 2 µL of DNaseI (0.125 µg/ml) was added to each reaction and samples were allowed to digest for 1 min. The reactions were stopped by adding 1 volume of 0.5 M EDTA and were cleaned up using a PCR cleanup kit (Qiagen) and eluted with 30µl EB buffer. Capillary electrophoresis was performed by the Roy J. Carver Biotechnology Center, and results were analyzed using GeneMapper software. Identities of the protected bases were determined by matching the GeneMapper results with a chromatogram produced using Thermo Sequenase Dye Primer manual cycle sequencing kit (USB Corporation).

Protein Purification

The detailed procedures used in this study to purify Xis2d and Exc have been described previously [6, 10, 12]. To summarize the Xis2d and Exc proteins were overexpressed on pET-27b(+) in BL21 (DE3) pLysS *ihfA*$^-$ and purified over a heparin-agarose column. The identity of the proteins was confirmed by mass spectrometry (Roy J. Carver Biotechnology Center).

pBend Assay

The 138 bp *tra* fragment was cloned between direct repeats of polylinkers containing multiple restriction enzyme sites on pBend2 using primers Bend138-F and Bend138-R. Insertion of the 138 bp fragment in between the multiple restriction enzyme sites was confirmed by sequencing. DNA fragments made by single digestions of pBend138 with *MluI, Nhe I, Spe I, EcoRV, SmaI, NruI, RsaI,* and *BamHI* were the same size, but had different ends. DNA fragments were then used for EMSA analysis as described above.

2.4 Results

Xis2d is a Dimer

The amino acid sequence of Xis2d predicts that a monomer of Xis2d is 14052.2 Daltons. In order to determine whether Xis2d is a monomer or multimer we employed size exclusion chromatography. The results show that Xis2d has a non-denatured molecular weight of approximately 28 kDa (Figure 2.2), indicating that it is a dimer in solution.

Binding of Xis2d to DNA

A 681 bp fragment of DNA, containing the region between the mobilization operon and the divergently transcribed transfer operon, was divided into six different segments (A-F) to determine which regions are bound by Xis2d (Figure 2.3a). Fragment A contains the leader region of the *tra* operon, the *tra* promoter, and part of the *mob* promoter. When Xis2d was mixed with fragment A, a slower migrating complex was observed indicating that Xis2d binds to this region (Figure 2.3b). Because transcriptional activators often bind upstream of the transcription initiation start site (TIS), fragment A

was divided into two different fragments to separate the regions upstream and downstream of the *tra* TIS (fragments B and C, respectively). As expected, Xis2d was capable of binding the smaller upstream fragment C, but was unable to bind the downstream fragment B (Figure 2.3b). Additional DNA fragments containing more of the upstream *tra* TIS region were created to determine if Xis2d binds upstream DNA. Fragment D contains the *tra* promoter and the *mob* promoter, fragment E contains part of the *mob* promoter and the area immediately downstream from the *mob* promoter, and fragment F contains the *mob* leader region and an *oriT* of CTnDOT. Xis2d bound to fragment D, but not to fragments E and F (Figure 2.3b).

Xis2d binding is only detectible when the area within fragment C is present, suggesting that Xis2d binds specifically to a region within this fragment. To further validate that Xis2d specifically binds the region between the *tra* and *mob* promoters within CTnDOT, a DNA fragment from the *immI* region of phage P22 was used to determine if Xis2d was capable of binding non-specific DNA under the conditions used. As seen in Figure 2.3b, no binding was detected. Thus we conclude that Xis2d binds DNA specifically to a site within fragment C.

Because partially purified protein preparations were used in this study, empty vector controls were tested for each DNA fragment. The empty vector substrate is the extract collected after cells containing the expression vector pET27b were subjected to the purification protocol used to purify Xis2d. This ensures that any of the *E. coli* proteins that elute from the column with Xis2d are not responsible for the observed results. As can be seen in Figure 2.3c, the addition of the empty vector preparations did

not alter the migration of the different DNA substrates. This indicates that none of the *E. coli* proteins present in the preparation are binding the tested DNA fragments.

Of the DNA fragments tested, three (fragments A, C, D) were capable of binding Xis2d. The results in Figure 2.3 show experiments where Xis2d is present at only one concentration. Other excisionase proteins bind to multiple sites during the excision reaction. For example, when Lambda Xis and P22 Xis bind DNA several bands appear as the protein is diluted, representing different numbers of excisionase proteins bound to the DNA [2, 18]. To determine whether Xis2d also binds to multiple sites, we performed experiments using dilutions of Xis2d to determine if decreasing concentrations of the protein would reveal complexes of higher mobility. As seen in Figure 2.4, Xis2d shows a single shift when incubated with DNA, and that shift is observed as the protein is diluted. Since Xis2d shows a single band it suggests that either there is only a single Xis2d binding site in the *mob* and *tra* region, or multiple sites that bind Xis2d cooperatively.

Footprinting of Xis2d

In order to identify the location of the base pairs bound by Xis2d between the *mob* and *tra* promoters, footprint analyses were performed. Fragment D was used for footprinting since it contains 97 bp that Xis2d does not bind. This provides an internal control for analysis of the results, since the area within this region should not show a footprint. All DNA positions mentioned below are given relative to the *tra* TIS.

Protection in the presence of Xis2d was detected over a region of 45 bp on the top strand from positions -87 to -42 (Figure 2.5). The bottom strand showed a similar footprint of 47 bp with protection ranging from positions -94 to -47 (Figure 2.6). This

corresponds to the area between the *mob* and *tra* promoters. When Xis2d was diluted from 470 nM to 80 nM of protein, full protection was maintained until a dilution was reached (80 nM) where the protein no longer protected any of the DNA (Figure 2.5). This 45bp area of protection may be bound by a single Xis2d dimer, which would explain why the entire protected region has the same affinity for Xis2d.

Peaks of enhancement are present on the footprint of both the bottom strand and the top strand. On the top strand there is a large peak of enhancement seen at -61 and two smaller peaks of enhancement seen at -51 and -71. On the bottom strand there are enhancement peaks at -55/56, -75, and -86. These peaks are located approximately 10 bp apart, with the exception of the bottom strand where peaks -75 and -55/56 are separated by double that distance. When the lambda repressor binds to its operator sites, the DNA forms loops that result in a similar enhanced cleavage pattern as seen in the footprint of Xis2d [8]. It was proposed that DNA is wrapped around ^{Tn916}Xis when it showed a similar enhanced cleavage pattern, which suggests that the DNA between the transfer and mobilization operons may be wrapped around the Xis2d protein [1].

Scanning Mutagenesis

Some of the base pairs that are protected in the footprint assay may not interact specifically with Xis2d to mediate the binding. Some base pairs may be blocked from access by DNaseI, by interacting non-specifically with Xis2d, or by being wrapped around Xis2d. To identify base pairs that are required for Xis2d binding, systematic 9 bp substitution mutations were made along the entire length of the area protected in the footprint assay. Nucleotides targeted for mutation were changed to the complementary base and the mutations made are shown in Figure 2.7a. Three different concentrations of

Xis2d were used to determine the binding capabilities of each mutated fragment (Figure 2.7b).

There was no effect on Xis2d binding when the regions from positions -95 to -72 (fragments 1-4) and -50 to -42 (fragment 11) were mutated. This suggests that the region between positions -72 and -50 interacts with Xis2d. When the bases from positions -77 to -69 (fragment 5), -68 to -60 (fragment 7), and -55 to -47 (fragment 10) were mutated, Xis2d showed reduced binding affinity for the DNA substrate. When bases -59 to -51 (fragment 9) were mutated a minimal amount of binding was detectible, and no binding was detectible when bases from positions -73 to -65 (fragment 6), and -64 to -56 (fragment 8) were mutated.

The region where Xis2d binding was affected by mutation (-72 to -50) has a region of dyad symmetry from -51 to -66, which could be a Xis2d binding site. The regions in which sequence changes did not alter Xis2d binding (positions -95 to -72, and -50 to -42) may be involved in non-specific interactions with Xis2d because they were protected from cleavage by DNaseI in the footprint experiments.

DNA Bending by Xis2d

The size of the footprint for Xis2d is large for a single dimer. However, if Xis2d binds DNA like IHF, then bending of the DNA could increase the size of the footprint [22]. The excisionase proteins of other systems, such as lambda Xis and P22 Xis, are known to bend the DNA they bind [2, 18].

Fragment C (containing the *tra* promoter and half the *mob* promoter) was cloned into pBend2 between direct repeats containing multiple restriction sites, as described in

the Materials and Methods. The tandem multiple restriction sites move the position of the cloned DNA in relation to the ends of the DNA fragment, depending on which restriction enzyme is used (Figure 2.8a). If Xis2d does not bend the DNA the migration of the fragments generated by the different restriction enzymes would be equivalent.

As seen in Figure 2.8b Xis2d bends the DNA that it binds. The slowest migrating complex was generated by *SpeI*, indicating that this complex contains Xis2d bound to the middle of the fragment (Figure 2.8b). This places the center of the bend around positions -62 to -57. As summarized in Figure 2.9, this corresponds to the region in the Xis2d footprint where binding is lost when the DNA is mutated.

Xis2d and Exc Interaction

Both Xis2d and Exc are needed for the activation of the *mob* operon. Exc does not bind specifically to the DNA in the intergenic region of the *mob* and *tra* operons (Figure 2.10). To determine if Exc interacts with Xis2d in this region an EMSA with both proteins was performed. Fragment D was incubated with 90 nM Xis2d and increasing concentrations of Exc were added. As seen in Figure 2.11, a supershift was observed at higher concentrations of Exc (1.5 to 6.0 μM). This indicates that Exc interacts with Xis2d. Since the topoisomerase function of Exc is not needed for the excision reaction, it is possible that Exc serves more of a structural role, and that it interacts with Xis2d through protein-protein interactions [29].

2.5 Discussion

Once the CTnDOT element excises from the chromosome, it is mobilized and transferred to a recipient cell. All three of these functions are needed for successful propagation of the element. Thus, it is understandable that the same protein (Xis2d) is

involved in performing and regulating all of these processes. While previous studies examined the role of Xis2d in the excision reaction, less was known about the role of Xis2d in the expression of the *tra* and *mob* operons.

This paper establishes that the Xis2d protein binds specifically to the region upstream of the *tra* and *mob* promoters in CTnDOT. Because Xis2d is a dimer, the simplest model would be that it recognizes a sequence with dyad symmetry. By scanning the region that this study shows to be important for Xis2d binding, an area of dyad symmetry was revealed that resembled Xis2d binding sites in the *attR* region of CTnDOT (Figure 2.12). In addition to the similarity to *attR* binding sites, the center of the bend induced by Xis2d binding is in the middle of this dyad symmetry. Therefore, the dyad symmetry in the *tra* and *mob* intergenic region was designated XD. Upon closer inspection the *attR* D1 and D2 sites also exhibit partial dyad symmetry, but the right sides of the dyads show weak conservation. Alignment of XD to the D1 and D2 sites of *attR* shows a consensus of GGCRNN(A/W)C (Figure 2.13).

In earlier work it was shown that mutations in the DNA upstream of the *tra* promoter affected transcription of the transfer genes. Mutating the DNA to the complement from positions -72 to -66 or -64 to -58 abolished detectible transcription of a *traA::uidA* fusion when CTnERL, a closely related element to CTnDOT, was provided *in trans* [12]. That previous work did not determine which of the excision proteins bound to the regions containing these mutations. From work done in this study, it is clear that both of these mutations eliminate the left half of the XD dyad symmetry (Figure 2.12). In the previous study Xis2d was still able to bind mutations made from -72 to -66 and -64 to -58, so Xis2d was able to bind by recognizing the right half of the XD symmetry.

However, without the intact XD site Xis2d is unable to make the appropriate contacts to activate *tra* transcription.

The binding pattern of Xis2d is different from other members of the excisionase family. ^{Tn916}Xis binds to three different sites, each one containing a 5' AT rich region and a 3' conserved binding sequence [1]. Two of these sites are located on *attL* and are involved in promoting excision, while the other is located on *attR* and prevents excision at high ^{Tn916}Xis concentrations [4, 7]. It has been proposed that ^{Tn916}Xis binds the sites cooperatively at high concentrations of protein [1]. The P22, L5, and Pukovnik Xis proteins bind a series of four direct repeats in what appears to be a head to tail arrangement [15, 18, 27]. Of these three Xis proteins, the Pukovnik Xis has been shown to form a filament [27]. Since L5 and P22 Xis are similar to Pukovnik Xis it is possible that they also form a similar filament. The P2 cox protein has several binding sites in a variety of arrangements depending on the target DNA and it has also been shown to form filaments [3]. In the Lambda *attR* site, a filament is formed by two Xis proteins binding specifically to a set of direct repeats, with another Xis binding non-specifically between the others [2]. There are no crystal structures for any of the proteins involved in CTnDOT integration or excision. Therefore, we cannot rule out the possibility that Xis2d is forming filaments that bind to DNA.

Xis2d is unusual because it participates in the excision reaction and is also involved in transcriptional activation of the *mob* and *tra* operons. No other ICE excisionases have been shown to have a similar dual functionality. However, the phage P2 cox protein is functionally similar to Xis2d. The cox protein is an excisionase that serves as a repressor of the P_c promoter on the P2 element, and also as an activator of the

P_{LL} promoter on the phage P4 [3, 14]. It has not been determined whether Xis2d is also able to regulate the promoters of unrelated elements.

Other known ICEs use a single excisionase protein. CTnDOT is unique since it contains an entire excision operon that encodes proteins that serve multiple functions. Xis2d is involved in multiple aspects of CTnDOT regulation and the other proteins of the excision operon appear to work with Xis2d to form elaborate multifunctional complexes. For example, while Exc does not appear to bind DNA in a sequence specific manner, it does appear to interact with Xis2d to form a complex that stimulates the transcription of the *mob* operon. To activate *tra* operon transcription both Xis2c and Xis2d are needed. Unfortunately Xis2c is unstable in our hands, but the strong structural similarity to Xis2d suggests that it binds DNA in a similar manner. Xis2c and Xis2d may form a complex that activates *tra* operon transcription.

Gaining an understanding of how Xis2d contributes to the regulation of these CTnDOT promoters is a preliminary step in unlocking the complexity of this system. Since the promoters of the *mob* and *tra* operons are separated by only 66 bp, and Xis2d is needed for the transcriptional regulation of both operons, it is possible that the initial step in the activation of P_{tra} and P_{mob} is the binding of Xis2d to the XD site. Then other required proteins can be recruited to drive transcription in either direction for the activation of the *mob* and *tra* operons.

2.6 Acknowledgements

We would like to thank Margaret Wood for technical instruction and assistance. This work was funded by the National Institutes of Health, grants AI 22383 and GM 28717.

2.7 References

1. Abbani, M., M. Iwahara, and R.T. Clubb, *The structure of the excisionase (Xis) protein from conjugative transposon Tn916 provides insights into the regulation of heterobivalent tyrosine recombinases.* J Mol Biol, 2005. **347**(1): p. 11-25.

2. Abbani, M.A., et al., *Structure of the cooperative Xis-DNA complex reveals a micronucleoprotein filament that regulates phage lambda intasome assembly.* Proc Natl Acad Sci U S A, 2007. **104**(7): p. 2109-14.

3. Berntsson, R.P., et al., *Structural insight into DNA binding and oligomerization of the multifunctional Cox protein of bacteriophage P2.* Nucleic Acids Res, 2014. **42**(4): p. 2725-35.

4. Connolly, K.M., M. Iwahara, and R.T. Clubb, *Xis protein binding to the left arm stimulates excision of conjugative transposon Tn916.* J Bacteriol, 2002. **184**(8): p. 2088-99.

5. Costello, E.K., et al., *Bacterial community variation in human body habitats across space and time.* Science, 2009. **326**(5960): p. 1694-7.

6. Dichiara, J., *DNA-Protein Interactions in the CTnDOT Excisive Intasome*, in *Microbiology*. 2006, University of Illinois Urbana-Champaign: Urbana, Illinois.

7. Hinerfeld, D. and G. Churchward, *Xis protein of the conjugative transposon Tn916 plays dual opposing roles in transposon excision.* Mol Microbiol, 2001. **41**(6): p. 1459-67.

8. Hochschild, A. and M. Ptashne, *Cooperative binding of λ repressors to sites separated by integral turns of the DNA helix.* Cell, 1986. **44**(5): p. 681-687.

9. Jeters, R.T., et al., *Tetracycline-associated transcriptional regulation of transfer genes of the Bacteroides conjugative transposon CTnDOT.* J Bacteriol, 2009. **191**(20): p. 6374-82.

10. Keeton, C.M. and J.F. Gardner, *Roles of Exc protein and DNA homology in the CTnDOT excision reaction.* J Bacteriol, 2012. **194**(13): p. 3368-76.

11. Keeton, C.M., et al., *Interactions of the excision proteins of CTnDOT in the attR intasome.* Plasmid, 2013. **70**(2): p. 190-200.

12. Keeton, C.M., et al., *The excision proteins of CTnDOT positively regulate the transfer operon.* Plasmid, 2013. **69**(2): p. 172-179.

13. Kim, J., et al., *Bending of DNA by gene-regulatory proteins: construction and use of a DNA bending vector*. Gene, 1989. **85**(1): p. 15-23.

14. Lewis, J.A. and G.F. Hatfull, *Control of directionality in integrase-mediated recombination: examination of recombination directionality factors (RDFs) including Xis and Cox proteins.* Nucleic Acids Res, 2001. **29**(11): p. 2205-16.

15. Lewis, J.A. and G.F. Hatfull, *Control of directionality in L5 integrase-mediated site-specific recombination.* J Mol Biol, 2003. **326**(3): p. 805-21.

16. Li, L.Y., N.B. Shoemaker, and A.A. Salyers, *Location and characteristics of the transfer region of a Bacteroides conjugative transposon and regulation of transfer genes.* J Bacteriol, 1995. **177**(17): p. 4992-9.

17. Maloy, S.R. and J. Gardner, *Dissecting nucleic acid-protein interactions using challenge phage.* Methods Enzymol, 2007. **421**: p. 227-49.

18. Mattis, A.N., R.I. Gumport, and J.F. Gardner, *Purification and characterization of bacteriophage P22 Xis protein.* J Bacteriol, 2008. **190**(17): p. 5781-96.

19. Moon, K., et al., *Regulation of excision genes of the Bacteroides conjugative transposon CTnDOT.* J Bacteriol, 2005. **187**(16): p. 5732-41.

20. Park, J. and A.A. Salyers, *Characterization of the Bacteroides CTnDOT regulatory protein RteC.* J Bacteriol, 2011. **193**(1): p. 91-7.

21. Peed, L., A.C. Parker, and C.J. Smith, *Genetic and functional analyses of the mob operon on conjugative transposon CTn341 from Bacteroides spp.* J Bacteriol, 2010. **192**(18): p. 4643-50.

22. Rice, P.A., et al., *Crystal structure of an IHF-DNA complex: a protein-induced DNA U-turn.* Cell, 1996. **87**(7): p. 1295-306.

23. Salyers, A.A., A. Gupta, and Y. Wang, *Human intestinal bacteria as reservoirs for antibiotic resistance genes.* Trends Microbiol, 2004. **12**(9): p. 412-6.

24. Salyers, A.A., N.B. Shoemaker, and L.Y. Li, *In the driver's seat: the Bacteroides conjugative transposons and the elements they mobilize.* J Bacteriol, 1995. **177**(20): p. 5727-31.

25. Salyers, A.A., et al., *Conjugative transposons: an unusual and diverse set of integrated gene transfer elements.* Microbiol Rev, 1995. **59**(4): p. 579-90.

26. Shoemaker, N.B., et al., *Evidence for extensive resistance gene transfer among Bacteroides spp. and among Bacteroides and other genera in the human colon.* Appl Environ Microbiol, 2001. **67**(2): p. 561-8.

27. Singh, S., et al., *The structure of Xis reveals the basis for filament formation and insight into DNA bending within a mycobacteriophage intasome.* J Mol Biol, 2014. **426**(2): p. 412-22.

28. Stevens, A.M., et al., *Tetracycline regulation of genes on Bacteroides conjugative transposons.* J Bacteriol, 1993. **175**(19): p. 6134-41.

29. Sutanto, Y., et al., *Characterization of Exc, a novel protein required for the excision of Bacteroides conjugative transposon.* Mol Microbiol, 2002. **46**(5): p. 1239-46.

30. Wang, Y., et al., *Translational control of tetracycline resistance and conjugation in the Bacteroides conjugative transposon CTnDOT.* J Bacteriol, 2005. **187**(8): p. 2673-80.

31. Wang, Y., N.B. Shoemaker, and A.A. Salyers, *Regulation of a Bacteroides operon that controls excision and transfer of the conjugative transposon CTnDOT.* J Bacteriol, 2004. **186**(9): p. 2548-57.

32. Waters, J.L. and A.A. Salyers, *Regulation of CTnDOT conjugative transfer is a complex and highly coordinated series of events.* MBio, 2013. **4**(6): p. e00569-13.

33. Waters, J.L., G.R. Wang, and A.A. Salyers, *Tetracycline-related transcriptional regulation of the CTnDOT mobilization region.* J Bacteriol, 2013. **195**(24): p. 5431-8.

34. Whittle, G. and A.A. Salyers, *Bacterial Transposons—An Increasingly Diverse Group of Elements,* in *Modern Microbial Genetics*. 2002, John Wiley & Sons, Inc. p. 385-427.

35. Whittle, G., N.B. Shoemaker, and A.A. Salyers, *Characterization of genes involved in modulation of conjugal transfer of the Bacteroides conjugative transposon CTnDOT.* J Bacteriol, 2002. **184**(14): p. 3839-47.

2.8 Tables and Figures

Table 2.1: Bacterial Strains and Plasmids

Strain or Plasmid	Relevant Phenotype	Description and/or reference
Strains		
DH5αMCR	RecA$^-$	Strain for plasmid maintenance and purification. (GibcoBRL)
BL21(DE3) pLysS *ihfA*$^-$	Cm^r	Novagen strain for overexpression of proteins with an *ihfA* gene deletion (J. Gardner, unpublished results)
Rosetta(DE3) pLysS *ihfA*$^-$	Cm^r	Novagen strain for overexpression of proteins containing rare codons with an *ihfA* gene deletion (M.Wood, unpublished results).
Plasmids		
pLYL72	Amp^r	Subclone of CTnDOT containing 18-kb transfer region, mobilization region, and *oriT* [16]
pGW40.5	Amp^r Cm^r	Translation fusion of *tra* promoter to *uidA* reporter gene[9]
pPY190	Amp^r	Contains the *immI* region of phage P22 [17]
pBend2	Amp^r	Contains two unique coding sites flanked by direct repeats of polylinkers containing multiple restriction enzyme sites [13]
pBend138	Amp^r	Contains the 138 bp *tra* fragment cloned into pBend1 (This study)
pET-27b(+)	Kan^r	Plasmid for protein overexpression (Novagen)

Table 2.2: Primers Used in this Study

Primer name	Sequence (5'- 3')
***Tra* and *mob* region:**	
Out-tra-shift-F	CCGTCAGGGGACGGATTGGG
Tra-promoter-F	GGTATCGGACAGATGCTTGACCC
In-tra-shift-F	CGTGCTGCCACTTGCTTGGG
In-tra-shift-R	GGTGTGCTTTCAGTCCTTCATCC
Out-tra-shift-R	CCGGTCACGGCAGCGTATTG
Up-tra-R	GCTTTAAGGGCGTAACTTTGCC
Leader-region-F	GGATGAAGGACTGAAAGCACACC
Bend138-F	GCAATGTCTAGACCGTCAGGGGACGG
Bend138-R	GCAATGGTCGACGGTGTGCTTTCAGTC
Non-specific DNA:	
Anti-Omnt	GATCATCTCTAGCCATGC
Intra-arc	CCGCTACCTTGCGTACCAAATCC

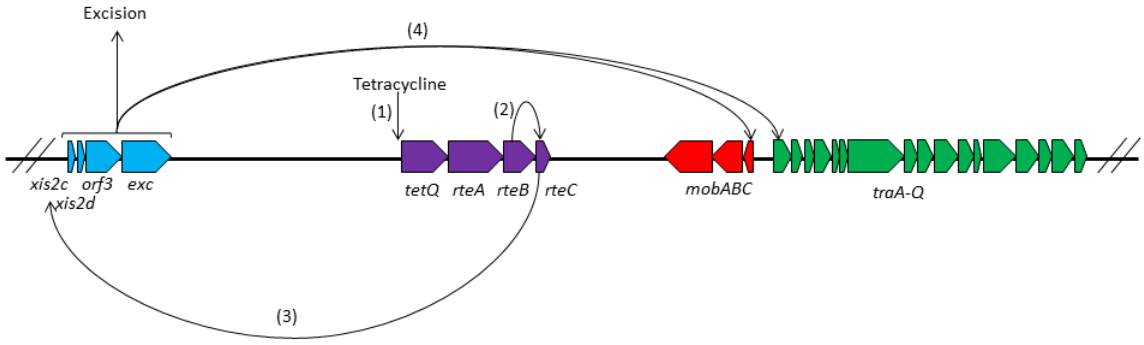

Figure 2.1: Summary of CTnDOT Regulatory Cascade. Upon exposure to tetracycline translation of the *tetQ-rteA-rteB* operon is stimulated. The RteB protein increases the transcription of *rteC*. RteC then acts upstream of the excision operon and increases transcription of that operon. The proteins in the excision operon are involved in excision of the CTnDOT element from the chromosome, as well as transcriptionally activating the divergently transcribed *mob* and *tra* operons.

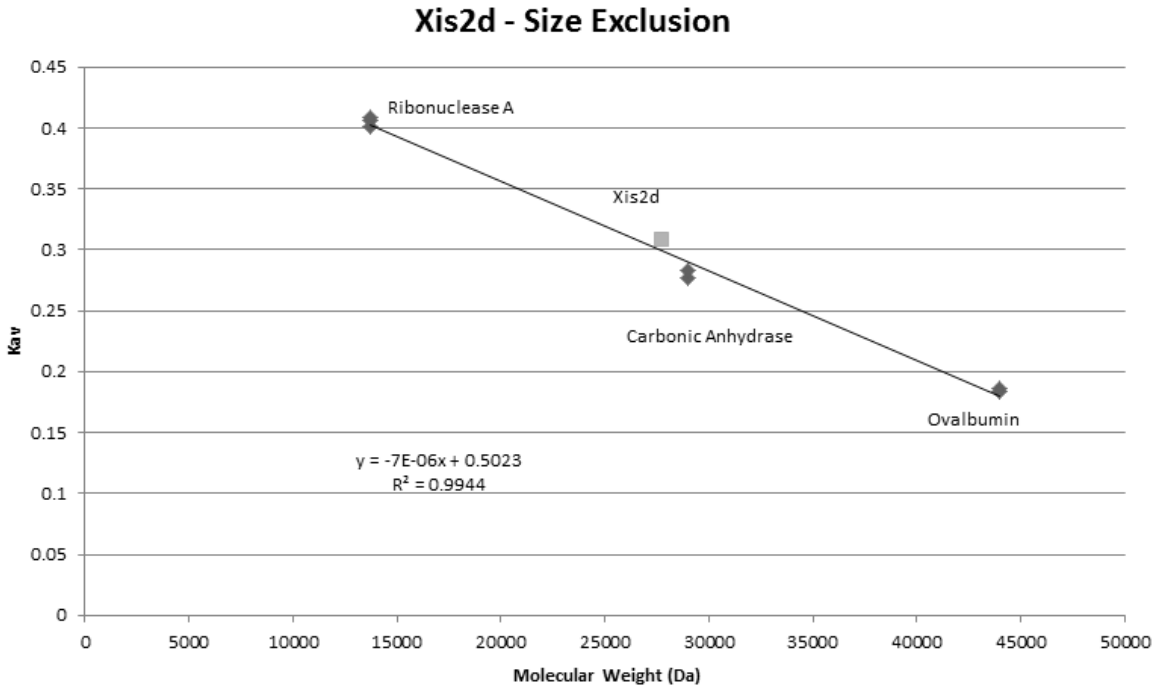

Figure 2.2: Size Exclusion Chromatography. The K_{av} values of Ribonuclease A, Carbonic Anhydrase, and Ovalbumin were plotted against the known molecular weights of the mentioned proteins to create a standard curve. Xis2d had a K_{av} value of 0.308, which corresponds to an approximate molecular weight of 28 kDa.

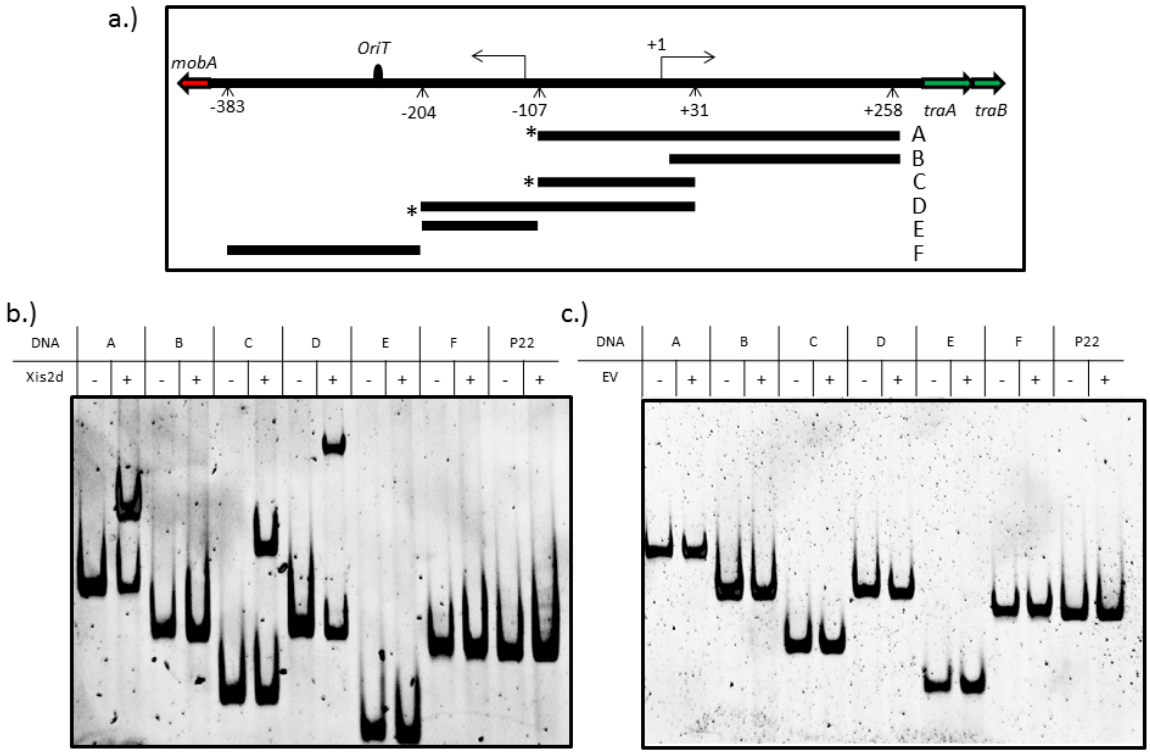

Figure 2.3: Xis2d Binding. (a) The upstream *tra* region was divided into six different fragments (A-F) to test for Xis2d binding capabilities. The transcription initiation start site for the *tra* operon is designated as +1 in this paper, with all mentioned positions in reference to this point. Arrows indicate the location of the promoters and the direction of transcription. A * indicates that binding was detected with the indicated fragment. (b) Electrophoretic mobility shift assay (EMSA) containing each DNA fragment being tested with (+) and without (-) the presence of Xis2d. The concentration of Xis2d was 400 nM. (c) EMSA containing each DNA fragment being tested with (+) and without (-) the presence of the Empty vector control.

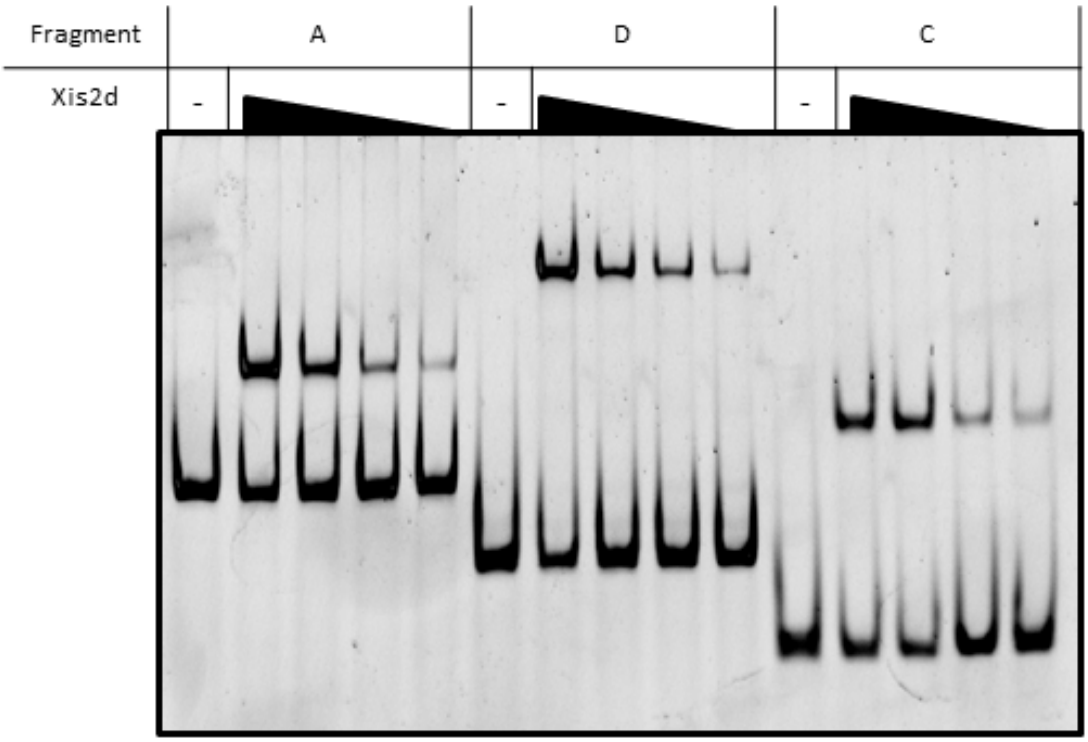

Figure 2.4: Xis2d Binding Dilutions. The three DNA fragments that interacted with Xis2d (Fragments A, C, and D) were tested with a range of Xis2d concentrations. The concentrations of Xis2d tested in this figure were 400 nM, 150 nM, 75 nM, and 40 nM.

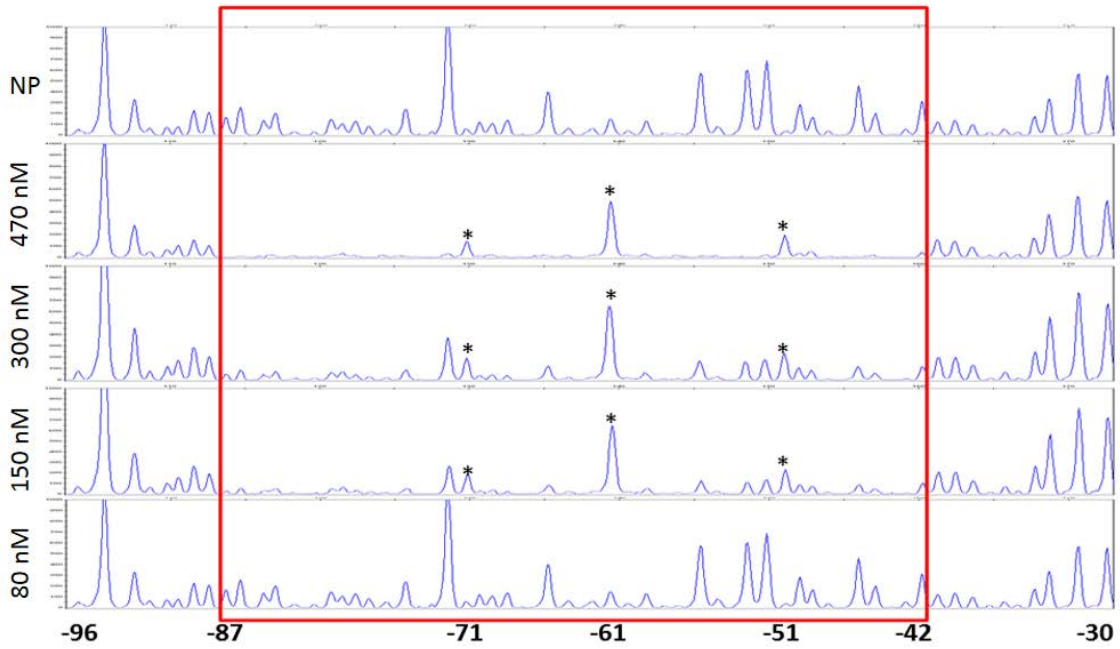

Figure 2.5: Xis2d Footprint. DNaseI footprint of Xis2d on the top strand of the 235 bp DNA fragment from position -96 to -30 relative to the *tra* TIS. The x-axis represents the length of the DNA fragment. The y-axis represents the florescent intensity, with the top of the scale set at 1000. The NP chromatogram is the no Xis2d control and the subsequent chromatograms show experiments performed with 470 nM, 300 nM, 150 nM, and 80 nM Xis2d. The red box highlights where footprints were observed, and the * symbol refers to peaks of enhanced cleavage.

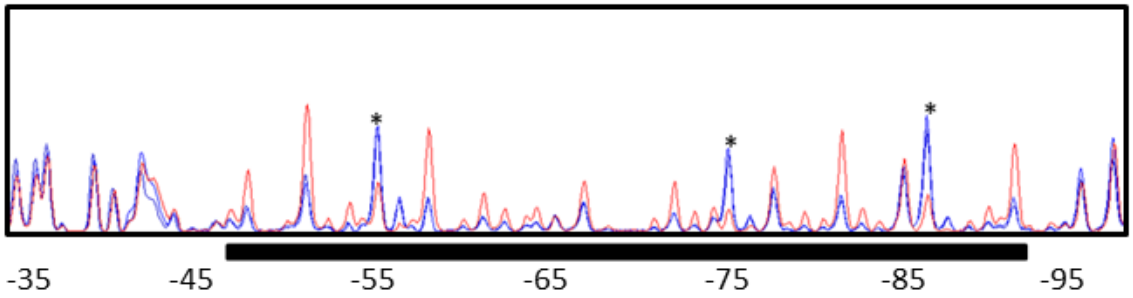

Figure 2.6: Xis2d Bottom Strand Footprint. DNaseI footprint of Xis2d on the bottom strand of fragment D from position -104 to -34 relative to the *tra* TIS. The x-axis represents the length of the DNA fragment. The y-axis represents the florescent intensity, with the top of the scale set at 1000. The red line represents the reaction without Xis2d present, while the blue lines represent the reaction in the presence of Xis2d. The black bar highlights where the footprint was observed, and the * symbol refers to peaks of enhanced cleavage. Xis2d concentration was 300 nM.

a.)

Fragment	Sequence	400 nM	100 nM
	-95 -85 -75 -65 -55 -45		
WT	ATGCTTGACCCGGTCAATGACTGCCAACCGGCGCAACGTGCTGCCACTTGCTTG	45%	3%
1	TACGAACTGCCGGTCAATGACTGCCAACCGGCGCAACGTGCTGCCACTTGCTTG	37%	3%
2	ATGCAACTGGGCCTCAATGACTGCCAACCGGCGCAACGTGCTGCCACTTGCTTG	34%	4%
3	ATGCTTGACGGCCAGTTAGACTGCCAACCGGCGCAACGTGCTGCCACTTGCTTG	37%	4%
4	ATGCTTGACCCGGAGTTACTGAGCCAACCGGCGCAACGTGCTGCCACTTGCTTG	32%	3%
5	ATGCTTGACCCGGTCAATCTGACGGTTCCGGCGCAACGTGCTGCCACTTGCTTG	**12%**	**1%**
6	ATGCTTGACCCGGTCAATGACTCGGTTGGCCCGCAACGTGCTGCCACTTGCTTG	**0%**	**0%**
7	ATGCTTGACCCGGTCAATGACTGCCAAGGCCGCGTTCGTGCTGCCACTTGCTTG	**15%**	**2%**
8	ATGCTTGACCCGGTCAATGACTGCCAACCGGGCGTTGCACCTGCCACTTGCTTG	**0%**	**0%**
9	ATGCTTGACCCGGTCAATGACTGCCAACCGGCGCAAGCACGACGGACTTGCTTG	**5%**	**0%**
10	ATGCTTGACCCGGTCAATGACTGCCAACCGGCGCAACGTGGACGGTGAAGCTTG	**13%**	**1%**
11	ATGCTTGACCCGGTCAATGACTGCCAACCGGCGCAACGTGCTGCCTGAACGAAC	39%	5%

b.)

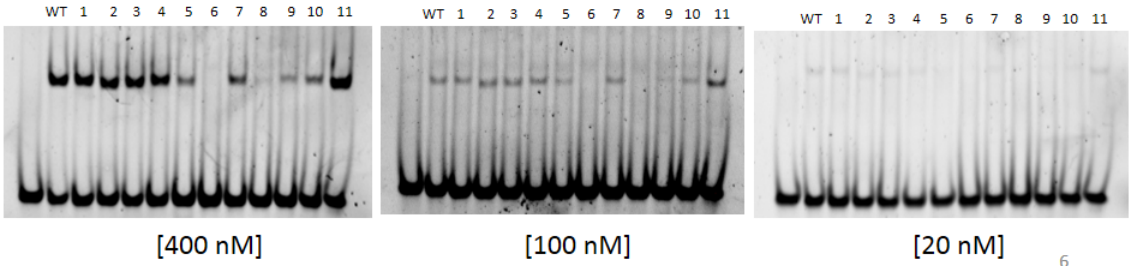

Figure 2.7: Scanning Mutagenesis. (a) The 54 bp region shown to be protected in the Xis2d footprint was sequentially mutated to the complement sequence to determine what regions of the fragment were important for binding. Red underlined bases highlight the area that was mutated in each fragment. The percentage of DNA shifted for different concentrations of Xis2d (400 nM and 100 nM) is reported to the right of each fragment. (b) EMSAs of the DNA fragments being tested with 400 nM, 100 nM, and 20 nM of Xis2d. The first lane of each EMSA is a DNA control and subsequent lanes correspond to each of the tested fragments listed in part a.

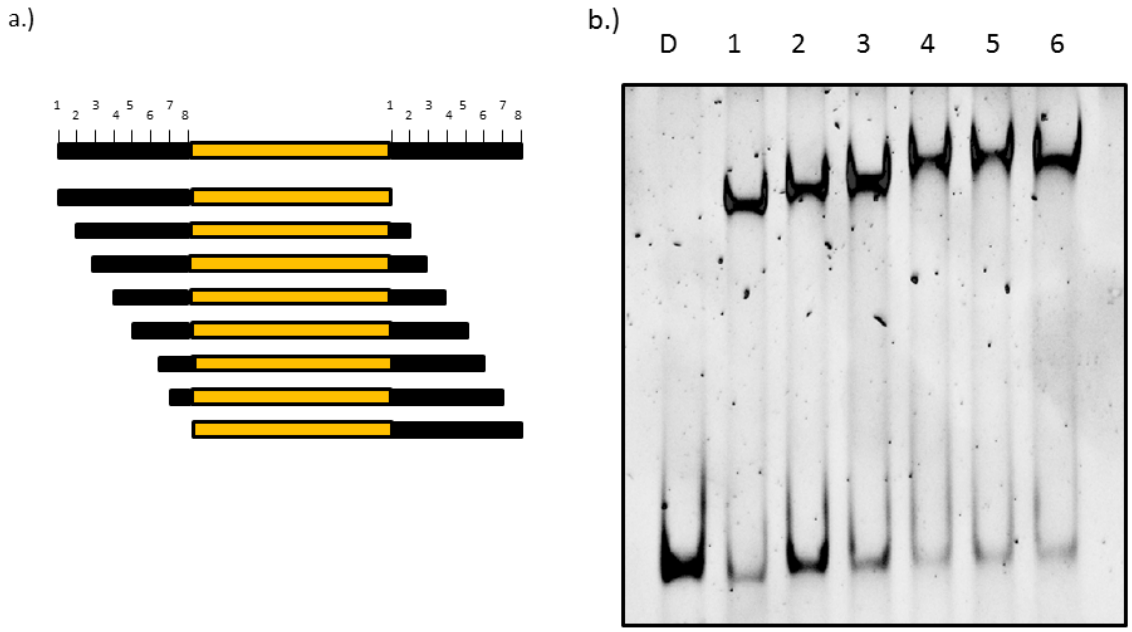

Figure 2.8: Xis2d Bending Assay. (a) Fragment D was cloned between direct repeats containing multiple restriction enzyme sites: MluI (1), NheI (2), SpeI (3), EcoRV (4), SmaI (5), NruI (6), RsaI (7), BamHI (8). Cutting with each of the restriction enzymes results in the Xis2d binding location shifting within the total fragment while retaining the overall fragment length. The *mob* and *tra* promoters are indicated by arrows, and the *tra* initiation start site is denoted as +1. (b) EMSA of Xis2d binding the different fragments from 5a. Lane "D" is a DNA control. Xis2d concentration was 400 nM.

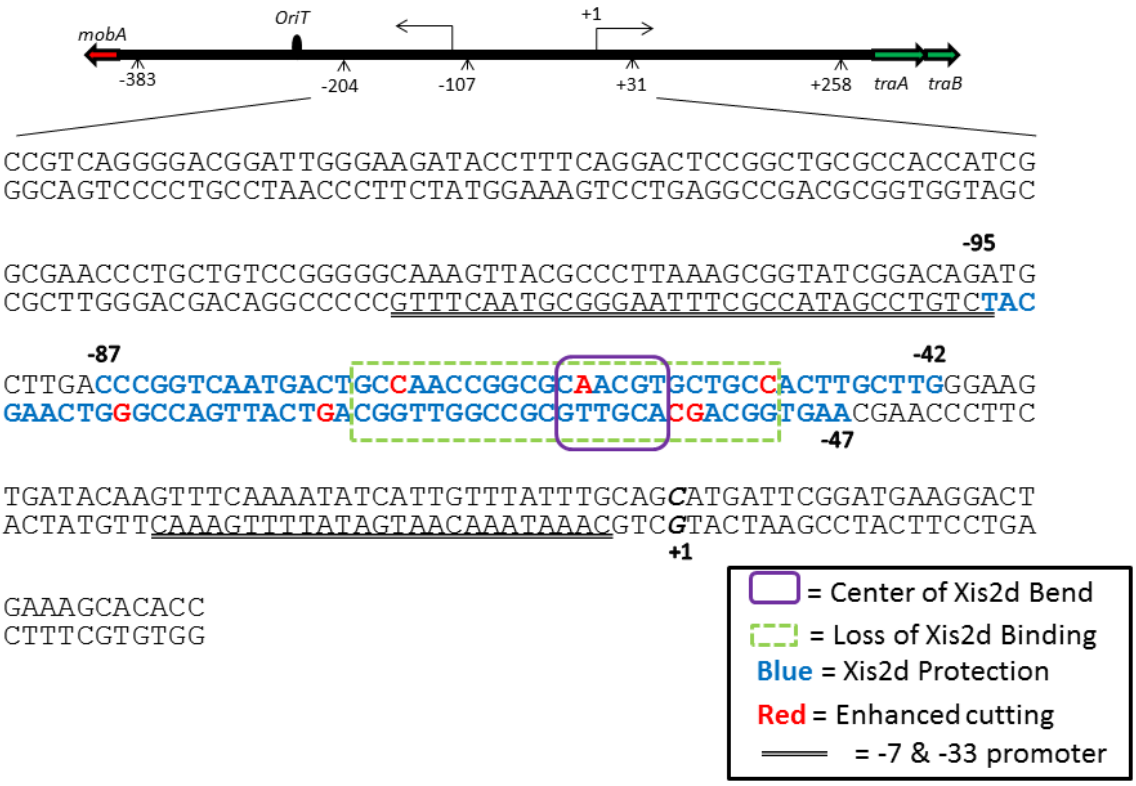

Figure 2.9: Summary of Xis2d Results. The sequence from positions -204 to +31 relative to the *tra* transcription initiation site (+1) is shown. The transcription initiation start site (+1) is bold/italicized and all noted positions are in reference to this point. The double underline bases span the -7 and -33 boxes of the *tra* and *mob* promoters. The bases in blue from positions -94 to -42 correspond to the bases that were protected in the footprinting assays when Xis2d was present. Of the protected bases those that are red correspond to areas where enhanced cutting was observed in the footprinting assays. The dashed green box encircles areas where Xis2d binding was lost when the sequence was mutated and the solid purple box indicates bases at the center of the bend induced by Xis2d binding.

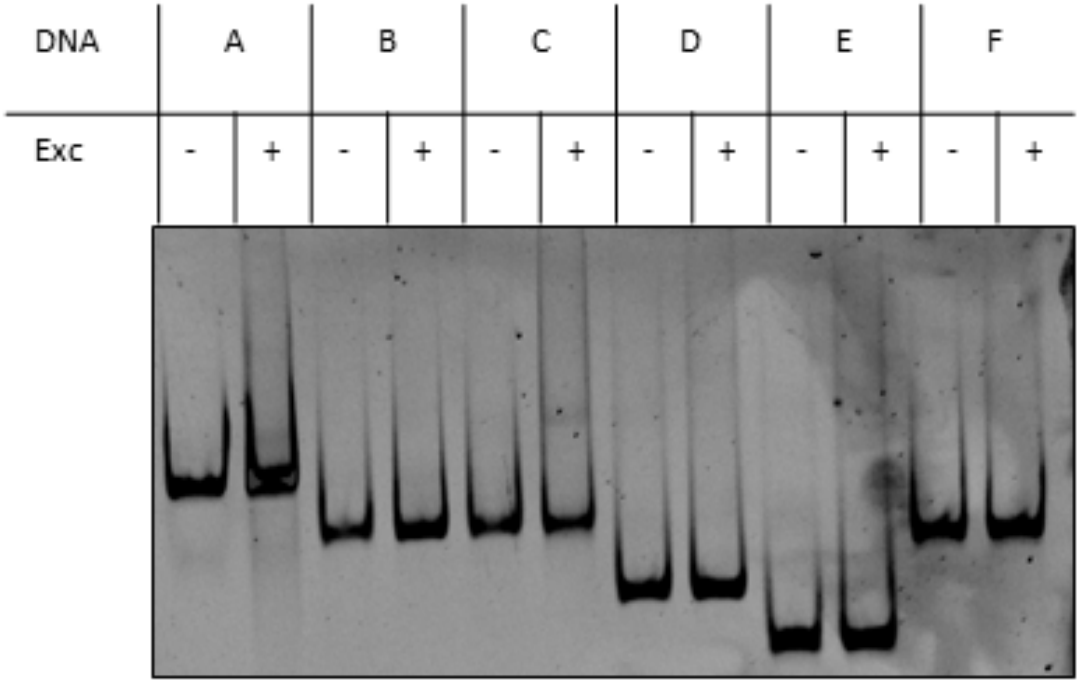

Figure 2.10: Exc Binding Results. The DNA fragments shown in Figure 3 (A-F) were tested with (+) and without (-) the presence of Exc. The concentration of Exc was 6.0 μM.

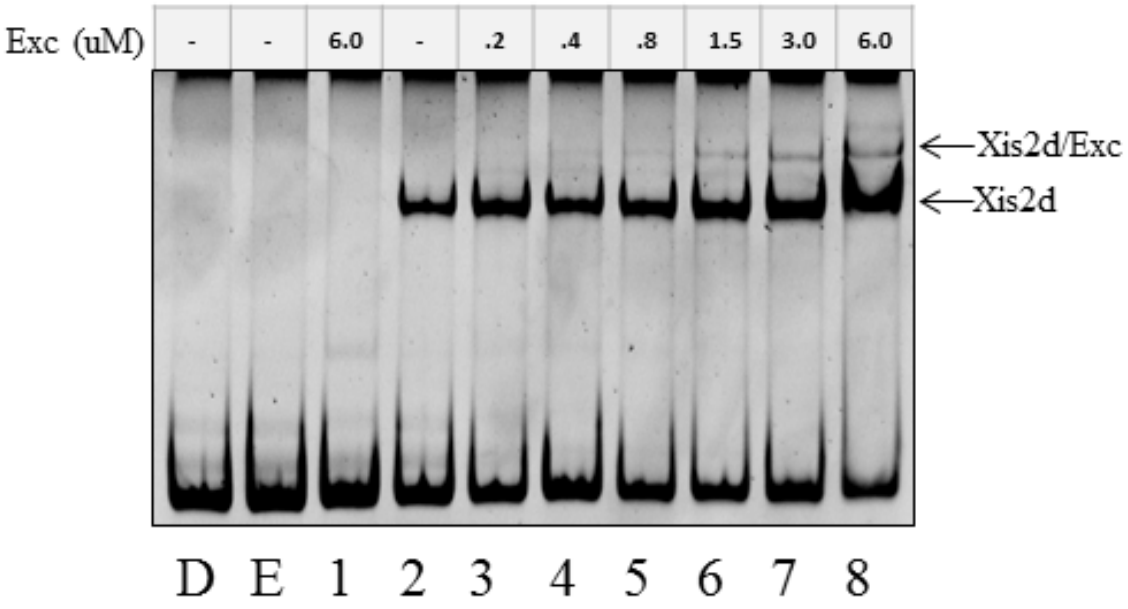

Figure 2.11: Xis2d and Exc Binding. Fragment D was incubated with Xis2d (0.09 uM) and increasing concentrations of Exc. Lane "D" is DNA control. Lane "E" is the empty vector control. Lane 1 is Exc alone (6 µM). Lane 2 is Xis2d alone (0.09 µM). Lanes 3-8 have the same concentration of Xis2d (0.09 +µM), but have increasing concentrations of Exc added. Concentrations of Exc listed in the table above the EMSA.

Figure 2.12: Xis2d Binds Dyad Symmetry. The dyad symmetry (XD) found in the intergenic region between the *tra* and *mob* operons compared to the Xis2d sites in the *attR* region (D1 and D2). The sequence shown for XD is from position -78 to -46. The underlined bases in the XD sequence comprise the dyad symmetry and the arrows designate the direction of the symmetry.

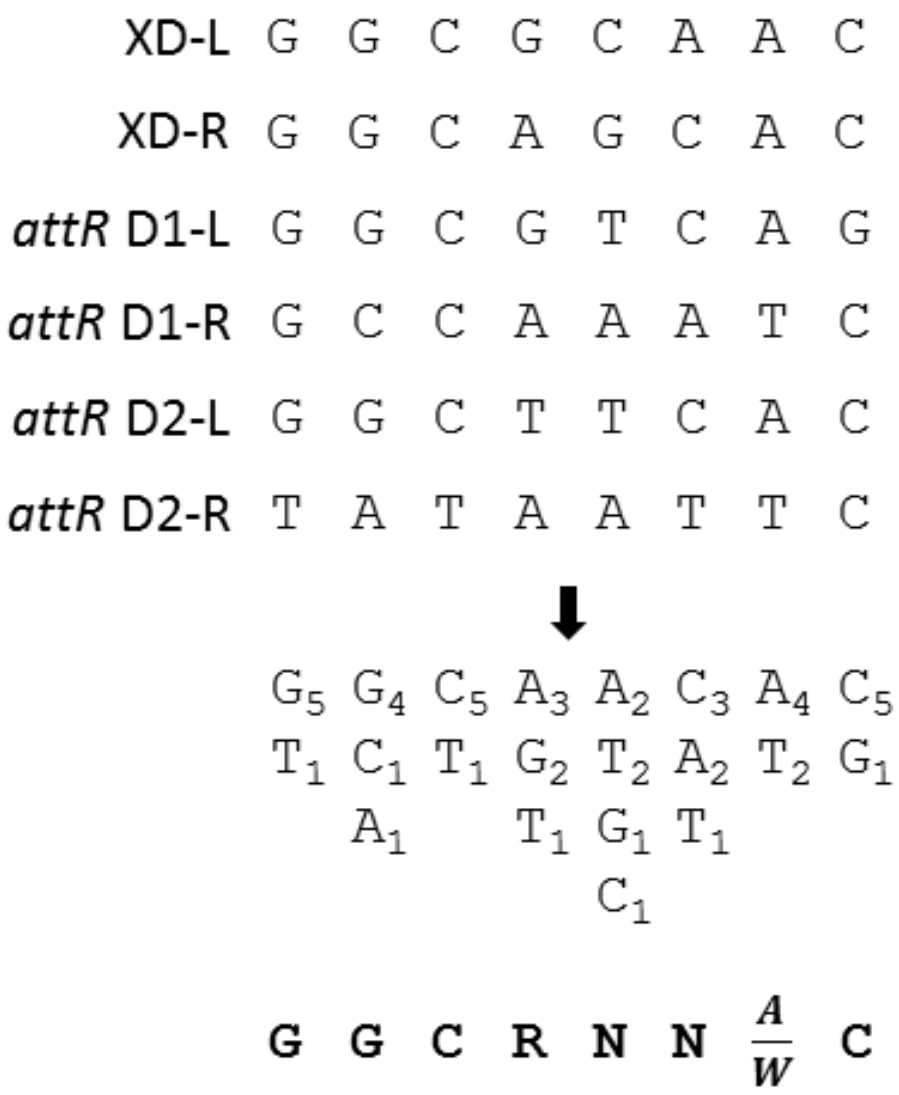

Figure 2.13: Xis2d Consensus Sequence. Alignment of the left (XD-L) and right (XD-R) halves of the XD dyad symmetry and the D1 (D1-L and D1-R) and D2 (D2-L and D2-R) sites of *attR*. A summary of the number of times of each nucleotide appears at a given position is shown below the sites. A consensus sequence is shown at the bottom.

CHAPTER 3: *IN VIVO* ANALYSIS OF CTNDOT EXCISION AND INTEGRATION

3.1 Abstract

CTnDOT is an integrative and conjugative element (ICE) that carries both erythromycin and tetracycline resistances. In order for this element to transfer itself to a new recipient cell, it must first excise itself from the host chromosome. Several studies have focused on studying the excision operon (*xis2c-xis2d-orf3-exc*), but many of these studies have provided conflicting results about how the different genes affect the excision reaction. This study quantifies excision levels *in vivo* by measuring the amounts of excision products (*attDOT* and *attB*) present. We found that the excision of CTnDOT was a rare occurrence, and that in-frame deletions of *xis2c*, *xis2d*, and *exc* reduced excision to background levels. Even the in-frame deletion of *orf3* showed a significant decrease in excision levels, which is the first detectable effect this gene has shown in any CTnDOT assay. This study also provided the first indication that the *orf2a* and *orf2b* genes, found upstream of the excision operon, contribute to the excision reaction. In particular, the addition of *orf2b* greatly increased the levels of excision. While the focus of this study is the excision of CTnDOT, the *in vivo* integration of CTnDOT was also studied and 18 alternative *attB* sites were identified.

3.2 Introduction

The *Bacteroides* genus has a proclivity for containing various arrays of mobile genetic elements. These elements often carry genes that increase the host's fitness in the unhospitable environment of the gastrointestinal tract. One of the best studied examples

of these types of elements is the integrative and conjugative element (ICE) named CTnDOT, which encodes resistances to both erythromycin and tetracycline.

CTnDOT can be maintained within a host cell, even when the selective pressure from antibiotics is removed from the environment. In the case of CTnDOT, excision from the host chromosome is regulated by the presence of tetracycline. CTnDOT contains *tetQ*, which encodes a ribosome protection resistance to tetracycline [16]. The presence of tetracycline initially stalls the ribosomes on the mRNA, which destabilizes a hairpin loop upstream of the *tetQ* promoter and increases the translation of TetQ and the regulatory proteins RteA and RteB [23, 26, 27]. The RteB protein then transcriptionally activates the regulatory gene *rteC*. RteC, in turn, transcriptionally activates the excision operon [17, 24]. The excision operon contains the genes *xis2c*, *xis2d*, *orf3*, and *exc*. The proteins encoded by the excision operon have been previously shown to contribute to the excision reaction, and serve as activators of the transfer (*tra*) and mobilization (*mob*) operons [3, 4, 8, 10, 11, 28, 29, 32]. The *xis2c* and *xis2d* genes encode small basic proteins that serve as recombination directionality factors (RDFs) for the excision reaction. These proteins, along with the host factor (BHFa), bind the ends of integrated CTnDOT (*attL* and *attR*) [10, 19]. The interaction between the RDFs and the integrase (IntDOT) facilitate the excision reaction.

As summarized in Figure 3.1, the excision reaction of CTnDOT consists of several sequential steps. When the element is integrated into the host chromosome it contains two attachment (*att*) sites, one on the left side (*attL*) and one on the right side (*attR*). Each attachment site contains core binding sites (B, D', B', or D), where the core binding domain of InDOT binds [7, 13]. The letter representing the core binding site

corresponds to origin of the DNA. If it originated from CTnDOT it is represented by the letter D, or if it originated from the *Bacteroides* chromosome it is represented with a B. Between the core binding sites there is a 7 bp overlap region (o) where the strand exchange occurs [14]. For CTnDOT the first two bases of the overlap region (GC) are conserved, however the remaining 5 bp can vary in sequence [14]. This is a unique feature since other known integrases, like lambda Integrase, require all bases in the overlap region to be conserved for excision to proceed [2].

Four IntDOT proteins likely bind to the DNA, one at each core binding site, and the *attL* and *attR* sequences are brought in close proximity to form a major complex known as an excision intasome [32]. Two of the IntDOT monomers nick the top strand of each overlap region, and the strands are exchanged to the partner site and ligated together [12]. This results in the formation of a structure known as a Holliday junction. Then the bottom strands of each overlap sequence are nicked by the other two IntDOT monomers, and the strands are exchanged and the products are ligated together [12]. This results in the formation of the *attDOT* sequence (D o D') and the *attB* sequence (B o B'). Since 5 bp in the overlap region (o) are not conserved, the resulting *attDOT* and *attB* sequences contain 5 bp of heterology when the sequences are initially formed. This heterology is fixed presumably through mismatch repair systems, and the final excised products are obtained.

Previous studies on CTnDOT excision have focused on determining how the excision proteins of CTnDOT contribute to the excision reaction. However, several of those studies have provided conflicting results with regards to the Exc protein. Previous *in vivo* studies using qualitative Southern blots indicated that Exc is required for

detection of the excised joined ends of the CTnDOT element, known as *attDOT* [4]. In contrast, *in vitro* studies suggested that Exc does not play an essential role in the excision reaction. An intermolecular assay was constructed using *attL* and *attR* on separate plasmids, which combine to form a single co-integrate plasmid containing *attDOT* and *attB* if the excision reaction was successful [25]. In this assay Exc was not required for the excised *attDOT* product to form. An intramolecular excision assay using *attL* and *attR* on a single plasmid with the *lacZα* gene cloned in-between detected excision by the loss of β-galactosidase activity [9]. In this assay Exc was shown to have a stimulatory effect on the excision reaction, however it was still non-essential for the excision reaction to occur.

This paper elucidates the contribution of each of the excision proteins in a quantitative *in vivo* excision assay. A qPCR assay was used to detect the amplification levels of *attDOT*, *attL/attR*, and *attB* with different combinations of excision proteins. $HiSeq_{2500}$ was also used to sequence CTnDOT samples that were un-induced and treated with tetracycline. The number of reads containing excised products was analyzed as an alternative way to detect excision. Additionally, the high-throughput sequencing gave insight into the integration of CTnDOT. Once CTnDOT excises itself from the chromosome it is possible for the element to use a different *attB* site for subsequent integration. In this study we have detected 18 new *attB* sites that CTnDOT has used for integration.

3.3 Materials and Methods

Strains, Plasmids, and Growth Conditions

The bacterial strains and plasmids used in this study are listed in Table 3.1. *Escherichia coli* strains were grown aerobically in Luria-Bertani (LB) media at 37°C with antibiotics when appropriate. *Bacteroides* strains were initially grown in PRAS chopped meat tubes (Remel) then sub-cultured into supplemented BHIS media at 37°C with appropriate antibiotics. Antibiotic concentration used: ampicillin (100 μg/ml), cefoxitin (15 μg/ml), chloramphenicol (10 μg/ml), erythromycin (10 μg/ml), gentamycin (200 μg/ml), kanamycin (50 μg/ml), tetracycline (1 μg/ml).

Hiseq$_{2500}$ Analysis

BT4007 was grown with and without tetracycline to three different stages: 0.3 OD_{650}, 0.6 OD_{650}, and overnight cultures. The DNA from each sample was extracted using DNeasy Blood and Tissue Kit (Qiagen). Standard shotgun libraries were constructed, and 160 nt paired-end sequencing was performed by the Roy J. Carver Biotechnology Center. The *attL*, *attR*, and *attDOT* sequences were found using junctionfinder_v2.sh script. The location of re-integration events was found using the search_new_attB.pl to map sequenced reads containing *attL/attR* to the VPI-5485 reference genome.

Construction of Excision Plasmids

To test how each of the excision genes effect excision levels, several plasmids containing various arrangements of the excision genes were constructed to be used in an *in vivo* excision assay. The following constructs were made using the indicated primers to amplify the excision region from plasmid pKSO1: pWTexcision [Excision-smaI-fwd,

Excision-smaI-rev], pWT+*orf2a-orf2b* [orf2a-ecoRI-fwd, Excision-ecoRI-rev], and pWT+*orf2b* [orf2B-ecoRI-fwd, Excision-ecoRI-rev]. To construct the plasmid containing the *orf3* deletion, the Excision-smaI-fwd and Excision-smaI-rev primers were used to amplify the excision region on plasmid pKS07. All resulting PCR products were then cloned into pAFD1. The in-frame deletions of *xis2c*, *xis2d*, and *exc* were constructed on pWTexcision using the lambda red recombination system using the strains, plasmids, and primers listed in Tables 3.1 and 3.2 [1, 5, 6, 18].

Construction of BT4001ΩQABCΩCefMinielement Strain

To test different excision plasmids *in vivo* a strain containing an integrated miniature form of CTnDOT was constructed. The pCefMinielement is based off of the plasmid pDJE2.3, which contains the IntDOT gene and the *attDOT* sequence. Sequencing of pDJE2.3 showed a point mutation in *intDOT* that ultimately changed an isoleucine to a valine residue. The QuikChangeII Kit (Agilent) was used with primers SDM-*intDOT*-fwd and SDM-*intDOT*-rev to regain the wild type sequence of *intDOT*. The resulting plasmid was named pWTMinielement. The resistance of this plasmid needed to be switched since both the excision plasmids and pWTMinielement encode resistance for erythromycin. Therefore, a Minielement that uses cefoxitin for selection was constructed. To construct pCefMinielement the primers Minielement-kpnI-fwd and Minielement-kpnI-rev were used to amplify the *intDOT* gene and *attDOT* sequence on plasmid pWTMinielement. The PCR product was then cloned into pGWA34.2 using the KpnI restriction site. The resulting plasmid, pCefMinielement, was transformed into the *E. coli* strain S17-1 and then mated into the *Bacteroides* strain BT4001ΩQABC using a bi-parental mating method[21]. The pGWA34.2 backbone of pCefMinielement is a

suicide vector, so it must integrate into the *Bacteroides* chromosome using *attDOT* and IntDOT in order to be maintained.

The location of the CefMinielement in the chromosome then needed to be determined for *attB* primer design. This was accomplished by incubating the chromosomal DNA of BT4001ΩQABCΩCefMinielement with EcoRI, which cuts once within the CefMinielement and infrequently within the *Bacteroides* chromosome. The digested DNA was ligated together and transformed into S17-1. Transformants that grew in the presence of ampicillin indicated that the *bla* gene within the backbone of pCefMinielement was present, and since EcoRI only cuts once within the CefMinielement the transformants must also contain the *attL* sequence. Sequencing of the chromosomal DNA flanking *attL* using primer L2 was performed to confirm the location of the integrated CefMinielement.

qPCR Excision Assay

The excision plasmid constructs were moved into the BT4001ΩQABC-ΩCefMinielement strain using a previously described mating assay [21]. The resulting strains were grown with and without tetracycline to three different stages: 0.3 OD_{650}, 0.6 OD_{650}, and overnight cultures. The DNA from each sample was extracted using DNeasy Blood and Tissue Kit (Qiagen). Quantitative PCR was performed using a Realplex2 Mastercycler (Eppendorf), with iTaq Universal SYBR Green Supermix (Bio-Rad) as a signal reporter. The sequences of primers used in this assay are listed in Table 2.2. The full length CTnDOT is integrated into a different *attB* site than the cefoxitin Minielement, which is why there are two sets of *attB* primers listed in Table 3.2. The *attL/attR* sequence was amplified using *attB*-fwd and *attDOT*-fwd primers.

Each 20 µL reaction consisted of: 300 nM of each primer, 40 ng DNA, 10 µL iTaq Universal SYBR Green Supermix (Bio-Rad). The PCR conditions consisted of an initial denaturation at 95°C for two min. Then 35 cycles of: denaturation at 95°C for 15 sec, annealing at 58°C for 15 sec, and extension at 68°C for 15 sec. A melting curve was performed with the following parameters: 95°C for 15 sec, 55°C for 15 sec, temperature increase for 20 min, 95°C for 15 sec. The relative quantification was determined using the $N=2^{-\Delta\Delta CT}$ equation, where N represents the relative fold difference. The ΔC_T was calculated by taking the average cycle threshold (C_T) value for an excision product (*attL/R, attDOT, attB*) and subtracting the average C_T value of the internal reference marker *rpoD*. The $\Delta\Delta C_T$ was calculated by subtracting the ΔC_T of the un-induced samples from the ΔC_T of the tetracycline induced samples.

3.4 Results

Studying CTnDOT Excision Using HiSeq$_{2500}$

Previous *in vivo* studies on CTnDOT excision focused on using qualitative Southern blots to analyze excision levels by detecting the presence of the *attDOT* sequence using a complementary probe [4]. In this study we use HiSeq$_{2500}$ data to provide a more quantitative assay, by detecting products of excision events in the sequenced reads of cells carrying CTnDOT.

Bacteroides thetaiotaomicron cells with CTnDOT integrated into the BT2413 Gene, which is annotated as a homoserine o-succinyltransferase, were grown in the presence and absence of tetracycline. The induced and un-induced cells were collected at three different growth stages: exponential phase (0.3 OD_{650}), stationary phase (0.6 OD_{650}), and overnight growth (O/N). These three different growth stages were assessed

to determine how quickly the excision reaction is detectible *in vivo* for both the induced and un-induced samples.

Table 3.3 summarizes how many reads containing *attDOT* and *attL/attR* were detected in the $HiSeq_{2500}$ excision assay for each of the samples. For every *attL* sequence there should be a corresponding *attR* sequence, since excision happens at both sites simultaneously. Therefore, the number of *attL* and *attR* reads were averaged for each of the samples to determine the approximate number of integrated CTnDOT elements within the population of cells. The number of reads containing the *attDOT* excised product was divided by that number to get an approximate excision frequency for the sample.

The excision frequency of CTnDOT in the induced samples is very low, with frequencies ranging from 0-1.7% (Table 3.3). The un-induced samples seemed to be unable to achieve excision, except for a single read of *attDOT* that was collected in the stationary (0.6 OD_{650}) DNA of sample C. Sample B did not contain reads for any excision events, for reasons not known. It is worth noting that excision events were higher during exponential phase (0.3 OD_{650}), and appeared to get less frequent as time proceeded. This indicates that *in vivo* excision happens relatively rapidly, whereas the *in vitro* excision reaction takes 24 hours for efficient excision [9]. The reduced number of excision reads seen in the later samples could mean that the excision products that occurred during exponential phase have since re-integrated into a host chromosome.

Discovering Alternative *attB* Sites

There have been many studies focused on the *in vitro* integration reaction of CTnDOT, however not much is known about integration *in vivo*. Integration occurs in one of three situations. The first involves the excised CTnDOT having transferred a single strand to a recipient cell, which is circularized and replicated before integrating into the recipient chromosome. The second situation involves the single strand left behind in the donor cell after transfer is initiated, which presumably can replicate and re-integrate into the donor chromosome. This allows the donor cell to retain the antibiotic resistances encoded by the element. The third situation involves the integrated element excising from the chromosome and re-integrating without the initiation of transfer.

After excision occurs and the concentration of tetracycline reduces, the integration reaction is capable of happening since the IntDOT protein is constitutively expressed [3]. The integration and re-integration events of the element do not necessarily have to occur at the same *attB* site. A previous study isolated CTnDOT constructs that were integrated into 7 different *attB* sites [3]. Comparison of the B core sites generated a GTA NN TTTGC consensus sequence, with cleavage occurring between the T and G [3]. There are 564 locations within the *Bacteroides* chromosome that perfectly match this consensus sequence and could be potential *attB* sites. There are also additional sites that closely resemble the B core consensus sequence, which could indicate that there are over a thousand potential sites of integration for CTnDOT.

Many ICEs have a preferred site of integration within the host chromosome. For example phage lambda integrates into a single *attB* site, however there are alternative

sites where phage lambda is capable of integrating at frequency 100-1000x lower than the normal *attB* site [20]. Perhaps one of the reasons ICEs appear to be prevalent within the *Bacteroides* sp. is that there are many possible *attB* sites found throughout the chromosome, and elements that are encountered by the host have more opportunities to integrate within the chromosome.

This study identifies alternative *attB* sites that are used by CTnDOT. The paired end reads of the sequences that contained *attL* and *attR* sequences from the $HiSeq_{2500}$ assay were mapped to the *Bacteroides* chromosome. If the paired end reads mapped to the original *attB* site the reads were ignored, since it cannot be determined if the element simply remained integrated, or excised and then reintegrated. However, if the paired end reads mapped to somewhere else on the *Bacteroides* chromosome the location was scanned for the consensus sequence of the B core site, GTA NN TTTGC [3]. As can be seen in Table 3.4, there were several paired end reads that mapped to other areas of the *Bacteroides* chromosome. Interestingly there appear to be integration events occurring with and without the presence of tetracycline, meaning there are some background excision and integration events that occur without the induction of the regulatory cascade. However, the products of excision, the *attDOT* sequence, are generally not detected without the samples being induced with tetracycline. This means that excision must be too rare in un-induced samples to be detectable.

Summarized in Table 3.5 are the 18 alternative *attB* sites that were detected within the $HiSeq_{2500}$ data more than once. Only the first location presented has been identified with the previous *in vivo* integration study, the remaining *attB* sites are new discoveries [3]. For two regions there was more than one highly conserved B core

consensus sequence found, so the integration event could have happened at either location. Ten of these consensus sequences were found in the middle of annotated genes, while ten of these consensus sequences where found in the intergenic regions of the chromosome. In Figure 3.2a the new *attB* sites were aligned, along with the previously discovered *attB* sites. Prior to this study there were not enough examples of the B' core type site to establish a consensus sequence. In Figure 3.2b it can been seen that the B' core type site is not as strongly conserved as the B core type site, but it does show a strong tendency towards adenine and thymine. The B' core type site of most elements is an inverted repeat of the B core type site. The most commonly used nucleotides for each position within the B' core type site (AAA TA TAA) form a near perfect inverted repeat of the GTA NN TTT sequence of the B core type site. As expected, the 5 bp following the conserved GC sequence in the overlap region do not show a strong consensus, or trend (Figure 3.2c) The first base pair within that 5 bp region does show a tendency for thymine, but overall there appears to be an even distribution of nucleotides used in this region.

Testing Excision Operon Constructs for *in vivo* Excision Levels Using qPCR

A minimal excision assay was constructed to study some of the fundamental components of the excision reaction *in vivo*. The minimal excision assay uses a cefoxitin resistant Minielement (pCefMinielement) that encodes the constitutively expressed IntDOT protein and the *attDOT* sequence. Once the CefMinielement is introduced into the *Bacteroides* host strain, the *attDOT* sequence and a chromosomal *attB* site undergo site selective recombination with the help of the Bacteroides host factor (BHFa) and IntDOT (Figure 3.3). The *Bacteroides* strain used contains the

central regulatory region, *tetQ-rteA-rteB-rteC*, irreversibly integrated into the NBU1 integration site on the chromosome. This allows all excision constructs to be expressed under their native promoter and remain inducible by tetracycline.

As depicted in Figure 3.4, the excision genes provided *in trans* stimulate the excision of the integrated CefMinielement when tetracycline induces the regulatory cascade. Primers can then be used to amplify the excised *attDOT* product, the chromosomal *attB* site, or the integrated *attL* and *attR* sites. This procedure was used to test samples from three different growth phases: exponential (0.3 OD_{650}), stationary (0.6 OD_{650}), and overnight growth (O/N). This was done to gain a better understanding of when the excision reaction generates detectable levels of excised product *in vivo*.

Before testing the CefMinielement strain for excision, the full length CTnDOT was assayed to compare the levels of excision in the minimal excision system to that of the full length element. CTnDOT showed a significant increase in the detection of *attDOT* and *attB* products when induced with tetracycline (Figure 3.5, Table 3.6). There was no change in the *attL/attR* products, which means that there were equivalent amounts in the induced and un-induced samples. This is most likely because the majority of the cells did not undergo an excision reaction, and the element remained integrated within the chromosome. Also, some of the elements that did excise may have re-integrated back into the same *attB* site, since the IntDOT proteins needed for integration are already in the area from their participation in the excision reaction. This trend of equivalent amounts of *attL/attR* products was observed for all of the tested excision operon constructs.

To test how different combinations of the excision genes effect excision levels, several different excision operon constructs were made and expressed *in trans* with the integrated CefMinielement (Figure 3.6). The wild type excision operon, containing *xis2c-xis2d-orf3-exc*, showed increased levels of *attDOT* and *attB* detection when induced with tetracycline. The levels were generally lower than those reported for the full length element, but the CefMinielement is 58 kb smaller than CTnDOT and it is integrated into a different *attB* site (Figure 3.7). These factors may contribute to the discrepancies between CTnDOT and the minimal excision system. Compared to CTnDOT, the exponential phase *attDOT* levels were about 18x reduced in the CefMinielement strain containing the WT excision operon, and the excision levels of the stationary and overnight growth samples were reduced by about half (Figure 3.5, Table 3.6). The CefMinielement strain containing the WT excision operon also showed about 10x lower levels of *attB* detected during exponential phase than the full length CTnDOT element, but showed roughly equivalent levels of *attB* detection during stationary phase and after overnight growth.

Previous qualitative *in vivo* studies indicated that the *orf3* gene is not required for excision, so all subsequent studies until now have eliminated this gene from analysis [4]. Not much is known about *orf3*, but it does contain two conserved domains of unknown function (DUF4099 and DUF3945). Even though this gene is not required for excision, its location within the excision operon suggests that it could contribute to the excision reaction. Therefore, the minimal excision system was used to quantify the contribution of *orf3* to the excision reaction. When the CefMinielement was tested with the in-frame deletion of *orf3*, the amount of detectable *attDOT* was 7-18x lower than

when the CefMinielement was tested with the WT excision operon (Figure 3.5, Table 3.6). The *attB* levels were approximately 5-7x lower than those reported for the wild type excision operon. This supports the proposal that *orf3* is not essential for excision, but it indicates that *orf3* deletions significantly reduce excision levels.

Other excision constructs were also tested with the CefMinielement to determine if they effected excision levels. Double mutant constructs, containing an *orf3* deletion, were tested for comparison with the results of previous *in vitro* assays. There was very little to no excision detected within the p*Δorf3Δxis2c*, p*Δorf3Δxis2d*, and p*Δorf3Δexc* constructs with and without tetracycline (Figure 3.5, Table 3.6). The highest levels of excision detected in the double mutants was a 10x increase in the amount of *attB* found in the overnight growth of the p*Δorf3Δexc* samples when tetracycline was present (Figure 3.5, Table 3.6). Since this study shows that a deletion of *orf3* reduces the levels of CefMinielement excision, singular in-frame deletions of the other excision genes were tested to determine if presence of *orf3* is able to compensate for the absence of that excision gene in the excision reaction. The pΔ*xis2c* and pΔ*exc* constructs produced no detectable *attDOT* and *attB* products under any of the tested conditions (Figure 3.5, Table 3.6). Therefore, it is still upheld that Xis2c, Xis2d, and Exc are required for *in vivo* excision.

Orf2a and Orf2b Influence Excision

As shown in Figure 3.8, there are two small open reading frames upstream of the excision operon called *orf2a* and *orf2b*. These proposed genes have a very similar predicted secondary structure to Xis2c and Xis2d, so it was hypothesized that they may contribute to the excision reaction. Preliminary data suggests that these genes are in an

operon, and are constitutively expressed (data not shown). An excision construct containing *orf2a, orf2b,* and the WT excision operon was tested with the CefMinielement. The levels of *attDOT* and *attB* detected was roughly equivalent to the levels detected for the WT excision operon (Figure 3.9, Table 3.6). When a construct containing *orf2b* and the WT excision operon was tested with the CefMinielement, the levels of *attDOT* and *attB* detected in the exponential phase sample were equivalent to the levels found with full length CTnDOT. The levels of *attDOT* and *attB* for both stationary phase and overnight growth were about 3-6x higher than the levels found in the full length CTnDOT. It is possible that *orf2b* enhances the excision reaction, while *orf2a* regulates how much excision occurs to minimize excessive excision.

3.5 Discussion

The excision reaction of CTnDOT is a complex sequence of events that is needed for propagating the element into new hosts. From this study it is clear that CTnDOT excision is inefficient, with an excision frequency of around 1%. Excision levels may be low because tetracycline is not the natural inducer of the regulatory cascade. As mentioned in the introduction, tetracycline increases the translation of the *tetQ-rteA-rteB* operon though a translational attenuation mechanism [26]. The RteA protein resembles a histidine kinase sensor protein in a two component regulatory system, but the molecule this protein is induced by is unknown [23]. When this unknown inducer molecule is present it may increase the potency of the regulatory cascade, and cause excision frequencies to increase dramatically.

With all of the conflicting results from previous studies, this study provides clarification for what proteins are contributing to the excision reaction *in vivo*. This

study agrees with all previous assays regarding to the Xis2c and Xis2d proteins, as they are shown to be required for the detection of excised products in the qPCR assay. However, this study confirms that the qualitative Southern blots were correct in identifying Exc as a required protein for *in vivo* excision [4]. This indicates that something is lacking from the *in vitro* excision reactions that enable them to proceed at wild type levels without Exc. The *in vitro* intermolecular assay indicated that reactions lacking Exc showed wild type excision levels, however the DNA topology in this reaction is completely different than what occurs *in vivo*. The *in vitro* intramolecular assay provided *attL* and *attR* on the same DNA molecule, and showed Exc having an 3-5-fold enhancing effect on excision levels when *attL* and *attR* were separated by 4.7kb and had mismatched overlap regions [9, 25]. *In vivo* there have been no isolated examples of *attL/attR* overlap regions matching, and the space between the *att* sites is 8 kb for the CefMinielement, and 65 kb for CTnDOT. Therefore, Exc may be needed to stabilize the DNA-protein interactions at the *att* sites, near the overlap region, when larger elements are excised *in vivo*.

An unexpected discovery from this study was the results obtained for *orf3*. When *in vivo* Southern blots were performed with the excision operon containing an in-frame deletion of *orf3*, the attDOT excision products was detected [4]. This caused *orf3* to be labeled as non-essential, and largely ignored in subsequent studies. The work presented within this study indicates that while excised products are detected with an in-frame deletion of *orf3*, the levels are minimal compared to the levels produced by the wild type excision operon. These results are the first instance where *orf3* has shown a functional role that validates the inclusion of this protein within the excision operon.

The predicted secondary structure of Orf3 shows two domains of unknown function. These domains may be involved in stabilizing the protein-protein interactions occurring within the confined *attL/attR* region during the excision reaction.

It is possible that Orf3 increases the speed of the excision reaction. The *in vitro* intramolecular excision reaction is very slow, and reactions were allowed to proceed overnight to obtain efficient excision levels [9]. In this study excised products were detectable in exponential phase, which cells reached in about 4 hours. The lack of Orf3 in the *in vitro* reaction could explain why excision proceeded so slowly.

This study also showed that Orf2a and Orf2b, which are structurally similar to Xis2c and Xis2d, contribute to the excision reaction. Even though the *orf2a* and *orf2b* genes are present within the same operon, they appear to have opposing effects on the excision reaction. The levels of CefMinielement excision with *orf2b* present were 3-6x higher than when the WT excision operon was expressed alone. This does not prove that Orf2b is working as an additional excisionase at the *att* sites. Both Xis2c and Xis2d work as transcriptional activators, so Orf2b could be transcriptionally activating something that increases the efficiency of the excision reaction. When *orf2a* and *orf2b* are expressed together with the WT excision operon, the levels of excision are equivalent to levels seen with the WT excision operon alone. This could mean that there is an additional layer of CTnDOT regulation that restricts the efficiency of the excision reaction. Orf2a could be accomplishing this regulation by binding the *att* sites in a way that lowers the efficiency of excision, or it could serve as a transcriptional repressor of an accessory gene that increases the efficiency of the excision reaction. In future studies

the region these proteins are acting upon could be identified using DNA binding assays with the purified forms of these proteins.

While the excision reaction is a pivotal step of CTnDOT propagation, the excised element must integrate for the host cells to maintain antibiotic resistance to erythromycin and tetracycline. The integration reaction relies on the recombination of the *attDOT* and *attB* sequences using the element encoded recombinase, IntDOT. Prior to this study there were only 7 known *attB* sites within the *Bacteroides* chromosome. This study identified 18 alternative *attB* sites that were used for CTnDOT integration. It is most likely that these integration events are the result of CTnDOT excising from the chromosome and re-integrating into a new *attB* site without the initiation of transfer. This is because transfer is highly inefficient in liquid culture, and all samples were grown in liquid BHIS media (Nadja Shoemaker, unpublished results).

It is interesting to note that a previous genechip assay indicated that when strains containing CTnDOT were induced by tetracycline, some host chromosomal genes appeared to be regulated by the element [15]. One of the genes that were down-regulated upon tetracycline exposure was *BT0387*, which is annotated as NADH dehydrogenase subunit 2. As seen in Table 3.5, this gene contains an alternative *attB* site. This *attB* site was previously identified in another study, which could indicate that this is a preferred site of integration [3]. The NADH dehydrogenase may not have been down-regulated by the gene products of the CTnDOT element, but rather down-regulated by the element integrating within this gene and abolishing its expression. *Bacteroides* appear to be built for harboring integrative and conjugative elements, due to the larger number of potential *attB* sites within the chromosome.

3.6 Acknowledgements

I would like to give a big thanks to Rachel Whitaker, Dave Krause, and Samantha DeWerff for contributing to the development of the HiSeq$_{2500}$ excision assay, and for enabling me to access the pertinent data from the vast amounts sequenced reads generated.

3.7 References

1. Baba, T., et al., *Construction of Escherichia coli K-12 in-frame, single-gene knockout mutants: the Keio collection.* Mol Syst Biol, 2006. **2**: p. 2006.0008.

2. Bauer, C.E., J.F. Gardner, and R.I. Gumport, *Extent of sequence homology required for bacteriophage lambda site-specific recombination.* J Mol Biol, 1985. **181**(2): p. 187-97.

3. Cheng, Q., et al., *Integration and excision of a Bacteroides conjugative transposon, CTnDOT.* J Bacteriol, 2000. **182**(14): p. 4035-43.

4. Cheng, Q., et al., *Identification of genes required for excision of CTnDOT, a Bacteroides conjugative transposon.* Mol Microbiol, 2001. **41**(3): p. 625-32.

5. Cherepanov, P.P. and W. Wackernagel, *Gene disruption in Escherichia coli: TcR and KmR cassettes with the option of Flp-catalyzed excision of the antibiotic-resistance determinant.* Gene, 1995. **158**(1): p. 9-14.

6. Datsenko, K.A. and B.L. Wanner, *One-step inactivation of chromosomal genes in Escherichia coli K-12 using PCR products.* Proc Natl Acad Sci U S A, 2000. **97**(12): p. 6640-5.

7. Dichiara, J.M., A.N. Mattis, and J.F. Gardner, *IntDOT interactions with core- and arm-type sites of the conjugative transposon CTnDOT.* J Bacteriol, 2007. **189**(7): p. 2692-701.

8. Jeters, R.T., et al., *Tetracycline-associated transcriptional regulation of transfer genes of the Bacteroides conjugative transposon CTnDOT.* J Bacteriol, 2009. **191**(20): p. 6374-82.

9. Keeton, C.M. and J.F. Gardner, *Roles of Exc protein and DNA homology in the CTnDOT excision reaction.* J Bacteriol, 2012. **194**(13): p. 3368-76.

10. Keeton, C.M., et al., *Interactions of the excision proteins of CTnDOT in the attR intasome.* Plasmid, 2013. **70**(2): p. 190-200.

11. Keeton, C.M., et al., *The excision proteins of CTnDOT positively regulate the transfer operon.* Plasmid, 2013. **69**(2): p. 172-179.

12. Laprise, J., S. Yoneji, and J.F. Gardner, *Homology-dependent interactions determine the order of strand exchange by IntDOT recombinase.* Nucleic Acids Res, 2010. **38**(3): p. 958-69.

13. Malanowska, K., et al., *Mutational analysis and homology-based modeling of the IntDOT core-binding domain.* J Bacteriol, 2009. **191**(7): p. 2330-9.

14. Malanowska, K., A.A. Salyers, and J.F. Gardner, *Characterization of a conjugative transposon integrase, IntDOT.* Mol Microbiol, 2006. **60**(5): p. 1228-40.

15. Moon, K., J. Sonnenburg, and A.A. Salyers, *Unexpected effect of a Bacteroides conjugative transposon, CTnDOT, on chromosomal gene expression in its bacterial host.* Mol Microbiol, 2007. **64**(6): p. 1562-71.

16. Nikolich, M.P., N.B. Shoemaker, and A.A. Salyers, *A Bacteroides tetracycline resistance gene represents a new class of ribosome protection tetracycline resistance.* Antimicrob Agents Chemother, 1992. **36**(5): p. 1005-12.

17. Park, J. and A.A. Salyers, *Characterization of the Bacteroides CTnDOT regulatory protein RteC.* J Bacteriol, 2011. **193**(1): p. 91-7.

18. Quick, L.N., A. Shah, and J.W. Wilson, *A series of vectors with alternative antibiotic resistance markers for use in lambda Red recombination.* J Microbiol Biotechnol, 2010. **20**(4): p. 666-9.

19. Ringwald, K. and J. Gardner, *The Bacteroides thetaiotaomicron protein Bacteroides host factor A participates in integration of the integrative conjugative element CTnDOT into the chromosome.* J Bacteriol, 2015. **197**(8): p. 1339-49.

20. Shimada, K., R.A. Weisberg, and M.E. Gottesman, *Prophage lambda at unusual chromosomal locations. I. Location of the secondary attachment sites and the properties of the lysogens.* J Mol Biol, 1972. **63**(3): p. 483-503.

21. Shoemaker, N.B., et al., *Regions in Bacteroides plasmids pBFTM10 and pB8-51 that allow Escherichia coli-Bacteroides shuttle vectors to be mobilized by IncP plasmids and by a conjugative Bacteroides tetracycline resistance element.* J Bacteriol, 1986. **166**(3): p. 959-65.

22. Simon, R., U. Priefer, and A. Puhler, *A Broad Host Range Mobilization System for In Vivo Genetic Engineering: Transposon Mutagenesis in Gram Negative Bacteria.* Nat Biotech, 1983. **1**(9): p. 784-791.

23. Stevens, A.M., et al., *Genes involved in production of plasmidlike forms by a Bacteroides conjugal chromosomal element share amino acid homology with two-component regulatory systems.* J Bacteriol, 1992. **174**(9): p. 2935-42.

24. Stevens, A.M., et al., *Tetracycline regulation of genes on Bacteroides conjugative transposons.* J Bacteriol, 1993. **175**(19): p. 6134-41.

25. Sutanto, Y., et al., *Factors required in vitro for excision of the Bacteroides conjugative transposon, CTnDOT.* Plasmid, 2004. **52**(2): p. 119-30.

26. Wang, Y., et al., *Translational control of tetracycline resistance and conjugation in the Bacteroides conjugative transposon CTnDOT.* J Bacteriol, 2005. **187**(8): p. 2673-80.

27. Wang, Y., N.B. Shoemaker, and A.A. Salyers, *Regulation of a Bacteroides operon that controls excision and transfer of the conjugative transposon CTnDOT.* J Bacteriol, 2004. **186**(9): p. 2548-57.

28. Waters, J.L. and A.A. Salyers, *Regulation of CTnDOT conjugative transfer is a complex and highly coordinated series of events.* MBio, 2013. **4**(6): p. e00569-13.

29. Waters, J.L., G.R. Wang, and A.A. Salyers, *Tetracycline-related transcriptional regulation of the CTnDOT mobilization region.* J Bacteriol, 2013. **195**(24): p. 5431-8.

30. Whittle, G., N.B. Shoemaker, and A.A. Salyers, *Characterization of genes involved in modulation of conjugal transfer of the Bacteroides conjugative transposon CTnDOT.* J Bacteriol, 2002. **184**(14): p. 3839-47.

31. Whittle, G., et al., *Identification of a new ribosomal protection type of tetracycline resistance gene, tet(36), from swine manure pits.* Appl Environ Microbiol, 2003. **69**(7): p. 4151-8.

32. Wood, M.M. and J.F. Gardner, *The Integration and Excision of CTnDOT.* Microbiol Spectr, 2015. **3**(2): p. Mdna3-0020-2014.

3.8 Tables and Figures

Table 3.1: Bacterial Strains and Plasmids

Strain or Plasmid	Phenotype	Description
Stains		
BT4001ΩQABC	Rif^r Tp^r Tc^r Thy^-	BT4001 with site-specific insertion of tetQ, rteA, rteB, rteC in the chromosome [30]
BT4001ΩQABC ΩCefMinielement	Rif^r Tc^r Cef^r	BT4001ΩQABC with the Cefoxitin Minielement integrated in the chromosome (This study)
S17-1	$RecA^-$ Tp^r Str^r Spc^r	IncPα RP4 inserted into the chromosome [22]
Plasmids		
pAFD1	Amp (Erm)	*E. Coli-Bacteroides* shuttle vector (A. M. Stevens, Unpublished)
pKS01	Amp (Cef)	Contains genes *orf2A, orf2B, xis2C,* xis*2D, orf3, exc, orf2E rteR,* and *orf4A* [4]
pKS07	Amp (Cef)	Contains an in-frame deletion of *orf3.* Genes present are *orf2A, orf2B, xis2C,* xis*2D, exc, orf2E and rteR* [23]
pWTExcision	Amp (Erm)	Contains genes *xis2c*, *xis2d*, *orf3*, and *exc* (This study)
p*Δorf3*	Amp (Erm)	Contains genes *xis2c*, *xis2d*, and *exc* (This study)
p*Δorf3Δexc*	Amp (Erm)	Contains genes *xis2c* and *xis2d* [11]
p*Δorf3Δxis2c*	Amp (Erm)	Contains genes *xis2d* and *exc* [11]
p*Δorf3Δxis2d*	Amp (Erm)	Contains genes *xis2c* and *exc* [11]
p*Δexc*	Amp (Erm)	Contains genes *xis2c*, *xis2d*, and *orf3* (This study)
p*Δxis2c*	Amp (Erm)	Contains genes *xis2d*, *orf3*, and *exc* (This study)
pWT+*orf2a-orf2b*	Amp (Erm)	Contains genes *orf2A*, *orf2B*, *xis2c*, *xis2d*, *orf3*, and *exc* (This study)
pWT+*orf2b*	Amp (Erm)	Contains genes *orf2B*, *xis2c*, *xis2d*, *orf3*, and *exc* (This study)
pGWA34.2	Amp (Cef)	*E. coli-Bacteroides* suicide vector containing *cfxA* [31]
pCefMinielement	Amp (Cef)	The IntDOT and *attDOT* region of pWTMinielement cloned into pGWA34.2 (This Study)
pWTMinielement	Amp (Erm)	pDJE2.3 with a wild type *intDOT* gene (This Study)
pDJE2.3	Amp (Erm)	pGERM based plasmid that contains intDOT and attDOT of CTnDOT. Contains a point mutation in *intDOT* [3]
pKD4	Kan	Contains kanamycin resistance cassette flanked by FLP sites [6]
pJW104	Cmr temps	Contains the lambda red recombination genes with a chloramphenicol resistance marker [18]
pCP20	Amp Cm	Contains a temperature inducible FLP recombinase gene [5]

Table 3.2: Primers Used in This Study

Primer Name:	Sequence (5'→ 3')
Cloning	
Excision-smaI -fwd	GCAATGCCCGGGCCATATTCATGCAATTATCGG
Excision-smaI -rev	GCAATGCCCGGGCGTTTCGGCGGCACGGTCGGC
Excision-bamHI-fwd	GCAATGGGATCCCCATATTCATGCAATTATCGG
Excision-ecoRI-rev	GCAATGGAATTCGTTAATACTATTTCTTCCG
Minielement-kpnI-fwd	GCAATGGGTACCCGTCATTACCGGTTACGCTGACC
Minielement-kpnI-rev	GCAATGGGTACCCATGATTACGCCAAGCTTGCATGC
Orf2A-ecoRI-fwd	CGAATCGAATTCTCATAACGGCTTGCGGTAGTTCGC
Orf2B-ecoRI-fwd	CGAATCGAATTCTCATCTGCCGTGCGGATAGAGCGT
Lambda Red	
Exc-del-fwd	AATAAAATCCAAAGTATCAACAAAAAAGCAAGAAAACATGGTGTAGGCTG GAGCTGC
Exc-del-rev	ACAAGTGGCAAAGTTAATACTATTTCTTCCGTCCTGAAAAATGGGAATTAG CCATGG
Xis2c-del-fwd	TATGTTCATGAAAATAAACAAAAAGAAAGGACTGAATATGGTGTAGGCTGG AGCTGC
Xis2c-del-rev	CGTGTGAGCAGTTCCATAGCTATGTCCTCCTTCCTTTGGGATGGGAATTAGC CATGG
Xis2d-del-fwd	GAACGGGAGGCACACCCAAAGGAAGGAGGACATAGCTATGGTGTAGGCTG GAGCTGCTTC
Xis2d-del-rev	TGAAAAATGTTTTAATGGGTTATTTATGAAAGAAATTATGATGGGAATTAG CCATGGTCC
SDM	
SDM-*intDOT*-fwd	GCGGTTGGCGATGTCAAGCAGGCGGATATTGGACACCACACCCGTTTTCTG GCGG
SDM-*intDOT*-rev	CCGCCAGAAAACGGGTGTGGTGTCCAATATCCGCCTGCTTGACATCGCCAA CCGC
qPCR	
***attDOT*-fwd**	GCTTCACGAATTATAGCCACTTC
***attDOT*-rev**	GCGATTAACCTACGCTCATTTC
CTnDOT-*attB*-fwd	GCAACCTCCCTATTATGTGCTAT
CTnDOT-*attB*-rev	CGTAGCACGCGAAGTATCAA
ME-*attB*-fwd	GCAGCATTCTGATTCGTATTAGTTAG
ME-*attB*-rev	TCGTGTGCAGGAATATTGTATCT
***rpoD*-fwd**	ACGCTGTATGGTGGATTCGTCAGT
***rpoD*-rev**	ACCTGATTCAACGGGAGACGAACA
Other	
L2	GGGCAATGGTGTTCCGACGGATAAAA

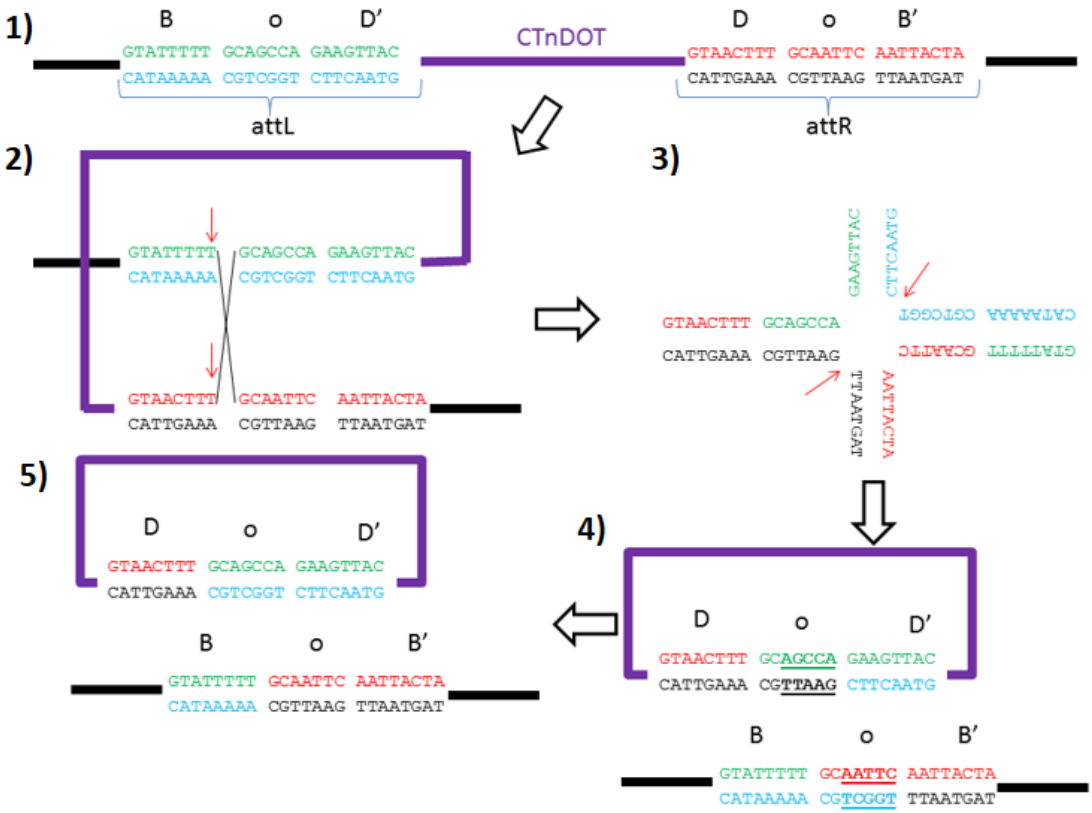

Figure 3.1: Summary of CTnDOT Excision. When CTnDOT is integrated it contains *attL* and *attR* sites located at the ends of the integrated element (1). Four IntDOT monomers bind the core sites (B, B', D, and D'). Two of the IntDOT proteins make nicks in the top strands of DNA (2). The IntDOTs then exchange and ligate the strands to form a Holliday junction intermediate (3). Then the other two IntDOTs become active and nick the bottom strands of the DNA (3). The strands are exchanged and ligated to form *attDOT* (D o D') and *attB* (B o B') (4). Due to the 5 bp of heterology in the overlap region (o) mismatch repair must replace the bases in either the top or bottom strand to correct the resulting products (4-5). Nicking of the DNA is indicated by red arrows.

Table 3.3: Summary of HiSeq$_{2500}$ Excision Results for CTnDOT. The number of *attDOT* reads for samples A, B, and C are presented for each of the different growth phases tested (0.3 OD_{650}, 0.6 OD_{650}, and Overnight). "–TET" refers to samples not treated with tetracycline, and "+TET" refers to samples treated with tetracycline. The average number of *attL/attR* reads detected during each growth phase are listed at the bottom of the table. The frequency of excision for each sample was determined by dividing the *attDOT* reads by the average *attL/attR* reads.

		0.3 OD_{650}		0.6 OD_{650}		Overnight	
		-TET	+TET	-TET	+TET	-TET	+TET
A	*attDOT*	0	8	0	7	0	2
	Freq.	**0%**	**1.4%**	**0%**	**1.2%**	**0%**	**0.3%**
B	*attDOT*	0	0	0	0	0	0
	Freq.	**0%**	**0%**	**0%**	**0%**	**0%**	**0%**
C	*attDOT*	0	9	1	2	0	1
	Freq.	**0%**	**1.6%**	**0.2%**	**0.4%**	**0%**	**0.2%**
attL/attR Avg.		547	572	568	565	587	607

Table 3.4: Re-integration of CTnDOT at New *attB* Sites. The paired end reads of *attL/attR* that mapped to a new chromosome location are enumerated for samples A, B, and C. The average number of *attL/attR* reads detected during each growth phase are listed at the bottom of the table. The frequency of new integration events for each sample was determined by dividing the number of new integration reads by the average number of *attL/attR* reads. Samples (A, B, C) were collected at exponential phase (0.3 OD_{650}), stationary phase (0.6 OD_{650}) and overnight growth. "–TET" refers to samples not treated with tetracycline, and "+TET" refers to samples treated with tetracycline.

		0.3 OD_{650}		0.6 OD_{650}		Overnight	
		-TET	+TET	-TET	+TET	-TET	+TET
A	*attDOT*	0	8	0	7	0	2
	Freq.	**0.0%**	**1.4%**	**0.0%**	**1.2%**	**0.0%**	**0.3%**
B	*attDOT*	0	0	0	0	0	0
	Freq.	**0.0%**	**0.0%**	**0.0%**	**0.0%**	**0.0%**	**0.0%**
C	*attDOT*	0	9	1	2	0	1
	Freq.	**0.0%**	**1.6%**	**0.2%**	**0.4%**	**0.0%**	**0.2%**
attL/attR Avg.		547	572	568	565	587	607

Table 3.5: New Integration events of CTnDOT. The paired end reads of sequences containing the *attL/attR* sequences were mapped to the *Bacteroides* chromosome. The locations were scanned for the B core consensus sequences, GTA NN TTTGC. The location and sequence of the B core sites are listed, along with the annotations of the nearest reference genes. The number of paired end reads that mapped to these locations are summarized for the induced (+tet) and un-induced (-tet) samples. Only paired end reads that mapped to a location more than once were analyzed. An * next to the B core sequence indicates a perfect match to the GTA NN TTTGC consensus sequence.

	Chromosome Location	B core consensus sequence	Nearest reference	Annotation of nearest reference	# of reads detected
1	477673 to 477682	GTA TA TTTGC*	BT0387	NADH Dehydrogenase Subunit 2	1 (+tet), 5 (-tet)
2	620068 to 620077	GTA CT TTTGC*	BT0500 to BT0501	Transporter & Hypothetical Protein	19 (+tet), 19 (-tet)
3	778384 to 778393	GTA TC TTTGC*	BT0631 to BT0632	Hypothetical Protein & GTP-binding Protein LepA	4 (+tet), 2 (-tet)
4	1018559 to 1018568	GTA TA TTTGC*	BT0823 to BT0824	Glucuronate Isomerase & LacI Family Transcriptional Regulator	3 (+tet), 7 (-tet)
5	1490625 to 1490634	GCA CC TTTGC	BT1194	OmpA Family Outer Membrane Protein	10 (+tet), 10 (-tet)
6	2628644 to 2628653	GTA TC TTTGC*	BT2095 to BT2096	Surface Layer Protein & Transcriptional Regulator (FucR Homolog)	3 (+tet)
7	2652882 to 2652891	TTG TT TTTGC	BT2110 to BT2111	Putative Chitobiase & Putative Alpha-1,2-mannosidase	2 (+tet)
8	3156201 to 3156210	AGC AT TTTGC	BT2526	Hypothetical Protein	3 (+tet), 1 (-tet)
9	3217165 to 3217174	GAT TC TTTGC	BT2577	Hypothetical Protein (upstream of transposase)	1 (+tet), 1(-tet)
10	3593829 to 3593838	TTC TT TTTGC	BT 2873	Putative Stress Protein	8 (+tet),4 (-tet)
11	3610989 to 3610998	ATA CT TTTGC	BT2890 to BT2891	Transposase and Hypothetical Protein	1 (+tet), 1 (-tet)
12	3861444 to 3861453	GTA TC TTTGC*	BT3047 to BT3048	Hypothetical Proteins	2(+tet), 1 (-tet)
13	4189588 to 4189697 4190784 to 4190893	GGA GT TTTGC GTC CA TTTGC	BT3277 BT3278	RNA Polymerase ECF-type Sigma Factor Anti-sigma Factor FrrF Homolog	2 (+tet)
14	4228096 to 4228015	GGC AA TTTGC	BT3298	Hypothetical Protein	30(+tet), 32(-tet)
15	4578232 to 4578241	GTA AA TTTGC*	BT3539 to BT3540	Hypothetical Proteins	1 (+tet), 6 (-tet)
16	4795555 to 4795564 4795298 to 4795307	GTA GC TTTGC* GTA CT TTTGC*	BT3692 BT3691 to BT3692	Phosphate Acetyltransferase Hypothetical Protein & Phosphate Acetyltransferase	1 (+tet), 2 (-tet)
17	5215830 to 5215839	GTA TA TTTGC*	BT4002	ParaA Family ATPase	7 (+tet), 6 (-tet)
18	5814070 to 5814079	GTA TC TTTGC*	BT4411 to BT4412	Hypothetical Proteins	6 (+tet), 2 (-tet)

a)

	B			o	B'			
Cheng 1	GTA	AA	TTT	GC	GCAAT	TAA	AA	TAC
Cheng 2	GTA	CT	TTT	GC	GGTGA	AAT	TT	TAT
Cheng 3	GTA	GC	TTT	GC	TGGAC	GAA	TG	TCT
Cheng 4	GTT	GT	TTT	GC	ACTAC	AAA	GA	TAA
Cheng 5	GTA	TA	TTT	GC	TTTAT	AAA	AA	TGA
BT4007	GTA	TT	TTT	GC	AGCCA	AAT	TA	CTA
ΩCefMinielement	GTA	TC	TTT	GC	GCCCG	AAT	TA	ATT
1	GTA	TA	TTT	GC	TTTAT	AAA	AA	TGA
2	GTA	CT	TTT	GC	CGCCT	CAA	AA	TTT
3	GTA	TC	TTT	GC	ACACC	AAA	AA	GAC
4	GTA	TA	TTT	GC	AGCGA	TTA	TT	TAT
5	GCA	CC	TTT	GC	CCGTA	TTG	TT	CAT
6	GTA	TC	TTT	GC	ACCTG	CAA	GG	TTC
7	TTG	TT	TTT	GC	ATAGG	AGT	GT	ATA
8	AGC	AT	TTT	GC	TAGTA	AAT	TG	TTA
9	GAT	TC	TTT	GC	CCAAT	CAG	CA	AAC
10	TTC	TT	TTT	GC	AGAAG	TAT	AC	AGA
11	ATA	CT	TTT	GC	ACTGT	TTT	GA	ATA
12	GTA	TC	TTT	GC	TGTAG	ATA	AC	AAC
13a	GGA	GT	TTT	GC	GCCAA	AAA	TA	CAA
13b	GTC	CA	TTT	GC	CAGAA	CCA	GT	GTT
14	GGC	AA	TTT	GC	TCCTG	TAA	TA	TAC
15	GTA	AA	TTT	GC	AGAAA	AAT	AA	CAC
16a	GTA	GC	TTT	GC	TGATG	TTA	CC	CAG
16b	GTA	CT	TTT	GC	AGCGC	AAA	TT	ACA
17	GTA	TA	TTT	GC	AAGCT	CAA	AC	AGA
18	GTA	TC	TTT	GC	AGTGT	TAA	TA	AAG

b)

B'

A_{12}	A_{19}	A_{16}	T_{11}	A_{13}	T_{10}	A_{13}	A_{10}
T_8	T_5	T_8	A_8	T_6	A_9	T_8	C_7
C_5	G_1	G_2	G_5	C_4	C_5	G_3	T_7
G_1	C_1	C_0	C_2	G_3	G_2	C_2	G_2

c)

o

A_{12}	G_{11}	C_8	A_{10}	A_8
T_6	C_{10}	A_7	G_6	G_7
G_4	A_3	T_6	C_5	T_7
C_4	T_2	G_5	T_5	C_4

Figure 3.2: Aligment of *attB* sequences. a) The *attB* sites from previous *in vivo* assays (Cheng 1-5) and from this study were aligned. The *attB* sites contain the B core type site, the 7 bp overlap sequence, and the B' core type site. Sequence 1 and Cheng 5 represent the same *attB* site b) A summary of how many times each nucleotide was found within the B' core type site. The number of times a nucleotide was present in a given position is represented as a subscript number. c) A summary of how many times each nucleotide was found within the 5 bp heterologous region of the overlap sequence.

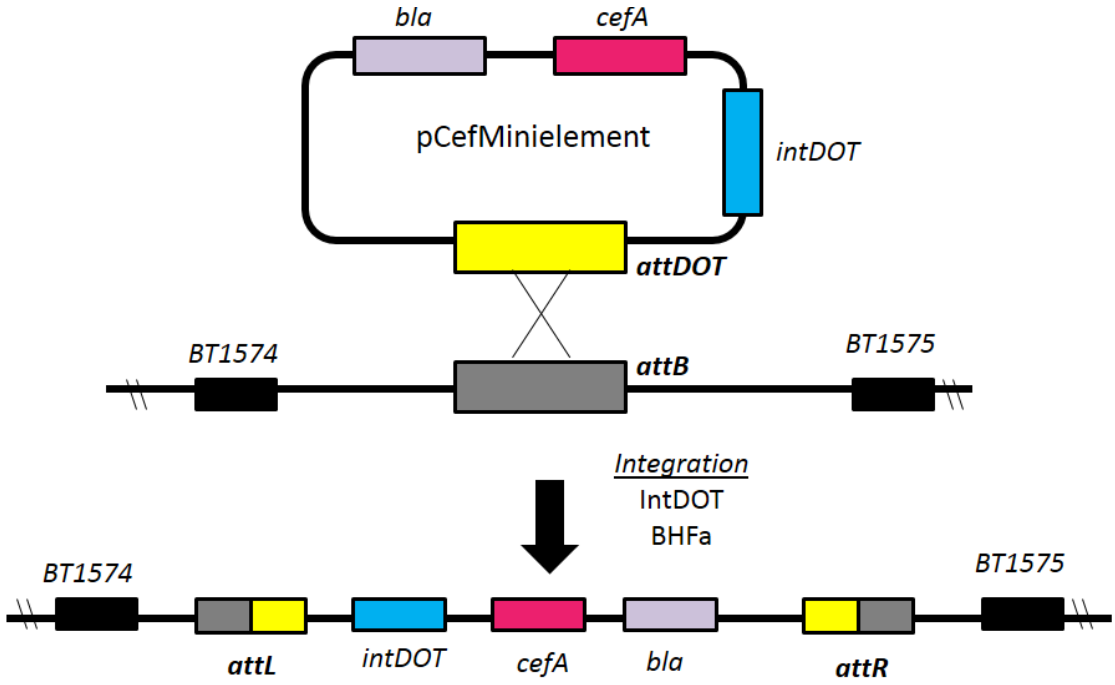

Figure 3.3: Integration of CefMinielement. A suicide vector containing the constitutively expressed integrase (*intDOT*) and the joined ends of the element (*attDOT*) was integrated into BT4001ΩQABC by selecting for cefoxitin resistance. IntDOT is able to bind and cleave the *attDOT* and *attB* sites with the help of a *Bacteroides* encoded host factor (BHFa), resulting in an integrated element containing *attL/attR* sites.

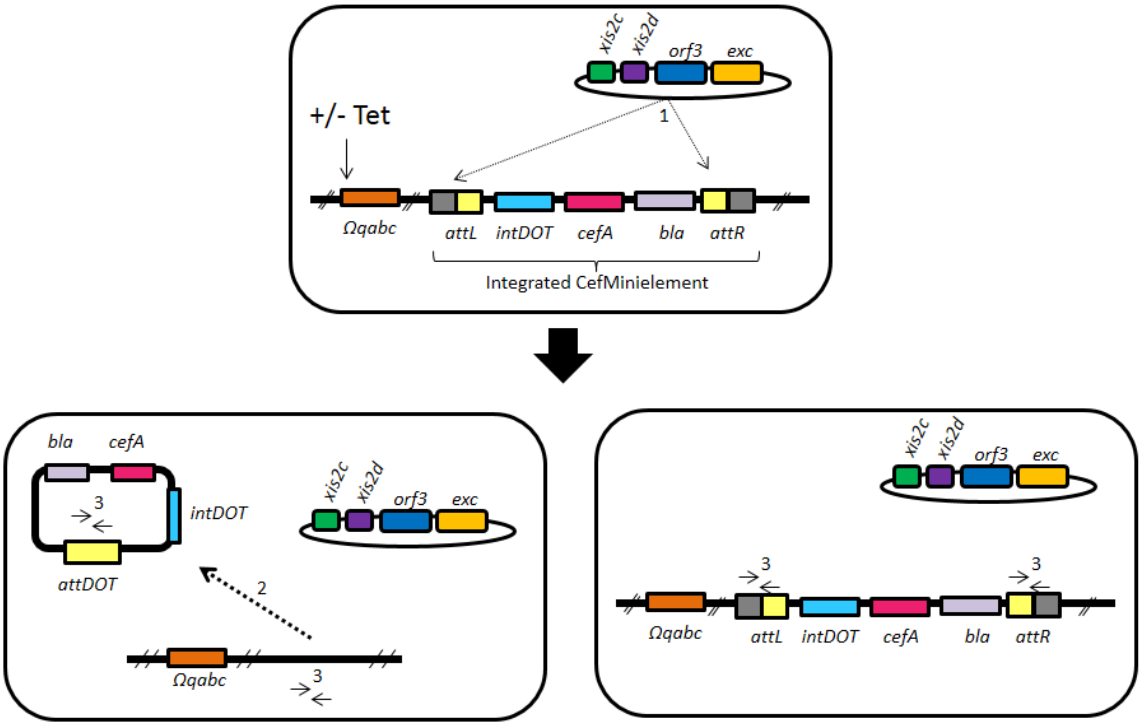

Figure 3.4: qPCR Excision Assay. The integrated CefMinielement is in a strain with the regulatory genes integrated elsewhere on the chromosome (ΩQABC). Different constructs of the excision region are provided *in trans* (here the WT excision operon is shown). Upon exposure to tetracycline the regulatory region will stimulate the expression of the excision operon (1). The excision operon then stimulates the excision reaction, and the element is able to remove itself from the chromosome (2). Primers are able to amplify the presence of the joined ends of excised mini-element (*attDOT*), the reformed chromosomal site (*attB*), or the integrated ends of the element (*attL/attR*) (3).

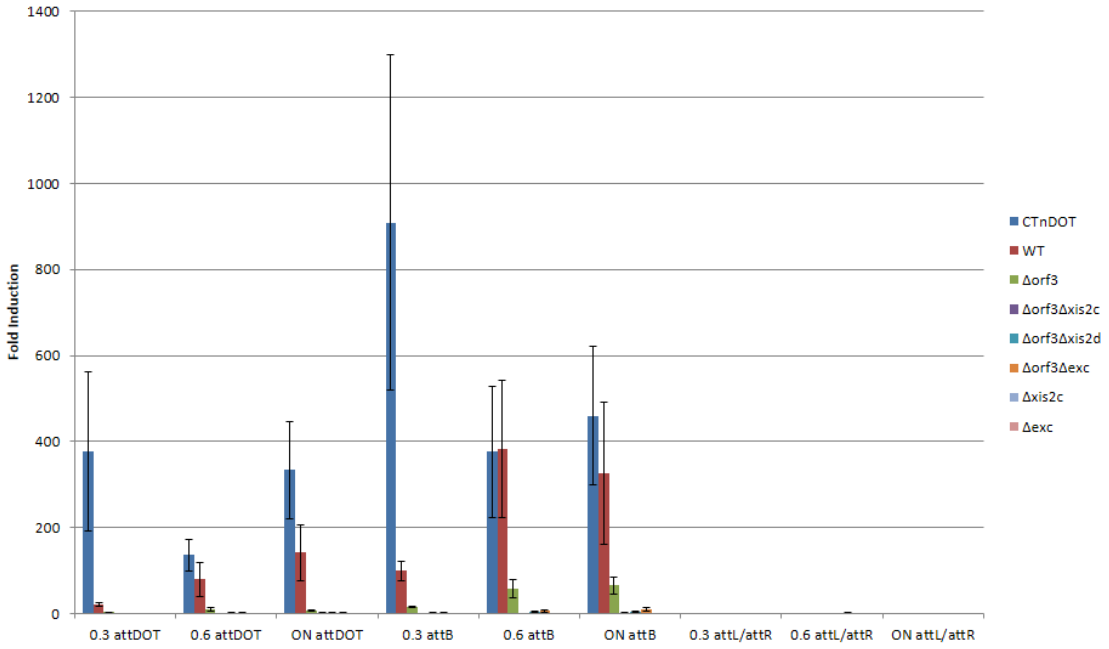

Figure 3.5: Summary of CTnDOT and CefMinielement Excision Levels. The fold increase calculated using the $2^{-\Delta\Delta CT}$ method of relative quantification is depicted for the detection of the excision products (*attDOT*, *attB*, and *attL/attR).* In addition to testing CTnDOT, the CefMinielement was used with the indicated excision plasmids.

Table 3.6: Summary of qPCR Excision Levels. A summary of the $2^{-\Delta\Delta CT}$ values for products used to measure excision levels. The excision products tested were the excised element (*attDOT*), the re-formed chromosomal insertion site (*attB*), and the integrated ends of the element (*attL/attR*). Samples for each construct were collected during exponential phase (0.3 OD), early stationary phase (0.6 OD), and after overnight growth (ON). CTnDOT refers to the full length element, while all other excision constructs were provided *in trans* with an integrated mini-element in the chromosome.

	0.3 attDOT	0.6 attDOT	ON attDOT	0.3 attB	0.6 attB	ON attB	0.3 attL/attR	0.6 attL/attR	ON attL/attR
CTnDOT	378 ± 185	137 ± 37	334 ± 113	909 ±391	376 ± 152	461 ± 162	1.4 ± 0.2	0.9 ± 0.2	1.0 ± 0.1
WT	21 ± 5	80 ± 39	142 ± 64	99 ± 22	383 ± 160	326 ± 166	1.2 ± 0.1	1.1 ± 0.1	1.2 ± 0.2
Δorf3	3 ± 1	10 ± 4	8 ± 1	15 ± 1	57 ± 21	65 ± 19	1.0 ± 0.1	1.2 ± 0.2	0.8 ± 0.1
Δorf3Δxis2c	1.2 ± 0.1	0.8 ± 0.1	1.3 ± 0.6	1.3 ± 0.1	0.8 ± 0.1	1.3 ± 0.6	1.1 ± 0.2	0.8 ± 0.2	0.8 ± 0.1
Δorf3Δxis2d	0.9 ± 0.1	2 ± 1.1	2 ± 1.2	2 ± 0.4	4 ± 1.5	4 ± 2.6	0.8 ± 0.2	1.1 ± 0.2	1.2 ± 0.1
Δorf3Δexc	1.0 ± 0.02	3 ± 0.9	2 ± 1	2 ± 0.6	6 ± 2	10 ± 3	0.7 ± 0.04	1.7 ± 0.2	1.1 ± 0.3
Δxis2c	1.0 ± 0.1	0.8 ± 0.1	1.3 ± 0.04	1.0 ± 0.1	0.8 ± 0.1	1.3 ± 0.04	1.0 ± 0.1	1.3 ± 0.2	1.0 ± 0.04
Δexc	0.9 ± 0.2	0.7 ± 0.3	1.2 ± 0.1	0.9 ± 0.2	0.9 ± 0.1	1.2 ± 0.1	0.9 ± 0.04	1.3 ± 0.2	1.1 ± 0.2
WT + orf2a-orf2b	23 ± 3	55 ± 10	118 ± 38	64 ± 27	149 ± 33	263 ± 69	1.1 ± 0.2	1.4 ± 0.2	0.7 ± 0.1
WT + orf2b	338 ± 54	811 ± 177	839 ± 135	861 ± 206	1838 ± 68	1717 ± 254	0.9 ± 0.02	1.1 ± 0.1	1.2 ± 0.1

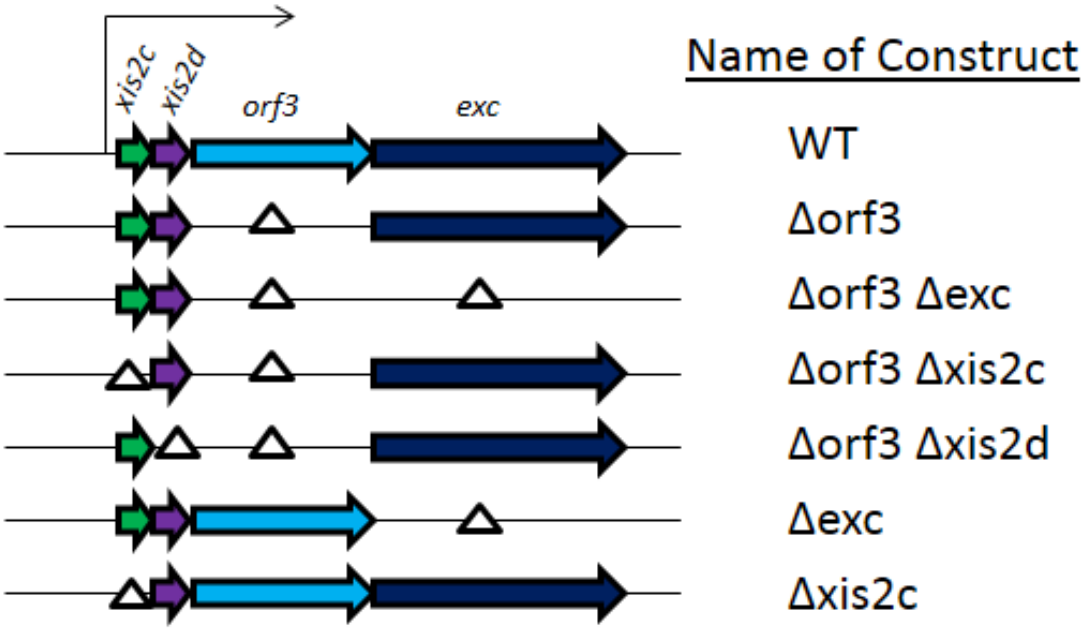

Figure 3.6: Excision Operon constructs. The excision operon is composed of the genes *xis2c, xis2d, orf3* and *exc*. Different combinations of these genes were tested in the minimal excision system with the CefMinielement. *Xis2c* and *xis2d* encode small recombination directionality factors (RDFs), *orf3* encodes a protein of unknown function, and *exc* encodes a type III topoisomerase. The black arrows represent the direction of transcription for both operons, and the small triangle represents an in-frame gene deletion.

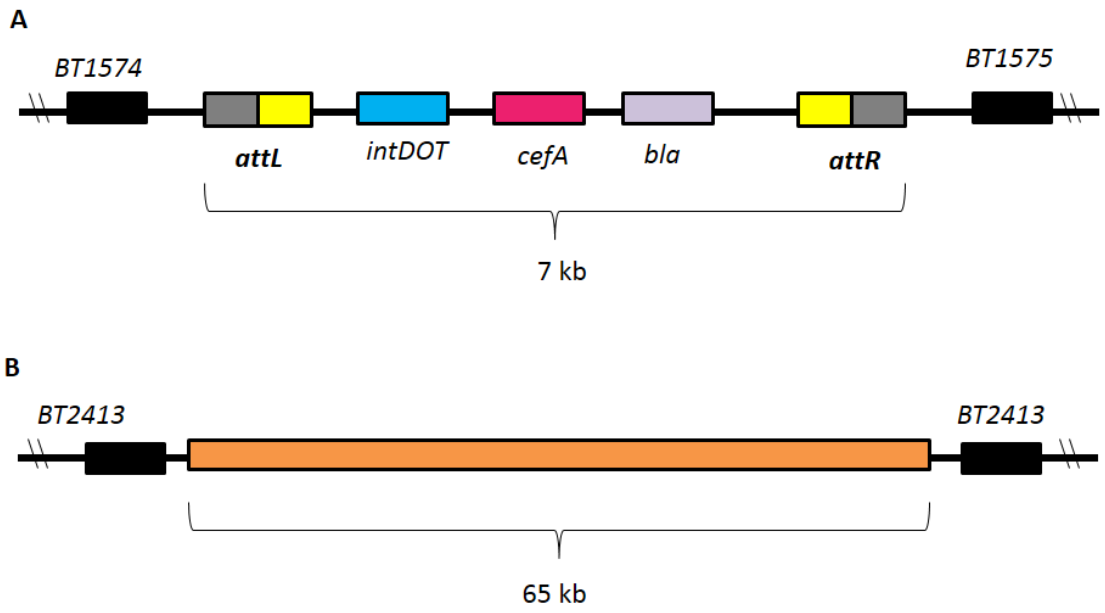

Figure 3.7: Comparison of the integrated CefMinielement (A) and WT CTnDOT (B). The CefMinielement is present in a strain containing central regulatory region *in cis* and the excision operon *in trans*. The CefMinielement is 7 kb in length and is integrated between the BT1574 (Hypothetical protein) and BT1575 (D-lactate Dehydrogenase) genes in the *Bacteroides* chromosome. CTnDOT is 65 kb in length is integrated within the BT2413 gene, which is annotated as a homoserine o-succinyltransferase.

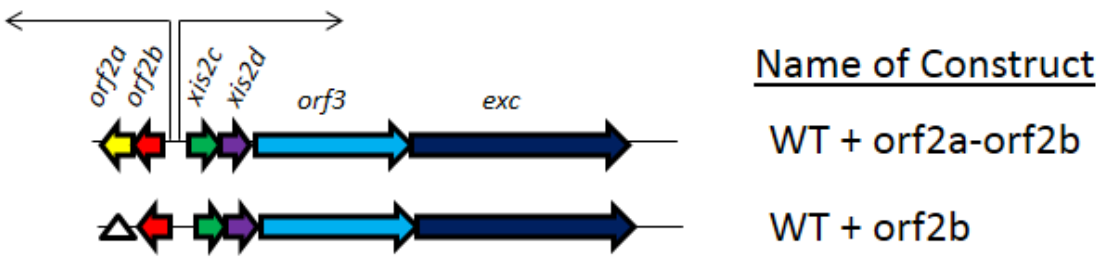

Figure 3.8: Orf2a and Orf2b. The excision operon is composed of the *genes xis2c, xis2d, orf3* and *exc*. The small *orf2a* and *orf2B* genes are divergently transcribed from the excision operon. The predicted secondary structures of Orf2a, Orf2b, Xis2c, and Xis2d are very similar. The black arrows represent the direction of transcription for both operons, and the small triangle represents a gene deletion.

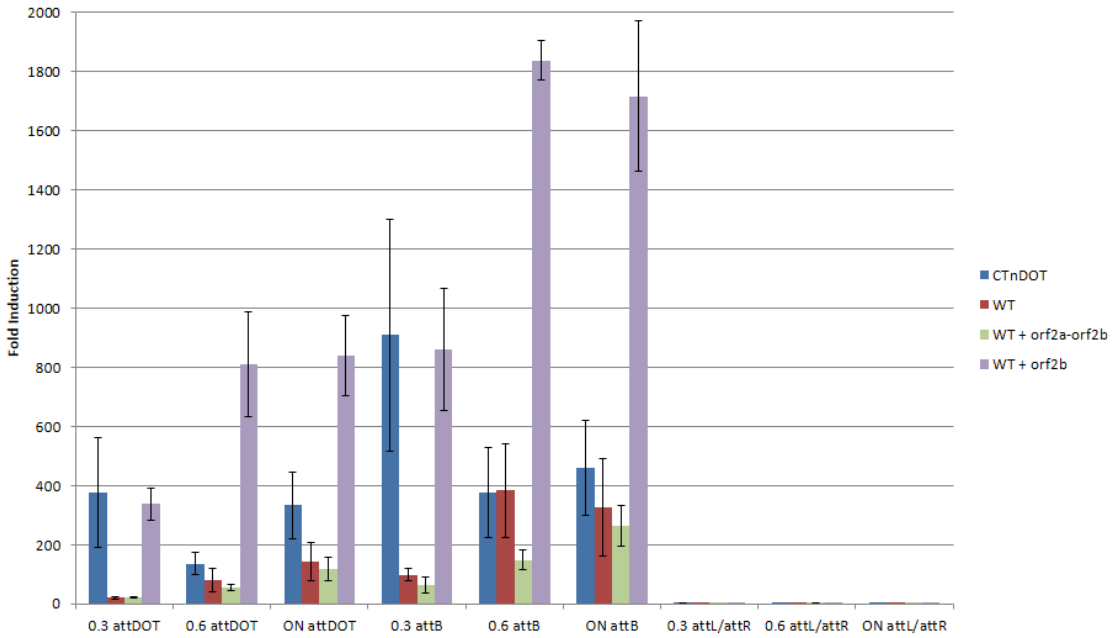

Figure 3.9: Excision Levels with the Addition of Orf2a and Orf2b. The fold increase calculated using the $2^{-\Delta\Delta CT}$ method of relative quantification is depicted for the detection of the excision products (*attDOT*, *attB*, and *attL/attR).* The fold increase of excision products for CTnDOT and the WT CefMinielement construct are shown for reference. Two additional plasmid constructs were tested with the CefMinielement: WT excision operon with *orf2a-orf2b*, and WT excision operon with *orf2b*.

CHAPTER 4: *IN VIVO BACTEROIDES* RANDOM MUTAGENESIS ASSAY

4.1 Introduction

The Excision Genes

The excision proteins of CTnDOT have been the focus of many studies, including those mentioned in Chapters 2 and 3 of this dissertation. However, previous studies have focused on the wild-type form of the excision proteins. There are four genes residing within the excision operon: *xis2c*, *xis2d*, *orf3*, and *exc*. The *xis2c* gene encodes a small (13.4 kDa), basic (10.7 pI) protein that contains a helix-turn-helix motif. Xis2c binds DNA to promote both the excision reaction and stimulate the transcription of the transfer operon [2, 3]. The *xis2d* gene encodes a protein that is structurally similar to Xis2c. Xis2d is also a small (14.1 kDa), basic (9.1 pI) protein, and it binds a G G C R N N A/W C consensus sequence [1]. Xis2d promotes the excision reaction and stimulates the transcription of both the mobilization and transfer operons. The *orf3* gene encodes a 59.7 kDa protein with two domains of unknown function (DUF 3945 and DUF 4099). Orf3 has recently been shown to contribute to the efficiency of the excision reaction (Chapter 3). The *exc* gene encodes a 77.5 kDa protein that contains a functional topoisomerase III domain. Exc is required for the in vivo excision reaction and transcriptionally activates the mobilization operon [1, 11].

As shown in Chapter 2 of this dissertation Xis2d and Exc exhibit protein-protein interactions at the promoter of the mobilization operon. These two proteins are assumed to make similar interactions when contributing to the excision reaction of CTnDOT.

There are likely protein-protein interactions between all four of the excision proteins, since they all function within a confined space when contributing to the excision reaction. It is currently unknown what residues within each of the excision proteins are responsible for these interactions.

In order to study the importance of the different residues within each of the excision proteins I have developed a random mutagenesis screen to find mutations that hinder the excision reaction. Hydroxylamine introduces random G:C →A:T mutations within the DNA, and the resulting DNA can be screened for excision competence [9]. I have based the screening process on the thymidine kinase (tdk) selection protocol used for chromosomal knockouts in other studies [5].

Thymidine Synthesis and Inhibition

When the nucleic acid base thymine is linked to a deoxyribose molecule, the resulting product is known as Thymidine. This nucleoside is present within the cell as a result of DNA degradation. A salvage pathway within cells takes scavenged thymidine and phosphorylates it in a three step process to create deoxythymidine triphosphate, which is one of the four nucleotide triphosphates used for DNA synthesis (Figure 4.1). The first phosphorylation step is catalyzed by the enzyme encoded by the thymidine kinase gene (*tdk*), which catalyzes the following reaction:

Deoxythymidine + ATP →deoxythymidine monophosphate + ADP

This reaction is not the only cellular reaction that produces deoxythymidine monophosphate (dTMP). A cellular metabolic product, deoxyuridine monophosphate (dUMP), is converted into dTMP by the enzyme thymidylate synthetase [6, 10]. This pathway is called the *de novo* thymidine synthesis pathway.

The *de novo* thymidine synthesis pathway can be inhibited by the nucleotide analog 5-fluoro-2-deoxyuridine (FUdR) [5]. FUdR is recognized by the enzyme encoded by the *tdk* gene, which subsequently phosphorylates the FUdR into 5-fluoro-2-deoxyuridine monophosphate (FdUMP) [10]. This phosphorylated analog inhibits the thymidylate synthetase enzyme in the *de novo* synthesis pathway [10].

4.2 Materials, Methods, and Results

Bacteroides Mating Assay

A bi-parental mating assay is used to transfer plasmids constructed within *E. coli* into *Bacteroides*. The *E. coli* (S17-1) containing the desired plasmid is grown overnight with shaking, in LB medium containing appropriate antibiotics. The *Bacteroides* host strain is grown statically overnight, in BHIS medium with the appropriate antibiotics. The overnight S17-1 growth is sub-cultured 1:100 in fresh LB medium with appropriate antibiotics. The overnight *Bacteroides* growth is sub-cultured 1:200 in fresh BHIS medium containing the appropriate antibiotics. Both cultures are grown to an approximate OD of 0.2 (OD_{600} for S17-1 and OD_{650} for *Bacteroides*). After outgrowth, 5 mL of each culture are spun down and re-suspended into a single 1 mL volume of BHIS. The resulting mixture is plated evenly across a non-selective BHIS agar plate and grown aerobically, agar-side down overnight. The overnight growth is collected and re-suspended in 5 mL of BHIS. A 100 uL aliquot of the resulting mixture is plated on BHIS agar containing appropriate antibiotics and grown anaerobically for 1-2 days.

Construction of *in vivo* Mutagenesis Screen

The *Bacteroides* strain *B.thetaiotaomicronΔtdk* contains a chromosomal knockout of the *tdk* gene [5]. Since this strain lacks a functional thymidine scavenging pathway, it relies solely on the *de novo* thymidine synthesis pathway. A Minielement containing a copy of the *tdk* gene was constructed, so that it could be inserted into the *B.thetaiotaomicronΔtdk* chromosome and restore they thymidine scavenging pathway. The plasmid pWTMinielement encodes the constitutively expressed tyrosine recombinase of CTnDOT (IntDOT), ampicillin resistance (*bla*), erythromycin resistance (*ermG*), and the *attDOT* sequence. The thymidine kinase gene, *tdk*, was amplified with primers *Tdk-EcoRI-F* and *Tdk-EcoRI-R* using the pExchange plasmid as a template. The resulting amplified product was cloned into the EcoRI site of pWTMinielement, resulting in the plasmid pTdkMinielement (Figure 4.2). This plasmid, pTdkMinielement, is a suicide vector capable of integrating into the *Bacteroides* chromosome when selected for with erythromycin (Figure 4.3). Once integrated, the host can utilize the thymidine scavenging pathway.

The integrated TdkMinielement provides the *attL/attR* sequences and the IntDOT protein, but it lacks the excision proteins required for excision to occur. If the excision operon is expressed *in trans*, the TdkMinielement would be capable of excising itself from the host chromosome. In order for the excision proteins to be expressed under their native promoter, the CTnDOT regulatory region needs to be integrated into the *B.thetaiotaomicronΔtdk* chromosome. The suicide plasmid pAMS7 contains the *tetQ-rteA-rteB-rteC* region, and integrates within the NBU1 site in the *Bacteroides* chromosome [8]. The resulting strain, tentatively called

*BTΔtdk*Ω*QABC*Ω*TdkMinielement*, would be adaptable for the study of excision mutants *in vivo*. If these cells were grown on minimal medium they would heavily rely on the *de novo* thymidine synthesis pathway, since they would not be able to scavenge much from the environment. If these cells on minimal medium were then exposed to FUdR, they would need to excise the TdkMinielement before the *de novo* thymidine synthesis pathway gets poisoned.

Hydroxylamine Mutagenesis of Excision Proteins

The hydroxylamine mutagenesis protocol was adapted from a protocol previously used to obtain IntDOT mutants [4]. A potassium phosphate stock solution was made by adding 10 mL of 0.5 M EDTA [pH 8] to 80 mL of 0.5 M KH_2PO_4. Then K_2HPO_4 was added to the EDTA-KH_2PO_4 solution until pH 6 was achieved, resulting in phosphate-EDTA buffer. A 7.2 M hydroxylamine stock solution was made by adding 1.28 g hydroxylamine-HCL, 0.28 mL NaOH [4 M], and 2.22 mL dd$H_2$0.

10 ng of pWTExcision DNA was incubated with 40 µL phosphate-EDTA buffer, 80 µL hydroxylamine stock solution, and 80 µL dd$H_2$0.Each reaction was incubated for 90 minutes at 37°C. Reactions were stopped by drop dialysis on TE buffer (10 mM Tris-HCl, 1 mM EDTA [pH 8]) using a 0.025 µM pore-size Millipore filter, for 1 hour.

Protocol for Mutagenesis Screen

The pWTexcision plasmids treated with hydroxylamine are transformed into S17-1. The resulting colonies are pooled together and the *Bacteroides* mating assay is used to introduce the plasmids into the host *Bacteroides* strain. After the non-selective overnight growth is collected and re-suspended in 5 mL of BHIS medium, 100 µL aliquots are made onto several BHIS agar plates containing appropriate antibiotics. The resulting

colonies are re-streaked onto two different types of minimal medium plates. All plates contain the appropriate antibiotics, but one set of plates contains FUdR (200 mg/mL). The cells are able to grow well on minimal medium because they have a functional *de novo* thymidine synthesis pathway. Cells containing functional excision proteins *in trans*, will be able to remove the integrated TdkMinielement from the host chromosome when FUdR is present (Figures 4.4 & 4.5). Colonies that are unable to grow in the presence of FUdR cannot excise TdkMinielement from the chromosome (Figure 4.5). The TdkMinielement provides a thymidine kinase protein that converts the FUdR into FdUMP, which poisons the thymidylate synthetase protein in the thymidine *de novo* synthesis pathway. Cells growing on minimal medium are unable to grow without a functional thymidine *de novo* synthesis pathway, resulting in cell death. The excision plasmids from the colonies that grew on minimal medium, but died on minimal medium containing FUdR will be sequenced to determine what mutations resulted in this phenotype.

4.3 Conclusions

Since the *in vitro* excision assays are not an accurate representation of *in vivo* excision, an *in vivo* mutational screen was required for isolating excision mutants (Chapter 3). Previous studies focused on CTnDOT excision have analyzed the wild-type proteins, but mutational analysis will provide greater insight into the structure-function relationship of the excision proteins.

This screen provides an adaptable way to isolate mutants within the excision operon. This assay allows for mutations to be screened within the entire excision operon, but it can be adapted to screen for mutations within a specific excision gene. To

accomplish this, the other excision genes must first be mated into the indicator strain containing the integrated TdkMinilement. Then the desired excision gene must be cloned onto a separate plasmid and subjected to mutagenesis, before being mated into the indicator strain containing the other excision proteins. Additionally, this assay has been described using hydroxylamine mutagenesis, which Hydroxylamine introduces random G: C to A: T mutations. This may limit the number of attainable mutations, but any other method of DNA mutagenesis could be used to compensate (error-prone PCR, UV mutagenesis, etc.).

Now that this *in vivo* mutagenesis screen has been developed, it needs to be used to isolate excision mutants. Once this occurs, the mutations can be characterized and functional properties can be assigned to specific structural regions of the proteins.

4.4 References

1. Hopp, C.M., J.F. Gardner, and A.A. Salyers, *The Xis2d protein of CTnDOT binds to the intergenic region between the mob and tra operons.* Plasmid, 2015. **81**: p. 63-71.

2. Keeton, C.M., et al., *Interactions of the excision proteins of CTnDOT in the attR intasome.* Plasmid, 2013. **70**(2): p. 190-200.

3. Keeton, C.M., et al., *The excision proteins of CTnDOT positively regulate the transfer operon.* Plasmid, 2013. **69**(2): p. 172-179.

4. Kim, S., B.M. Swalla, and J.F. Gardner, *Structure-function analysis of IntDOT.* J Bacteriol, 2010. **192**(2): p. 575-86.

5. Koropatkin, N.M., et al., *Starch catabolism by a prominent human gut symbiont is directed by the recognition of amylose helices.* Structure, 2008. **16**(7): p. 1105-15.

6. O'Donovan, G.A. and J. Neuhard, *Pyrimidine metabolism in microorganisms.* Bacteriol Rev, 1970. **34**(3): p. 278-343.

7. Simon, R., U. Priefer, and A. Puhler, *A Broad Host Range Mobilization System for In Vivo Genetic Engineering: Transposon Mutagenesis in Gram Negative Bacteria.* Nat Biotech, 1983. **1**(9): p. 784-791.

8. Stevens, A.M., et al., *Genes involved in production of plasmidlike forms by a Bacteroides conjugal chromosomal element share amino acid homology with two-component regulatory systems.* J Bacteriol, 1992. **174**(9): p. 2935-42.

9. Stolarski, R., et al., *Mechanism of hydroxylamine mutagenesis: tautomeric shifts and proton exchange between the promutagen N6-methoxyadenosine and cytidine.* Biochemistry, 1987. **26**(14): p. 4332-7.

10. Summers, W.C. and P. Raksin, *A method for selection of mutations at the tdk locus in Escherichia coli.* J Bacteriol, 1993. **175**(18): p. 6049-51.

11. Waters, J.L., G.R. Wang, and A.A. Salyers, *Tetracycline-related transcriptional regulation of the CTnDOT mobilization region.* J Bacteriol, 2013. **195**(24): p. 5431-8.

4.5 Tables and Figures

Table 4.1: Bacterial Strains and Plasmids.

Strain or Plasmid	Phenotype	Description
VPI-548Δtdk		*Bacteroides* Strain that has chromosomal knock-out of *tdk* [5].
S17-1	RecA$^-$ Tp^r Str^r Spc^r	IncPα RP4 inserted into the chromosome[7].
pExchange	Amp (Erm)	Plasmid used for making chromosomal knockouts with FUdR selection. Contains *tdk*, *amp^r*, *erm^r*, and RP4 replication origin [5].
pWTMinielement	Amp (Erm)	pDJE2.3 with a wild type *intDOT* gene (Chapter 3)
pTdkMinielement	Amp (Erm)	This Study
pAMS7	Amp (Tet)	Contains the *tetQ-rteA-rteB-rteC* region on the suicide vector pNFD13-2[8].
pWTExcision	Amp (Erm)	Contains genes *xis2c*, *xis2d*, *orf3*, and *exc* (Chapter 3)

Table 4.2: Primers Used in this Study.

Primer Name	Sequence	Tm
Tdk-EcoR1-F	GCAATG***GAATTC***CACTCATTTATTTAA	58.8°C
Tdk-EcoR1-R	GCAATG***GAATTC***GTTTATATCTTCTGT	60.4°C

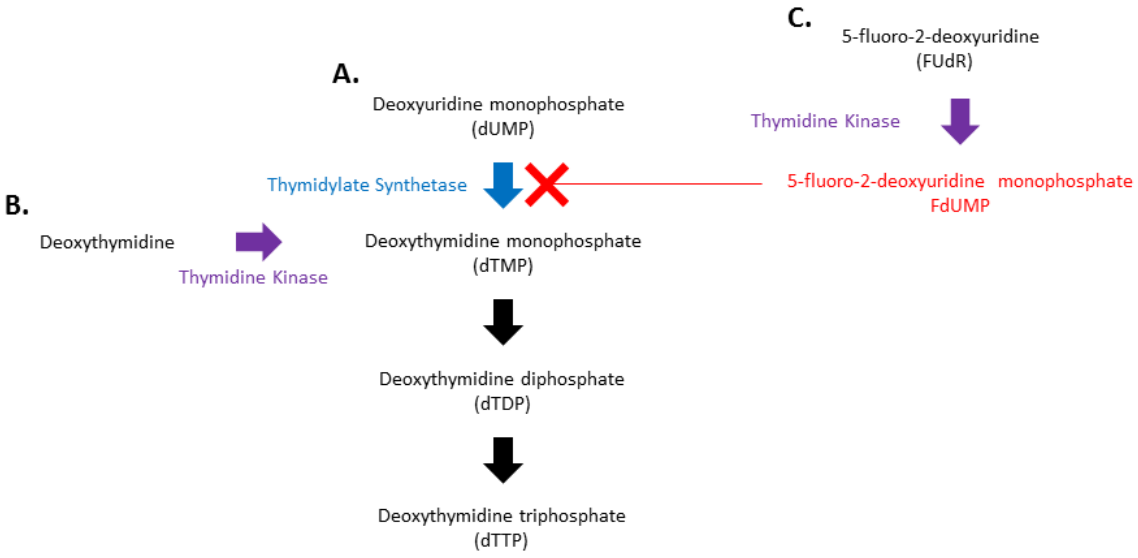

Figure 4.1: Inhibition of Thymidine Synthase. (A) The *de novo* thymidine synthesis pathway begins by using thymidylate synthetase to convert the metabolic product deoxyuridine monophosphate (dUMP) into deoxythymidine monophosphate (dTMP). (B) The thymidine scavenging pathway begins by phosphorylating deoxythymidine into dTMP. (C) The nucleoside analog 5-fluoro-2-deoxyuridine (FUdR) is recognized by thymidine kinase and converted into 5-fluoro-2-deoxyuridine monophosphate (FdUMP). FdUMP inhibits thymidylate synthetase, which results in the cell relying on the thymidine scavenging pathway for deoxythymidine monophosphate.

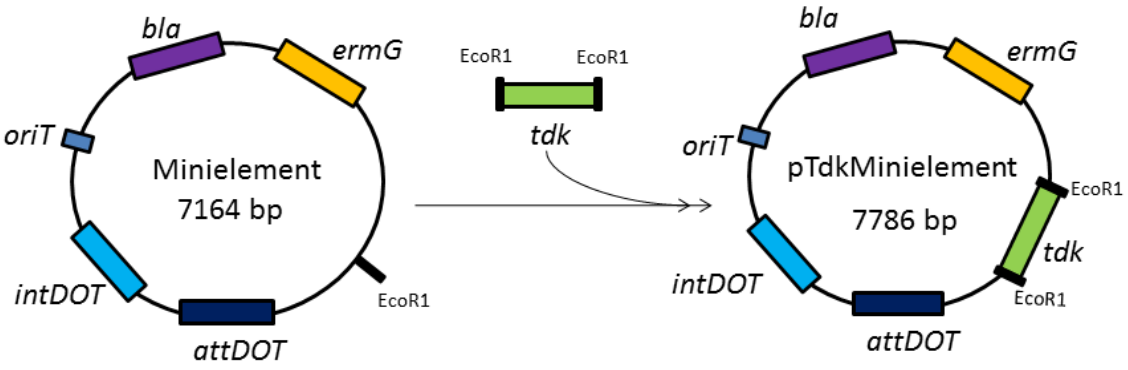

Figure 4.2: Construction of pTdkMinielement. The *tdk* gene was amplified with primers containing EcoRI restriction sites, and subsequently cloned into the pMinielement plasmid. The resulting plasmid , pTdkMinielement, is capable of integrating into the *Bacteroides* chromosome. Once integrated the host *Bacteroides* strain will gain a functional copy of thymidine kinase.

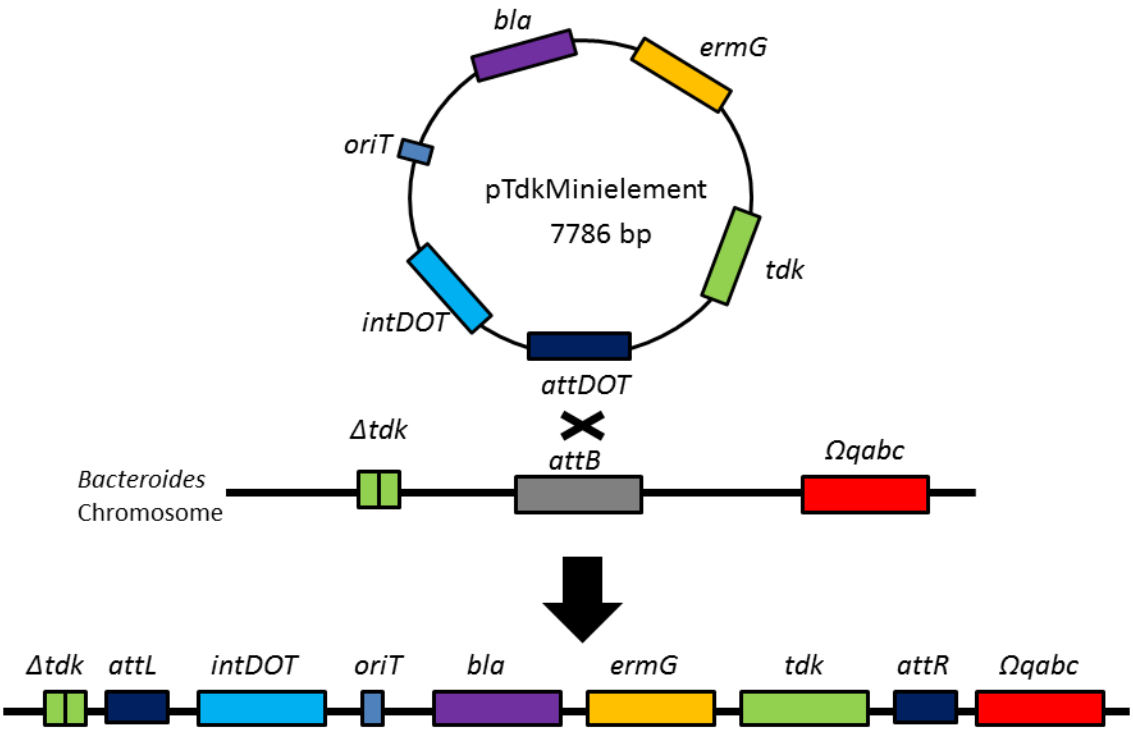

Figure 4.3: Insertion of pTdkMinielement into the Chromosome. The pTdkMinilement was mated into the *Bacteroides* strain *B.thetaiotaomicronΔtdk*Ω*QABC*. Once inside the host cell the pTdkMinielement will use the Bacteroides host factor (BHFa) and IntDOT to perform site selective integration of this plasmid. Once this plasmid has integrated into an *attB* site within the host chromosome the cells will gain resistance to erythromycin, and also gain a functional copy of thymidine kinase.

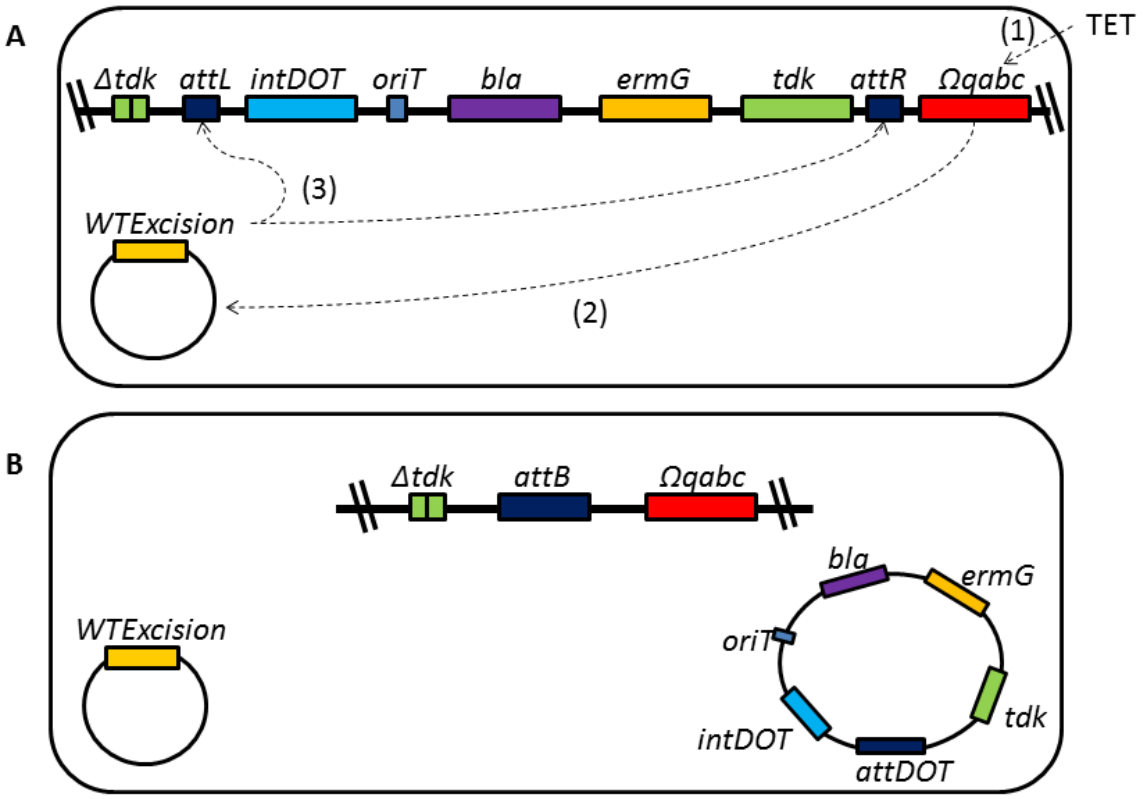

Figure 4.4: Excision of the Integrated pTdKMinielement. A.)(1)When cells are exposed to tetracycline the CTnDOT regulatory cascade is activated. (2) RteC activates the transcription of the excision genes, which have been treated with hydroxylamine. (3) The resulting excision proteins may bind the *attL/attR* sites of the integrated element, and promote the excision reaction. B.) Functional excision proteins will be able to excise the integrated pTdkMinielement from the chromosome. The resulting plasmid is unable to replicate in *Bacteroides*, so antibiotic resistances and thymidine kinase activity will be lost.

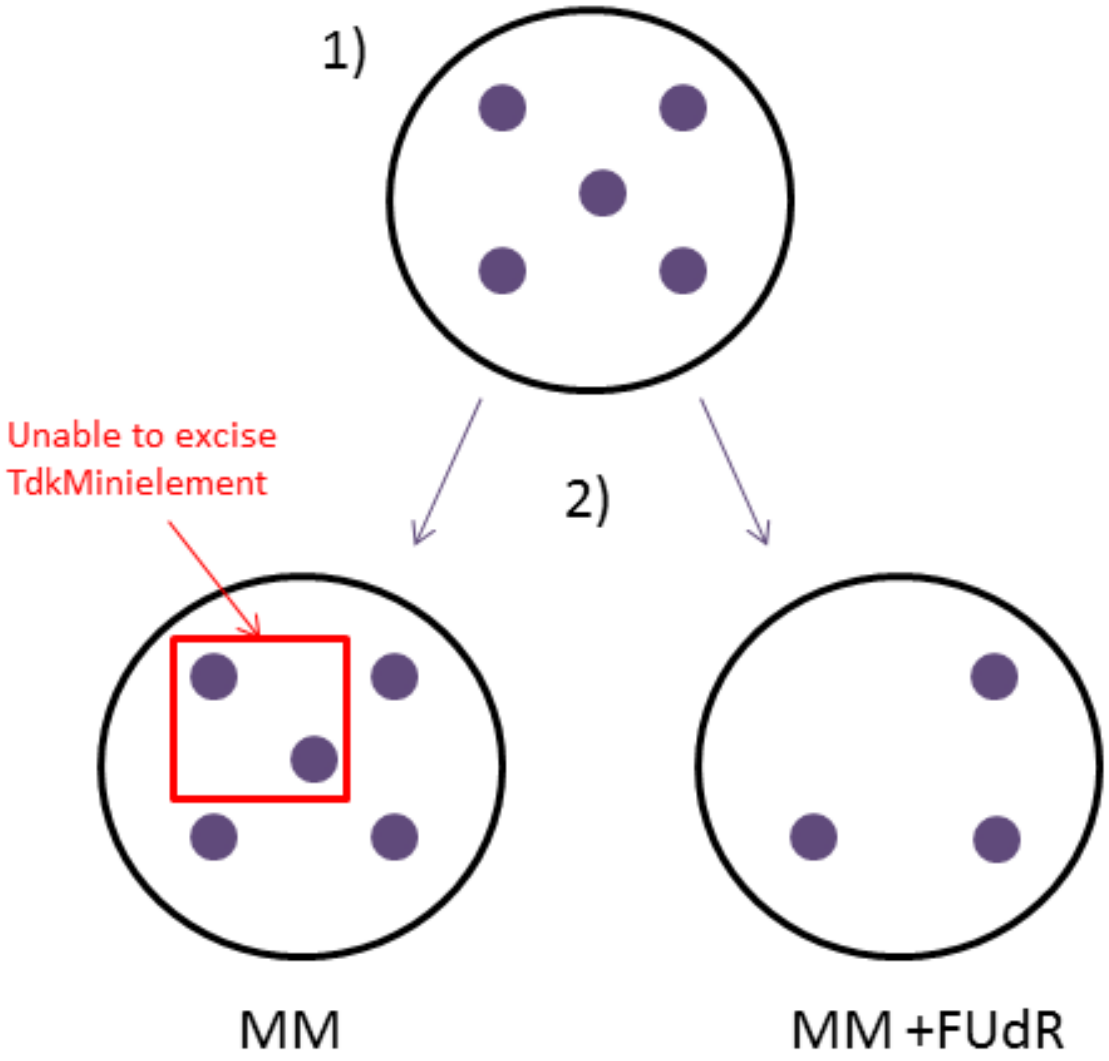

Figure 4.5: FUdR Mutagenesis Screen. (1)The hydroxylamine treated excision plasmids are mated into the *Bacteroides* host strain and selected for on antibiotics. (2) The resulting colonies are plated on two sets of plates. Both plates contain minimal medium (MM) with the appropriate antibiotics, but one plate contains 200 mg/mL FUdR. The colonies grow well on minimal medium because they have a functional *de novo* thymidine synthesis pathway. The colonies that are unable to grow on medium containing FUdR cannot excise the integrated TdkMinielement, meaning they use the thymidine kinase protein to phosphorylate FUdR into FdUMP. FdUMP poisons the thymidylate synthetase enzyme in the *de novo* pathway, and in minimal medium the thymidine scavenging pathway is not able to keep up with the thymidine demands of the cell. This results in cell death.

CHAPTER 5: CONCLUDING REMARKS AND FUTURE STUDIES

5.1 Concluding Remarks

The Salyers lab has published studies regarding the regulation of the CTnDOT family of elements since the early 1990s, and 26 years later there is still much to learn about these elements. It seems that new aspects of regulation are unlocked with every discovery concerning the complex regulatory cascade that governs CTnDOT propagation. Through the work published in this dissertation I have broadened our knowledge of how the excision proteins influence CTnDOT regulation.

It is clear that the excision proteins are relied on heavily for multiple levels of CTnDOT regulation. They are involved in promoting the excision reaction, and the transcriptional activation of both the mobilization (*mob*) and transfer (*tra*) operons [3, 4]. Prior to my investigations the mechanism for how the excision proteins were meditating the transcriptional regulation of the *mob* and *tra* operons was unknown. In Chapter 2, I show that native Xis2d is a dimer and binds with high affinity to a G G C R N N A/W C consensus sequence found between the *mob* and *tra* promoters. I proposed that Xis2d is the first excision protein recruited to the promoter region, since it is involved in the activation of both promoters. The other excision proteins are then likely recruited depending on which promoter needs to be activated. Xis2c is recruited if the transcription of the *tra* operon needs to be activated, whereas Exc is recruited if the *mob* operon needs to be transcriptionally activated. In Chapter 2, I showed the first evidence that Xis2d and Exc directly interact with each other. Exc does not interact with the *mob* promoter by

itself, but higher order complexes form in the presence of Xis2d. These findings have helped define the multifunctional complexes that form between the excision proteins to perform different roles within the lifecycle of CTnDOT.

In vitro studies, like those used in Chapter 2, are vital ways of gaining a detailed analysis of protein mechanism. However, not all *in vitro* studies are created equal. Many of the results obtained from intermolecular and intramolecular *in vitro* excision assays do not corrolate with results obtained during early *in vivo* experimentation. Therefore, in Chapter 3 I have constructed a versatile *in vivo* excision assay that can quantify relative excision levels. This assay not only confirmed that Xis2c and Xis2d are required for excision, it also confirmed that Exc is required for *in vivo* excision. Additionally, this assay is the first to conclude that a deletion of *orf3* has a detectable effect on CTnDOT excision. Without *orf3*, there was a noticeable decrease in the levels of excision, which validates why this gene is included within the excision operon.

The *in vivo* excision system also provided the first evidence towards identifying the function of the *orf2a* and *orf2b* genes, which are located within an operon just upstream of the excision operon. It appears that the presence of *orf2b* alone greatly increases the detectable levels of excision, and the presence of *orf2a* causes the excision levels to return to wild-type expression levels. This suggests that Orf2b enhances the efficiency of the excision reaction, while Orf2a may regulate excision to prevent excess. While the function of these proteins needs to be further studied, the results obtained with these two genes in the *in vivo* qPCR assay gave insight into previously unknown aspects of CTnDOT.

Chapter 3 also presented the most advanced sequencing data to date regarding CTnDOT. The first complete sequence of CTnDOT was obtained, and several new alternative *attB* sites were discovered. *Bacteroides* appears to be well suited for harboring integrative mobile elements, as there are many possible locations for integration throughout the *Bacteroides* chromosome.

The research conducted concerning the excision proteins has until this point focused on the wild-type form of these proteins. Chapter 4 introduces a new mutagenesis assay I devised, which identifies mutant proteins that are incapable of excising CTnDOT from the chromosome. Studying how mutations affect the functionality of the proteins will clarify the structure-function relationship of the excision proteins. This may elucidate what regions of the excision proteins are involved in protein-protein interactions when higher order complexes are formed.

While the work presented within this dissertation has furthered what is known about the regulation of CTnDOT, there is still much to be studied with regards to this subject. The potential future studies described below are aimed at gaining a greater understanding of the focus of this dissertation - the excision operon.

5.2 Future Studies

Purification and Analysis of Xis2c

The research presented in Chapter 2 of this dissertation focused on learning how the excision proteins mediate the transcriptional activation of the transfer and mobilization operons. One protein that is notably missing from that work is Xis2c. This is because a stable preparation of Xis2c has remained elusive. Xis2c's sister protein Xis2d

is easily purified, and preparations ofXis2d appear to remain stable for more than a year. The proteins have a very similar structure, but attempts to purify Xis2c have ultimately been unsuccessful.

Previous students had tried purifying Xis2c (and Xis2d) by attaching a polyhistidine tail to the protein. However, this eliminated protein activity, so simple Ni^{2+} chromatography could not be used in the purification of Xis2c (data not published). A multitude of different affinity columns were tested for the native purification of Xis2c. When cell lysates of overexpressed Xis2c were tested with HiTrap heparin HP columns, which are the same type of columns used to purify Xis2d, no detectable product was eluted. A HiTrap Blue HP column, which is designed to capture a wide range of biomolecules using a dye molecule that resembles a nucleotide cofactor, was also unsuccessful in achieving a purified Xis2c product. A HiTrap Q HP column, which contains a strong ammonium anion exchanger, also failed in the attempts to purify Xis2c. A HiTrap SP HP column, containing a strong sulfopropyl anion exchanger, did elute a Xis2c product from the column. However, the Xis2c product had low activity levels. Additionally, repetitions of this purification indicated that even minimal Xis2c activity was not always consistent.

The sequence of *xis2c* indicates that this gene contains several codons that are rarely used in *E. coli*. Therefore, the overexpression vector carrying *xis2c* was transformed into a Rosetta strain that carries additional tRNA genes for rare codons. This was also ultimately unsuccessful in purifying a stable form of the protein. I also questioned whether Xis2c needed Xis2d present for stability. Therefore, I cloned *xis2c*

and *xis2d* into a pACYCDuet overexpression vector (Table 5.1 & 5.2). While the Xis2d that came off the column was stable, Xis2c remains elusive.

Upon closer inspection of the region upstream of Xis2c I noticed two in-frame alternative start codons for the *xis2c* gene. One is 36 bp upstream of the current start codon, while the other is 30 bp upstream. This could mean that either 12, or 10 amino acids could be missing from the beginning of the overexpressed protein. The lack of these amino acids at the N-terminus of the protein could be contributing to the instability of Xis2c. I have cloned the version of Xis2c containing 12 extra amino acids into the pET27b(+) expression vector, but further testing is needed to assess the stability of the new Xis2c construct (Table 5.1 & 5.2).

Once a stable form of Xis2c has been purified there are several experiments that can be performed to gain a better understanding of where and how this protein is working. We know that Xis2c is required for both the excision reaction and the activation of the transfer operon (Chapter 3, [4]). A sample of Xis2c purified using an SP column was capable of shifting DNA upstream of the *mob* and *tra* operon. However, this sample lost activity before more experiments could be completed (Figure 5.1). Therefore, once a stable preparation of Xis2c has been achieved the area where Xis2c binds within these two locations needs to be determined through electrophoretic mobility shift assays (EMSA). Once the region is narrowed down, footprinting assays can be performed to determine exactly which base pairs in the DNA are being protected by Xis2c. Then when the protection profiles are compared, a consensus binding site can be extrapolated.

In addition to understanding the individual binding characteristics of Xis2c, cooperative assays may be performed to gain a greater understanding of how the excision proteins are interacting together with the DNA. In Chapter 2 of this dissertation I showed that Xis2d interacts with Exc via protein-protein interactions, as indicated by a supershift that appears on an EMSA containing both of those proteins. Xis2c likely interacts with both Xis2d and Exc in the excision reaction, since all three of the proteins are required *in vivo*. Xis2c also likely interacts with Xis2d in a different manner to activate the transcription of the *tra* operon, since Exc is not needed for the activation of this operon. Cooperative EMSAs can help determine if the different complexes have different affinity for the DNA in question. Cooperative EMSAs can also help determine the affinity of the proteins for each other based on what concentrations of protein are needed to sustain a super-shift in the DNA.

In Chapter 2 of this dissertation I determined that Xis2d bends the DNA once bound. Since Xis2c is structurally similar to Xis2d, it would seem reasonable that Xis2c has a similar function. Therefore, once a stable preparation of Xis2c has been obtained it should be tested in the pBend assay system. It would be interesting to see if Xis2c bends DNA by itself, and also if Xis2c works with Xis2d to create a larger bend in the DNA.

Purification and Analysis of Orf3

As Chapter 3 in this dissertation indicates, Orf3 appears to play a larger role in the excision reaction than previously thought. Previous *in vivo* and *in vitro* work indicated that *orf3* was not an essential gene for the excision reaction [1, 5]. Chapter 3 shows that excision is still able to occur without Orf3, but the frequency of excision upon the

induction of tetracycline is greatly reduced. Therefore, a purified form of the protein would be desirable for future testing.

Once Orf3 has been purified it needs to be tested for activity. Unfortunately, all the *in vitro* tests available for CTnDOT excision do not require this protein for success. It is possible that the addition of a purified Orf3 to the *in vitro* intermolecular excision assay would speed up the reaction. Previously this reaction was very slow and required overnight incubation, whereas *in vivo* excision can be detected during the exponential phase of growth [2]. The slow reaction rate of the *in vitro* intermolecular assay could be due to the lack of Orf3. If this is the case, the *in vitro* intermolecular excision assay may be an efficient test for determining Orf3 activity after purification.

Once an active purified Orf3 sample has been obtain it can be tested for DNA binding capabilities within the *attL* and *attR* regions. Once the individual binding capabilities of Orf3 have been determined, Orf3 can be tested for cooperative binding interactions. Excision happens within the defined *attL* and *attR* regions of CTnDOT, so it is not hard to imagine that all the proteins are interacting within that very limited space. Therefore, it would be interesting to see how DNA migration patterns change when all of the excision proteins are added to *attL* and *attR* DNA for EMSA analysis. It would also be interesting to see how the addition of IntDOT would affect these DNA binding patterns, since it is also interacting with the core and arm-type sites within *attL* and *attR* during the excision reaction.

Mutational Analysis of Excision Proteins

Once the properties of each of the excision proteins have been established with wild type proteins, the mutational screen mentioned in Chapter 4 may be used to obtain mutants of these proteins. These mutants can then be tested *in vitro* to determine what aspect of these proteins has been affected to cause them to be defective in the excision reaction. Simple EMSA analysis can be performed to test if they have lost the ability to bind DNA, and/or have lost the ability to make the protein-protein interactions needed for forming higher order complexes, like those seen formed between Xis2d and Exc in Chapter 2 of this dissertation.

Purification and Analysis of Orf2a and Orf2b

The Orf2a and Orf2b proteins have a proposed secondary structure that is very similar to the Xis2c and Xis2d proteins. Prior to the excision assay results mentioned in Chapter 3, these two proteins have largely remained unstudied. It appears that these two proteins, particularly Orf2b, have some impact on excision levels. It is currently unknown how these proteins are mediating their effect on the excision reaction. Therefore, purification of these proteins would allow for *in vitro* testing that could help determine if these two proteins are contributing to the excision reaction by binding DNA, and/or interacting with the proteins of the excision operon.

It is possible that in addition to their role in the excision reaction, the Orf2a and Orf2b proteins may serve as transcriptional regulators, like the similarly structured Xis2c and Xis2d. There is a transfer assay that has been used in lab previously that tests the ability of a plasmid, containing the transfer and mobilization genes of CTnDOT, to transfer itself into new hosts. On its own, this plasmid (pLYL72) transfers constitutively

to new host cells. But when CTnDOT regulatory genes are provided *in trans*, transfer becomes regulated. I have mated the new excision plasmid constructs containing the *orf2a* and *orf2b* genes into a strain containing pLYL72, to determine if Orf2a and Orf2b have an impact on the transfer and mobilization reactions (Table 5.1). While the strains have been constructed, they still need to be tested in the CTnDOT transfer assay.

5.3 References

1. Cheng, Q., et al., *Identification of genes required for excision of CTnDOT, a Bacteroides conjugative transposon.* Mol Microbiol, 2001. **41**(3): p. 625-32.
2. Keeton, C.M. and J.F. Gardner, *Roles of Exc protein and DNA homology in the CTnDOT excision reaction.* J Bacteriol, 2012. **194**(13): p. 3368-76.
3. Keeton, C.M., et al., *Interactions of the excision proteins of CTnDOT in the attR intasome.* Plasmid, 2013. **70**(2): p. 190-200.
4. Keeton, C.M., et al., *The excision proteins of CTnDOT positively regulate the transfer operon.* Plasmid, 2013. **69**(2): p. 172-179.
5. Sutanto, Y., et al., *Factors required in vitro for excision of the Bacteroides conjugative transposon, CTnDOT.* Plasmid, 2004. **52**(2): p. 119-30.

5.4 Tables and Figures

Table 5.1: Bacterial strains and Plasmids

Strain or Plasmid	Phenotype	Description
pCDco-expression	Cm^r	pACYCDuet vector containing Xis2c and Xis2d (C. Hopp, unpublished results)
pFull-Xis2c	Kan^r	pET27b(+) overexpression vector with Xis2c under alternative initiator codon 36 bp upstream of current AUG codon. (C. Hopp, unpublished results)
BT4001ΩQABC, pLYL72, pABCD3E	$Gent^r$,Cm^r, Erm^r	CTnDOT transfer assay system containing orf2a, orf2b, xis2c, xis2d, orf3, exc *in trans* (C. Hopp, unpublished results)
BT4001ΩQABC, pLYL72, pBCD3E	$Gent^r$,Cm^r, Erm^r	CTnDOT transfer assay system containing orf2b, xis2c, xis2d, orf3, exc *in trans* (C. Hopp, unpublished results)

Table 5.2: List of Primers

Name	Sequence
Xis2c-HindIII-R	GCAATGAAGCTTCTATGTCCTCCTTCCTTTGGGTGTGCC
Xis2c-NdeI-10-F	GCAATCCATATGAAAATAAACAAAAAGAAAGGACTG
Xis2c-NdeI-12-F	GCAATCCATATGTTCATGAAAATAAACAAAAAGAAAGGACTGAATATG
Xis2c-mutate-F	GGAGATATACCATGAAAGTGATAACAATGGAAAGTTCCGTATTTCGG
Xis2c-mutate-R	CCGAAATACGGAACTTTCCATTGT TATCACTTTCATGGTATATCTCC

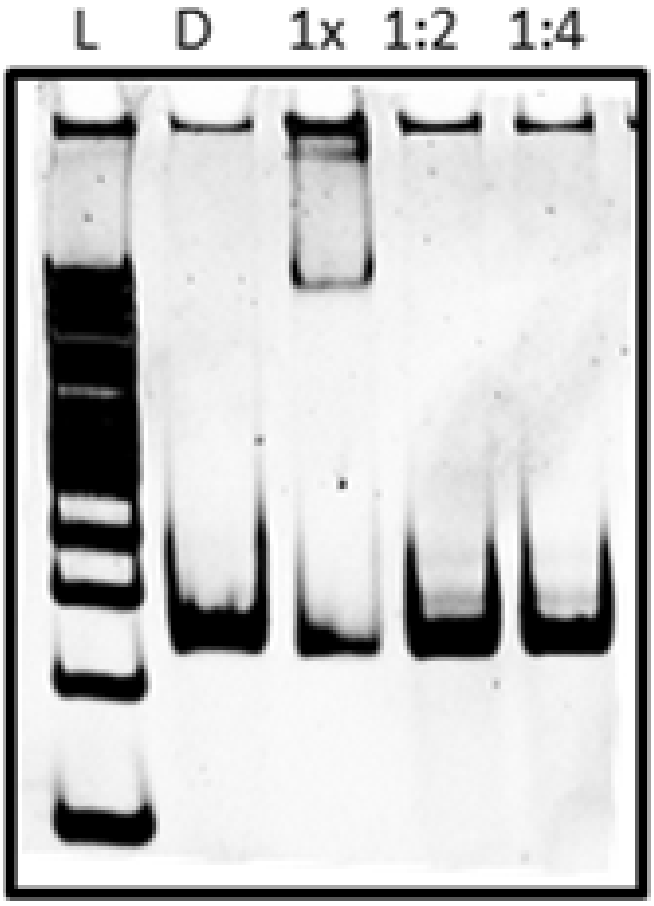

Figure 5.1: Xis2c Binding the Transfer Operon Promoter. Xis2c purified from an SP column was incubated with a 138 bp DNA fragment from the transfer region (Fragment D, Chapter 2). The Xis2c preparation was tested undiluted (1x), and at 1:2 and 1:4 dilutions. Lane L corresponds to the 100 bp DNA ladder. Lane D corresponds to a DNA only reaction.